Aus dem Institut für Physiologie und Pathophysiologie
Geschäftsführender Direktor: Prof. Dr. Dominik Oliver des
Fachbereichs Medizin der Philipps-Universität Marburg

Effects of Interleukin-1 on Glucose Uptake and Energy Homeostasis in Lymphocytes

Inaugural-Dissertation zur Erlangung des
Doktorgrades der Naturwissenschaften

Dem Fachbereich Medizin der
Philipps-Universität Marburg
vorgelegt von

Cornelius Meyer aus Heidelberg
Marburg, 2020

Angenommen vom Fachbereich Medizin der
Philipps-Universität Marburg am 24.07.2020

Gedruckt mit Genehmigung des Fachbereiches

Dekan: Prof. Dr. Helmut Schäfer

Referent: Prof. Dr. Adriana del Rey

Korreferent: Prof. Dr. Michael Bacher

Abstract

The research group in which this work was performed has shown that interleukin-1 (IL-1) induces a profound, long-lasting, and insulin-independent hypoglycemia, by mechanisms acting at peripheral and central levels. More recently, we reported that despite the concomitant hypoglycemia, IL-1 increases energetic activity in the brain *in vivo* and glucose uptake by neurons and astrocytes *in vitro*. The aim of this work was to study whether IL-1 can also affect glucose uptake by immune cells. For this purpose, murine spleen cells were stimulated with lipopolysaccharide (LPS) during 4 or 24 hours and endogenously produced IL-1 was neutralized with IL-1 receptor antagonist (IL-1Ra). Glucose incorporation was evaluated by uptake of the fluorescent glucose analog 2-(N-(7-Nitrobenz-2-oxa-1,3-diazol-4-yl)Amino)-2-Deoxyglucose (2-NBDG) and flow cytometry. The results showed that IL-1Ra decreases 2-NBDG uptake by LPS-stimulated cells to a degree comparable to that observed when glucose transporters are blocked with phloretin. Percentually, the decrease of 2-NBDG uptake in response to IL-1 blockade was larger in LPS-stimulated B cells than in unstimulated B cells after 24 h *in vitro*, suggesting an activation-dependent enhancement of glucose uptake by IL-1. Application of the agonist IL-1β during one hour increased 2-NBDG uptake by B cells, however, only to a comparably small extent, presumably because IL-1 receptors are already almost saturated under the *in vitro* conditions used in these studies. Neither Myeloid differentiation primary response 88 (MyD88), an innate immune signal adapter protein, nor the inward-rectifier potassium channel 6.2 (K_{ir}6.2) seem to play a relevant role in the intracellular signaling pathway involved in the effect of IL-1 on glucose uptake. Pharmacological inhibition of AKT/PKB did not prevent the effect of IL-1 on glucose uptake in B cells, while the results in T cells were not clear. The effect of endogenously produced IL-1 on spleen cell energetic metabolism was also investigated. Using live cell real-time metabolic flux analysis, it was found that blockade of endogenous IL-1 resulted in a reduction of the oxygen consumption rate (OCR) that gradually recovered to the basal value after one hour. The decrease in OCR was of a magnitude comparable to the inhibition of mitochondrial ATP generation elicited

i

by oligomycin. In the initial phase of IL-1Ra inhibition in non-stimulated spleen cells, the reduction of oxidative phosphorylation was paralleled by an increase in the extracellular acidification rate (ECAR), which is considered a marker of lactate production by glycolysis. The increase in ECAR induced by LPS stimulation could not be further augmented after IL-1Ra injection, probably because glycolysis could not be additionally accelerated. After the immediate effects of endogenous IL-1 blockade, which lasted for approximately 2 h, ECAR decreased below control values in both unstimulated and LPS-stimulated cells. The metabolic effects of IL-1 blockade were not MyD88-dependent. The results indicate that endogenously produced IL-1 can increase glucose uptake and energetic metabolism in immune cells and possibly contributes to the relocation of energy to the immune system.

Zusammenfassung

Die Arbeitsgruppe, in der diese Dissertation entstand, hat bereits gezeigt, dass Interleukin-1 (IL-1) eine ausgeprägte, langanhaltende und insulin-unabhängige Hypoglykämie verursacht. Diese IL-1-induzierte Hypoglykämie wird durch Mechanismen erzeugt, welche sowohl auf peripherer, als auch zentraler Ebene wirken. Erst kürzlich haben wir berichtet, dass IL-1 trotz der gleichzeitigen Hypoglykämie *in vivo* die energetische Aktivität im Gehirn steigert und *in vitro* die Glukose-Aufnahme von Neuronen und Astrozyten erhöht. Das Ziel dieser Arbeit ist es zu erforschen, ob IL-1 die Glukose-Aufnahme durch Immunzellen ebenfalls beeinflussen kann. Für diesen Zweck wurden murine Splenozyten mit Lipopolysaccharid (LPS) stimuliert und das während 4 oder 24 Stunden produzierte IL-1 mit IL-1 Rezeptor-Antagonist (IL-1Ra) neutralisiert. Die Glukoseaufnahme wurde mit dem fluoreszierenden Glukose-Analog 2-(N-(7-Nitrobenz-2-oxa-1,3-diazol-4-yl)-Amino)-2-Deoxyglukose (2-NBDG) und Durchflusszytometrie bestimmt. Die Resultate zeigen, dass IL-1Ra die 2-NBDG-Aufnahme in LPS-stimulierten Zellen zu einem Grad verringert, der vergleichbar mit der Blockade von Glukose-Transportern durch Phloretin ist. Prozentual war die Verringerung der 2-NBDG-Aufnahme infolge der IL-1 Blockade

in LPS-stimulierten B-Zellen nach 24 h *in vitro* höher als in nicht stimulierten B-Zellen, was auf eine aktivationsabhängige Zunahme der Glukoseaufnahme durch IL-1 schließen lässt. Der Agonist IL-1β erhöhte die 2-NBDG-Aufnahme in B-Zellen innerhalb einer Stunde. Allerdings war die prozentuale Erhöhung der 2-NBDG-Aufnahme vergleichsweise gering, da die IL-1 Rezeptoren unter den *in vitro* Bedingungen dieser Arbeit vermutlich fast alle bereits durch IL-1 gebunden waren. Weder Myeloid Differentiation Primary Response 88 (MyD88), ein Signal-Adapter Protein des angeborenen Immunsystems, noch der einwärts gleichrichtende Kaliumkanal 6.2 ($K_{ir}6.2$) scheinen eine relevante Rolle im Signalweg zu haben, der die Glukoseaufnahme durch IL-1 beeinflusst. Eine pharmakologische Inhibition von AKT/PKB konnte die Effekte von IL-1 auf die Glukoseaufnahme von B-Zellen nicht verhindern, während die Ergebnisse in T-Zellen nicht eindeutig waren. Die Effekte von endogen produziertem IL-1 auf den energetischen Metabolismus von Splenozyten wurden ebenfalls untersucht. Durch die Verwendung von *live cell real-time metabolic flux* Analysen wurde beobachtet, dass die Blockade von endogenem IL-1 in einer verringerten *oxygen consumption rate* (OCR) resultierte, die sich sukzessiv innerhalb einer Stunde wieder auf den Ausgangswert normalisierte. Die Verringerung der OCR war von vergleichbarem Ausmaß wie die Inhibition der mitochondriellen ATP-Erzeugung durch Oligomycin. In der initialen Phase der IL-1Ra-Inhibition in nicht stimulierten Splenozyten wurde die Verringerung der oxidativen Phosphorylierung von einem Anstieg der *extracellular acidification rate* (ECAR) begleitet, welche ein Marker für die Laktatproduktion durch Glykolyse ist. In LPS-stimulierten Splenozyten wurde die ECAR nach IL-1Ra-Injektion nicht weiter erhöht, da die Glykolyse wahrscheinlich nicht weiter beschleunigt werden kann. Die metabolischen Effekte der IL-1-Blockade sind nicht MyD88-abhängig. Die Resultate deuten darauf hin, dass endogen produziertes IL-1 die Glukoseaufnahme und den energetischen Metabolismus von Immunzellen erhöhen kann und möglicherweise damit zur Relokation von Energie zum Immunsystem beiträgt.

Contents

1 Introduction

Glucose is one of the principal sources of energy in the body. Thus, glucose homeostasis is paramount for survival and tightly regulated in order to assure adequate supply to all cells that require glucose. The regulation of glucose homeostasis is a highly dynamic process, which has to respond to dietary glucose delivery, changes in the rate of gluconeogenesis, and changes in glucose consumption of the organism. Besides the control of food uptake, glucose transport into cells or its substitution by gluconeogenesis are the main mechanisms that contribute to achieve a stable level of glucose in blood. A well-known physiological mechanism to control glucose levels is to favor its uptake by tissues that are sensitive to insulin, such as fat and muscle cells. However, this hormone is not the only endogenous molecule that can facilitate distribution of glucose towards a specific set of cells. There is growing evidence that interleukin-1 (IL-1) can also profoundly alter glucose homeostasis and stimulate glucose transport into specific cells under certain conditions [Besedovsky and del Rey, 2010, Besedovsky and del Rey, 2014].

1.1 Interleukin-1 and its family

IL-1 is a potent pro-inflammatory cytokine with a broad spectrum of effects. It is one of the key molecules involved in the activation of the immune response, and its synthesis can be induced by diverse stimuli, such as bacterial products, viruses, mitogens, antigens, sterile insults and other cytokines [Dinarello, 2011, Lukens et al., 2012]. Further, Interleukin-1β (IL-1β) has the remarkable capacity to induce its own production. Because of these features and its very high potency, few nanograms per Kg body weight of this cytokine are sufficient to elicit host defense mechanisms, such as fever and inflammation [Dinarello, 2015, Dinarello et al., 1986]. IL-1 has multiple immunological functions. It is a T cell growth factor [Mier and Gallo, 1980], activates T cells by stimulating IL-2 production [Smith et al., 1980] and IL-2 receptor expression [Kaye et al., 1984] and also plays a crucial role in the induction of IL-17-producing T cells [Sutton et al., 2006]. Fur-

thermore, IL-1 induces B cell proliferation and antibody production [Falkoff et al., 1983]. Besides its immunological functions, it also participates in other important biological processes, such as the maintenance of long-term potentiation in the hippocampus [Coogan et al., 1999, Schneider et al., 1998, Spulber et al., 2009], learning and memory consolidation [Besedovsky and del Rey, 2011, Avital et al., 2003, Ben Menachem-Zidon et al., 2011], slow-wave sleep, appetite suppression and neuroendocrine responses (reviewed in [Besedovsky and del Rey, 2011]).

Today, eleven IL-1 family members have been identified, with various physiological roles in the immune system. These proteins are encoded by 11 distinct genes and termed IL-1F1 to IL-1F11 [Sims and Smith, 2010, Weber et al., 2010]. Most relevant for this work are interleukin-1α (IL-1α), IL-1β and the natural receptor antagonist (IL-1Ra), which bind to the functional IL-1 receptor 1 (IL-1R1) and the decoy receptor IL-1 receptor 2 (IL-1R2).

1.1.1 The agonists

The molecule termed IL-1 later, has originally been described in the 1940s as an endogenous pyrogen present in granulocytic exudate fluid, but it was a long time solely characterized by its pro-inflammatory and pyrogenic effects, ([Beeson, 1948] reviewed in [Dinarello, 1991]). Its molecular characterization was not possible until the 1970s, when it was purified to homogeneity. With the emergence of genetic methods, the complementary DNAs for two IL-1 isoforms were cloned in 1984. These isoforms were termed IL-1α and IL-1β [Dinarello, 1991]. Although IL-1α and IL-1β share only 24 % amino acid sequence homology, they largely share biological functions [Dinarello, 2018, Dinarello, 1996, Pizarro and Cominelli, 2007]. The two IL-1 genes are expressed as 31 kDa precursor proteins that are subsequently cleaved to 17 kDa mature proteins. The synthesis takes place in the cytoplasm and no leader sequences are present for further processing in the endoplasmatic reticulum or Golgi apparatus (reviewed in [Dinarello, 1991]). However, the N-terminal amino acid sequence of pro-IL-1α contains a nuclear

localization signal. In addition to its ability to bind and activate its receptor, the intracellular precursor of IL-1α is able to enter the nucleus, where it induces the transcription of pro-inflammatory genes. The pro-IL-1β protein, in contrast, does not contain a nuclear localization signal and this precursor is not able to bind to the IL-1 receptor [Werman et al., 2004].

Both pro-IL-1α and pro-IL-1β are cleaved to the mature molecules by membrane associated proteases before they are released from the cytoplasm. Pro-IL-1α is processed by calpain, a calcium-activated cysteine protease [Watanabe and Kobayashi, 1994], and pro-IL-1β is cleaved by the specific IL-1β-converting enzyme (ICE or caspase 1) [Arend, 2002]. The activity of caspase 1 is regulated by the NACHT, LRR and PYD domains containing protein (NALP3) inflammasome, which senses signals such as bacterial toxins, viral products, and crystallized endogenous molecules. Inflammasomes are multiprotein complexes that control the inflammatory response and coordinate antimicrobial host defenses [Broz and Dixit, 2016]. In addition to the "classical" intracellular processing of IL-1α and IL-1β, an inflammasome-independent extracellular cleavage of the pro-peptides to their mature forms by serine proteases was described recently [Netea et al., 2015].

The most important immunological source of IL-1α and IL-1β are macrophages and monocytes, the sentinel cells of the innate immune system. However, IL-1α and IL-1β can be expressed by many other cell types in the periphery and the brain, amongst them epithelial cells, endothelial cells, fibroblasts, and neural cells [Weber et al., 2010, Bandman et al., 2002, Holzberg et al., 2003, del Rey et al., 2016].

Since the discovery and characterization of the two agonists IL-1α and IL-1β, the IL-1 family grew considerably. In terms of significance in physiology and disease however, the importance of the first three family members IL-1α, IL-1β and their receptor antagonist IL-1Ra are the best studied.

1.1.2 The functional receptor: IL-1 receptor type 1

The IL-1R1 is expressed in all cell types in the human body and its expression level is relatively stable. The largest changes in IL-1R1 expression that have been reported so far are two to threefold increases, which occur during disease [Dinarello, 2005]. This ubiquity and stability of expression is highlighting the importance of the IL-1 system. The number of IL-1R1 receptors expressed at the cell surface is very low, with only about 100 receptors per cell. Nevertheless, the IL-1 receptor system is very sensitive and there is evidence that occupancy of only 2-3 % of the receptors is sufficient to elicit a biologically relevant response. For example, only 10 pg/ml of IL-1 stimulates glucose uptake by astrocytes more than 300-fold with saturation of the effect at 25 pg/ml [Ye et al., 1992, Matsushima et al., 1986].

IL-1 receptors are part of the toll-like receptor (TLR) superfamily, which share the toll-IL-1 receptor (TIR) domain. This TIR domain is located at the intracellular part of the receptor and allows recruitment of adapter proteins from the cytosol and signal transduction of IL-1R1 (Figure 1).

1.1.3 Intracellular effects of IL-1 signaling

At present, two major signaling pathways downstream of the IL-1R1 have been described (Figure 1): the well-recognized classical myeloid differentiation primary response 88 (MyD88) dependent pathway and the less known phosphoinositide 3-kinase (PI3K) pathway. It has to be remarked that signaling via almost all TLRs is mediated by MyD88 as well, and likely also by PI3K via the phosphoinositide 3-kinase adapter protein (BCAP) [Troutman et al., 2012]. Signaling via both MyD88 and PI3K is complicated because it is widely ramified and involves many proteins, interactions, feedback loops and alternative inputs derived from the occupancy of other receptors.

The intracellular cascade triggered by stimulation of the IL-1R1 is described in somewhat more detail because many of the downstream events that occur also form part of mechanisms involved in glucose uptake and metabolism.
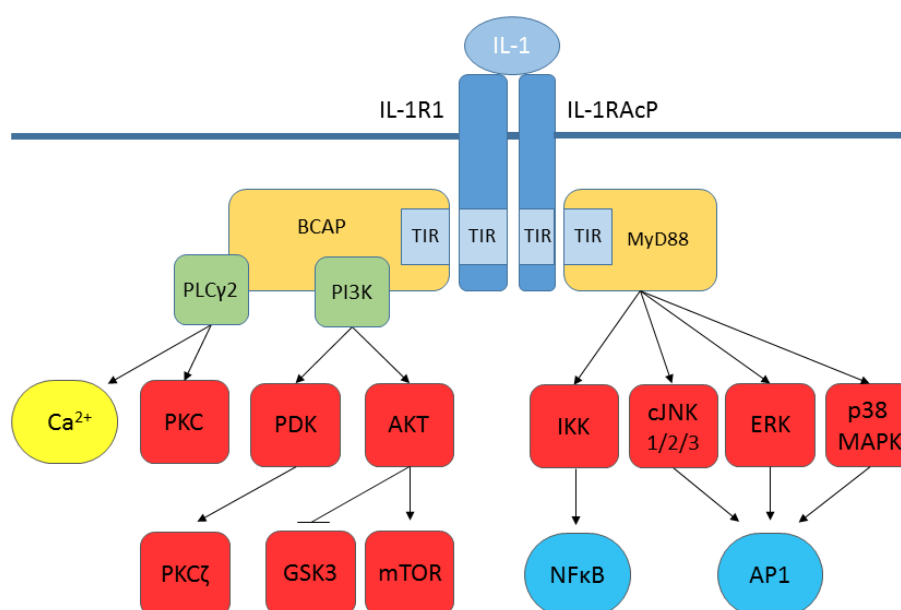
Figure 1. The intracellular signaling cascade of IL-1. The IL-1R1/IL-1RAcP complex associates with the adapter proteins BCAP and MyD88, and activates several downstream signaling cascades. BCAP connects IL-1R1 to PI3K and phospholipase Cγ2 (PLCγ2) signaling. PI3K activates AKT and phosphoinoisitide dependent kinase 1 (PDK1) by phosphatidylinositol (3,4,5)-trisphosphate (PIP$_3$) production. The master kinase AKT impacts many cellular functions, of which mechanistic target of rapamycin (mTOR) activation and glycogen synthase kinase 3 beta (GSK3B) inhibition by AKT are best described. PDK1 supports AKT activation and also activates the atypical protein kinase Cζ (PKCζ). PLCγ2 activity provides diacyl glycerol (DAG) for conventional and novel PKCs and also produces the second messenger inositol 1,4,5-trisphosphate (IP$_3$), which triggers calcium release from the endoplasmatic reticulum. The MyD88-mediated signaling cascade contains more than 30 proteins of which the most important are depicted. The MyD88-activated inhibitor of kappa B kinase (IKK) controls nuclear factor kappa-light-chain-enhancer of activated B cells (NFκB), a transcription factor which initiates transcription of pro-inflammatory genes, and notably also of IL-1β itself. Furthermore the c-Jun N-terminal kinases 1/2/3 (cJNK), extracellular-signal regulated kinase (ERK) and p38 mitogen-activated protein kinase (p38 MAPK) activate the transcription factor activator protein 1 (AP1), which is also responsible for the transcription of pro-inflammatory genes.

After binding of IL-1α or IL-1β to the IL-1R1, a conformational change occurs and the complex is able to associate with IL-1 receptor accessory protein (IL-1RAcP). Dimerization of the two TIR domains of IL-1R1 and IL-1RAcP allows binding of the

adapter protein MyD88. Subsequently, IL-1 receptor-associated kinase 4 (IRAK4) is able to attach to MyD88 and together with IL-1, IL-1RI, and IL-1RAcP a stable signaling module is formed. The MyD88-dependent pathway is complex and contains more than 30 proteins. The most important are the kinases IκB kinase (IKK), c-Jun N-terminal kinases (cJNK) 1/2/3 and p38 mitogen-activated protein kinase (p38 MAPK), which activate the transcription factors nuclear factor kappa-light-chain-enhancer of activated B cells (NFκB) and activator protein 1 (AP1). NFκB and AP1 then initiate the transcription of pro-inflammatory genes [Weber et al., 2010]. However, it is possible that the multiple kinases involved also influence relevant lymphocyte functions other than gene transcription. For example, it is known that the ERK and p38 MAPK-mediated pathways enhance glucose uptake by T cells in response to CD3/CD28 stimulation [Marko et al., 2010].

IL-1R1-mediated activation of PI3K occurs over the TIR domain-containing protein BCAP [Deason et al., 2018]. The most prominent target for PI3K-generated phosphatidylinositol in lymphocytes is AKT, a central regulator of metabolism (Section 1.4). AKT also connects the IL-1R1 signaling to energy homeostasis via mechanistic target of rapamycin (mTOR) kinases and to cell survival via the forkhead box (FOX) transcription factor [Laplante and Sabatini, 2012, Brunet et al., 1999]. PI3K/AKT activation results in elevated IL-1R1 expression and in a glucose transporter 1 (GLUT1) dependent increase of glucose uptake by T cells [Teshima et al., 2004, Yoshida et al., 2008, Frauwirth et al., 2002, Jacobs et al., 2008].

The adapter protein BCAP connects IL-1R1 also to PLCγ2/PKC-signaling. Direct phosphorylation of GLUT1 by PKC increases glucose transport [Lee et al., 2015] and in chondrocytes PKC enhances glucose uptake in response to IL-1 [Shikhman et al., 2004]. Notably, the positive feedback loop of IL-1-induced IL-1 transcription amplifies the IL-1 response in an autocrine/paracrine manner [Dinarello et al., 1987].

1.1.4 Decoy receptors, signal inhibiting proteins and the IL-1 receptor antagonist

IL-1 signaling is not only regulated by the amount of agonist available and the surface expression of IL-1R1. There are several proteins that negatively regulate IL-1 signaling at different levels.

Before IL-1β in the circulation reaches the cell surface, it can be bound and neutralized by the soluble forms of IL-1R1, IL-1R2, and IL-1RAcP released from the cell membrane by enzymatic cleavage. At the cell membrane, IL-1 has to compete with its antagonist IL-1Ra for receptor binding sites of the functional IL-1R1 and the decoy receptor IL-1R2 neutralizes IL-1. In addition, there are signal inhibiting co-receptors for the functional IL-1R1, namely the single Ig IL-1-related receptor (SIGIRR) [Wald et al., 2003] and the interleukin-1 receptor accessory protein b (IL-1RAcPb) described in neurons [Smith et al., 2009]. The decoy receptor and the co-receptors that inhibit IL-1R1 function are characterized by a missing or non-functional TIR domain that does not allow MyD88 binding (Figure 2), and therefore no MyD88-mediated signal is transduced. The intracellular signal cascade downstream the IL-1R1 is also negatively regulated. The short form of MyD88 (MyD88S) and the adapter protein IRAK-3 inhibit signaling [Kobayashi et al., 2002, Weber et al., 2010, Dinarello, 2011]. The adapter toll-interacting protein (TOLLIP) eventually marks the functional complex of IL-1R1 and its associated adapter proteins for internalization to endosomes [Brissoni et al., 2006].

1.1.5 Splice variants of IL-1 receptor 1

It has been reported that there are 7 promoters for the IL-1R1 [Li et al., 2010] that produce different splice variants, which are in part truncated versions of the original receptor [Qian et al., 2012]. One of these receptors does not induce MyD88 activity and signals exclusively via the AKT pathway. Further, this receptor lacks the binding site for IL-1Ra and is therefore unlikely to bind the receptor antagonist. Although it has been reported that this splice variant only functions with IL-1RAcPb in neurons, the protein itself is also

expressed in non-neuronal tissues. Unfortunately, as it is difficult to distinguish between the splice variants because of the structural homology, at present there is not a full picture of the expression patterns of the splice variants. Also, their properties regarding the mechanism of signaling and their affinities to IL-1 and IL-1Ra remain unclear.

1.1.6 The effects of IL-1β on glucose homeostasis

IL-1β was the first cytokine shown to stimulate the hypothalamus-pituitary-adrenal axis and to increase glucocorticoid blood levels [Besedovsky et al., 1986]. Contrary to the expectation, however, it was found that, in parallel to this hormonal change, IL-1β induces a marked and long lasting hypoglycemia [del Rey and Besedovsky, 1987]. Using models of insulin-resistant diabetic mice and rats, it was demonstrated that the hypoglycemic effect of IL-1β is independent of insulin [del Rey and Besedovsky, 1989]. It was further shown that IL-1β-induced hypoglycemia is caused by both peripheral and central effects of the cytokine [del Rey et al., 1998, Besedovsky and del Rey, 2010]. When IL-1Ra is injected intraperitoneal (i.p.), it significantly reduces LPS-induced hypoglycemia. Because IL-1Ra does not cross the blood-brain barrier, the results show that the effect is at least partially exerted at peripheral levels [Besedovsky and del Rey, 2010]. Blockade of IL-1β receptors in the brain results in marked attenuation of the hypoglycemia induced by peripheral administration of the cytokine and demonstrates central nervous system involvement [del Rey et al., 2006].

Mice injected with IL-1β i.p. that are simultaneously challenged with a glucose load not only return quicker to normal basal blood glucose levels, but are maintained at the hypoglycemic level induced by the cytokine during several hours. This effect can also be abrogated by blocking IL-1β receptors in the brain [del Rey et al., 2006].

These findings led to the proposal that IL-1β can change the set-point of glucose homeostasis at central levels [del Rey et al., 2006]. Remarkably, the early phase of IL-1β-induced hypoglycemia develops against increased levels of glucocorticoids, catecholamines and glucagon.
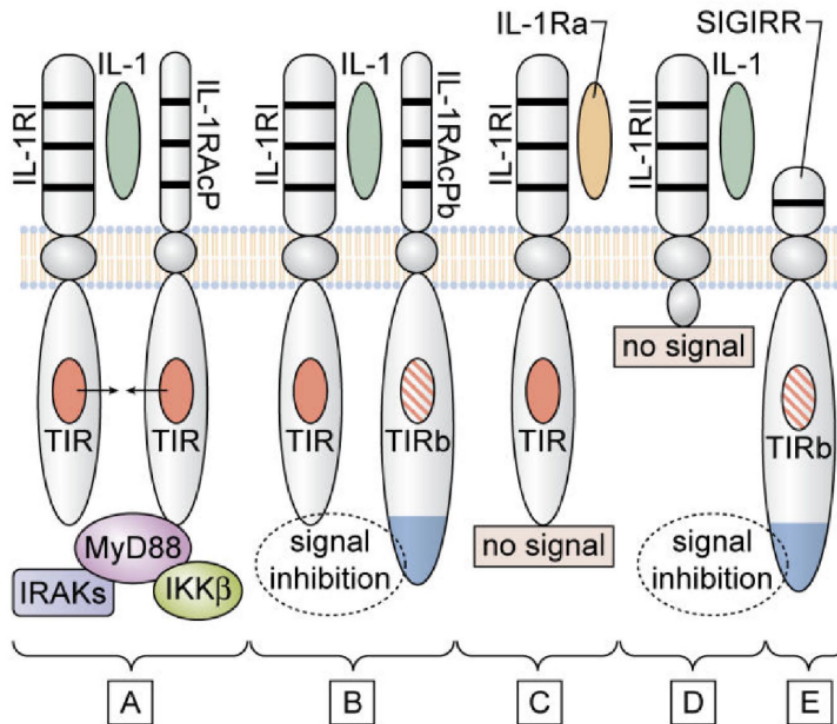
Figure 2. Signaling and Signal Inhibition of the IL-1R1. Adapted from 'Interleukin-1 in the pathogenesis and treatment of inflammatory diseases' [Dinarello, 2011]. Reprinted with permission.

A) IL-1R1 can bind the IL-1α precursor and both mature forms of IL-1α and IL-1β. After ligand binding, the heterodimeric IL-1R1/IL-1RAcP receptor complex is formed and the proximity of the two TIR domains allows MyD88 recruitment. Subsequently, the IL-1R -associated kinases (IRAKs) are phosphorylated and inhibit NFκB kinase β, resulting in NFκB activation and gene transcription.

B) The IL-1RAcP variant IL-1RAcPb is expressed in the brain and spinal cord. The heterodimeric receptor complex with IL-1α, IL-1β and IL-1R1 can be formed, but the complex fails to recruit MyD88, and thus there is no MyD88 signal transduction. The failure to recruit MyD88 may be caused by IL-1RAcPbs altered TIR domain (indicated as TIRb).

C) IL-1Ra binds to IL-1RI but there is no signal because IL-1Ra does not allow the formation of the receptor complex with IL-1RAcP.

D) IL-1 binds to IL-1RII but no signal is triggered because of the missing cytoplasmic segment and the consequential lack of a TIR domain.

E) The TIR domain of SIGIRR is non-functional (indicated as TIRb). SIGIRR is able to associate with IL-1-bound IL-1R1, but inhibits IL-1 signaling.

This endocrine counter-regulation against hypoglycemia is, however, no longer present at later phases of IL-1β-induced hypoglycemia [del Rey and Besedovsky, 1987]. Therefore, it has been proposed that IL-1β blocks the physiological counter-regulatory response to hypoglycemia. However, the mechanism responsible for the observed long-lasting decrease in glucose blood levels is not yet known [del Rey et al., 2006]. A component that might contribute to altered glucose distribution in response to IL-1β could be that IL-1β stimulates glucose uptake by cells in the periphery, such as immune cells, in addition to its central effects [Besedovsky and del Rey, 2014].

1.2 Lymphocyte function is coupled to their metabolism

Over the last years, it has been recognized that lymphocyte function is closely linked to metabolism [Fox et al., 2005, MacIver et al., 2013, Donnelly and Finlay, 2015]. Quiescent lymphocytes depend predominantly on adenosine triphosphate (ATP) generating metabolic processes for basal energy generation and replacement biosynthesis, whereas clonal expansion of proliferating lymphocytes requires a high metabolic flux to promote cell growth. Therefore, the key aspect of metabolism changes from a survival sustaining production of ATP to the synthesis of new biomass [MacIver et al., 2013, Caro-Maldonado et al., 2014]. Since cells undergo substantial metabolic changes during activation, especially concerning glycolysis and oxidative phosphorylation, this process is frequently termed metabolic reprogramming. The rate of oxidative phosphorylation is mainly increased in order to supply the cell with energy in form of ATP. Aerobic glycolysis, in contrast, although it also generates ATP, primarily provides the precursors that are essential for the synthesis of nucleotides, amino acids and lipids, necessary for cell growth and proliferation [Donnelly and Finlay, 2015].

A successful transition to the activated state in T and B cells is only possible if they are able to fulfill the required biosynthetic and bioenergetic demands. Co-stimulatory factors contribute decisively to the provision of energy for proliferation and effector functions by allowing the uptake and utilization of extracellular nutrients [Fox et al., 2005].

It is well described that co-stimulation via CD28 serves as a signal that substantially enhances glucose metabolism in T cells [Jacobs et al., 2008]. A comparable receptor that enhances signaling pathways associated with glucose metabolism in B cells is CD40 [Elgueta et al., 2009, Boothby and Rickert, 2017]. It has been shown that both T and B cells cannot be activated if they fail to upregulate their glucose metabolism [Jacobs et al., 2008, Caro-Maldonado et al., 2014].

Successful lymphocyte activation requires feedback from the activated metabolism in form of reactive oxygen species (ROS) from the mitochondria. T cells lacking ROS-dependent signaling events are not able to undergo antigen-specific expansion [Sena et al., 2013]. Equally, suppression of ROS generation in B cells results in impaired *in vitro* BCR-induced activation and proliferation [Wheeler and Defranco, 2012].

In macrophages, it has been shown that a raise in mitochondrial ROS in response to bacterial products, and danger signals such as extracellular ATP, increase caspase-1 activation and IL-1β production, which in turn can be expected to affect metabolism [Pétrilli et al., 2007, Martinon et al., 2004, Mariathasan et al., 2004, Zhou et al., 2010]. This mechanism could also be important in lymphocytes.

Interestingly, the metabolic reprogramming of lymphocytes is reversible. After a successful immune response, the metabolic phenotype of activated effector T and B cells, which is characterized by glycolysis and lactate production, can return to a quiescent, oxidative phenotype again [Pearce et al., 2009, van der Windt et al., 2012, Boothby and Rickert, 2017].

For our experiments on IL-1-induced glucose uptake, it is important to mention that there are co-stimulatory signals that raise glucose uptake and metabolism, and that IL-1 is a co-stimulatory factor for lymphocytes [Huber et al., 1998, Khoruts et al., 2004, Ben-Sasson et al., 2009, Ben-Sasson et al., 2013]. In addition, IL-1 has been shown to increase glucose uptake by several cell types [Bird et al., 1990, Garcia-Welsh et al., 1990, Shikhman et al., 2004, del Rey et al., 2016, Tsuchiya et al., 2018]. On this basis, we hypothesize that IL-1 is able to enhance glucose uptake and metabolism in lymphocytes.

1.3 Metabolic differences between T and B lymphocytes

There have been substantial efforts to understand metabolism and especially the codependency of metabolism and activation in lymphocytes. However, the interest was particularly focused on T cells. The knowledge of B cell metabolism was much more limited and poorly understood [Caro-Maldonado et al., 2014]. It has become evident that T and B cells react with distinct metabolic programs to fulfill the substantially increased bioenergetic and biosynthetic demands for a successful activation. Further there is a remarkable metabolic heterogeneity in the different lymphocyte subsets [Michalek et al., 2011, MacIver et al., 2013].

In T cells, metabolic reprogramming is induced by the transcription factor c-Myc, which regulates glycolysis, glutaminolysis, cell growth, and the PI3K/AKT pathway [Wang et al., 2011, Frauwirth et al., 2002]. Glucose uptake and metabolism are increased in T cells after activation, and glycolysis becomes the predominant form of energy generation, resembling a cancer-like phenotype. Simultaneously, the oxidation of fatty acids is decreased and the oxidation of glutamine is increased [Wang and Green, 2012, Vander Heiden et al., 2009]. B cells, however, are metabolically distinct from T cells. B cells also increase glycolysis in response to activation, although they do not switch to a predominant utilization of glucose via glycolysis but instead increase metabolism in a more balanced fashion [Caro-Maldonado et al., 2014].

1.4 AKT signaling and its role in metabolism

AKT, also known as protein kinase B (PKB), is a serine/threonine kinase important for signal integration downstream of antigen receptors, cytokines, growth factors, and other stimuli. AKT signaling influences essential cellular functions such as survival, growth, proliferation, cellular metabolism, and glucose uptake. However, it is increasingly accepted that most AKT substrates are not exclusively controlled by AKT, allowing a context-dependent redundant regulation of cellular functions. Together with feedback mecha-

nisms, threshold effects, and crosstalk with other signaling pathways, the regulation of many AKT-targets does not work in a linear nor in a binary on-off fashion (reviewed in [Manning and Toker, 2017]).

The canonical pathway leading to AKT activation is initiated by ligand-bound receptors that recruit PI3K to the plasma membrane. Activated PI3K subsequently converts phosphatidylinositol 4,5-biphosphate (PIP_2) to phosphatidylinositol (3,4,5)-triphosphate (PIP_3), and thus provides a membrane anchor to which AKT can attach with its pleckstrin homology (PH) domain. AKT binding of PIP_3 has two effects: AKT is kept localized at the cell membrane in proximity to its substrates, and also induces a conformational change that allows its phosphorylation by PDK1, enabling the catalytic activity of AKT [Calleja et al., 2007]. Although AKT is generally able to phosphorylate its substrate after activation by PDK1, another phosphorylation by mTOR complex 2 is required to exert maximal catalytic activity [Sarbassov et al., 2005].

PI3K-AKT signaling is only transient in nature and needs constant activation to be sustained. The protein phosphatase and tensin homolog (PTEN), limits AKT signaling by degrading PIP_3, and therefore prevents membrane recruitment. Also, the time that activated AKT remains at the cell membrane is relatively short [Calleja et al., 2007]. In recent years, evidence accumulated that AKT reverses its conformational change upon disengagement of PIP_3 and is rapidly dephosphorylated by phosphatases, thus returning to an inactive state [Ebner et al., 2017, Lučić et al., 2018]. The activity of AKT is thereby restricted to membranes with active PI3K.

There are three isoforms of AKT, but most of the substrates are phosphorylated by all three isoforms. Preferences in substrate specificity seem to be achieved by spatial separation, and different thresholds of AKT activity. While some substrates are phosphorylated at a low levels of AKT activity, others require higher levels of AKT activity in order to be sufficiently phosphorylated [Manning and Toker, 2017].

Many AKT substrates, such as small G proteins responsible for vesicle trafficking, exert a direct effect on cellular functions, while others serve as signaling nodes, which integrate several inputs and distribute their signal to multiple outputs. The most important

signaling nodes downstream of AKT concerning energy homeostasis and metabolism are mTOR, GSK3, and forkhead box O (FoxO) transcription factors [Manning and Toker, 2017]. While mTOR is activated, GSK3 and FoxO are suppressed by PI3K-AKT signaling.

The mTOR complex adjusts upstream signals to the availability of nutrients, and stimulates biosynthetic processes underlying cell growth [Saxton and Sabatini, 2017]. GSK3 regulates cellular metabolism by directly phosphorylating metabolic enzymes, and also indirectly by controlling their abundance via transcription factors such as c-Myc. FoxO controlled genes regulate key aspects of cell faith, such as induction of apoptosis, cell cycle arrest, growth inhibition, and also catabolism (reviewed in [Manning and Toker, 2017]).

GSK3 and mTOR activity are also particularly important in the regulation of glucose uptake. AKT enhances GLUT1 surface expression by stimulating mTOR and suppressing GSK3 (see Section 1.6). Furthermore, AKT activity results in enhanced GLUT1 transcription. GSK3 [Gregory et al., 2003] and mTOR [Land and Tee, 2007] control GLUT1 expression via the transcription factors c-Myc [Osthus et al., 2000] and hypoxia-inducible factor 1α (HIF-1α) (reviewed in [Ferrer et al., 2014]).

Contributing to the situation-dependent adaption of PI3K-AKT signaling, there is crosstalk with other major signaling pathways. In addition, especially important in the context of glucose uptake and metabolism, many AKT targets are redundantly targeted by ERK, AMP-activated protein kinase (AMPK), and PLCγ-PKC pathways (reviewed in [Manning and Toker, 2017]).

PI3K-AKT signaling is important in T and B cell functions. However, the effects of PI3K-AKT signaling are not the same in different lymphocyte subtypes. Suppression of PI3K can result in diverse dysfunctions, such as attenuated immune response, but also enhanced inflammation, disrupted peripheral tolerance or promoted autoimmunity [So and Fruman, 2012].

1.5 Glucose transporters in lymphocytes

Glucose transporters (GLUTs) are responsible for the most important mechanism by which glucose enters into mammalian cells. They are a family of integral membrane proteins with 14 different members described today [Thorens and Mueckler, 2010]. Although 11 of the 14 known GLUTs are able to transport glucose under experimental conditions, it is likely that glucose is not the primary substrate for many of them. GLUT1-4 are the classical transporters, which primarily transport glucose [Thorens and Mueckler, 2010, Mueckler and Thorens, 2013]. GLUTs are uniport transporters with a single glucose binding site, and facilitate the transport of glucose driven by the concentration gradient over the membrane. GLUTs have the capacity to influence glucose metabolism by controlling the amount of glucose that enters the cell [Barros et al., 2005]. Thus, their expression and surface translocation are highly regulated for example by cytokines, hormones, growth factors, oxidative stress, and metabolic stress, depending on the cell type [Barros et al., 2009].

Lymphocytes differentially express the glucose transporters GLUT1, GLUT3 and GLUT4, dependent on the method of stimulation [McBrayer et al., 2012, Maratou et al., 2007]. GLUT1 has a high K_m (6.9 mM for 2-deoxyglucose), which results in comparably low affinity for glucose and assures its provision for basal metabolic needs. GLUT3 and GLUT4 have a higher affinity for glucose than GLUT1 (K_m 1.4 mM and 4.6 mM for 2-deoxyglucose, respectively, reviewed in [Simpson et al., 2008]). The lower K_m results in higher transport rates during situations of low substrate availability and allows the cell to efficiently incorporate the sugar in environments with low glucose levels.

Although GLUT3 and GLUT4 are expressed in lymphocytes, it is assumed that they primarily rely on the surface expression of GLUT1 for glucose uptake [Maciver et al., 2008, Macintyre et al., 2014, Liu et al., 2014]. Supporting the pivotal role of GLUT1, and important in the context of this work, it has been shown that GLUT1 is drastically upregulated and GLUT3 is considerably downregulated in splenic B cells after LPS stimulation [Caro-Maldonado et al., 2014]. Thus, it is unlikely that GLUT3 con-

tributes to the upregulation of glucose uptake by LPS-stimulated B-cells. The mechanism of differential expression of GLUT1 and GLUT3 could be related to the activity of GSK3, which inhibits GLUT1 surface expression and supports GLUT3 transcription [Buller et al., 2008, Watanabe et al., 2012]. Thus, the suppression of GSK3 by AKT results in enhanced GLUT1 surface expression and reduced GLUT3 transcription.

Considering the role of GLUTs in the context of IL-1-mediated glucose uptake, the significance of GLUT1 is further highlighted. Although there is no data available for lymphocytes, it was reported that IL-1β enhances GLUT1 mRNA expression in chondrocytes, but not mRNA expression of GLUT3 or GLUT4. It was further shown that IL-1β facilitates the incorporation of GLUT1, but not GLUT3, into the cell membrane [Shikhman et al., 2001, Shikhman et al., 2004].

GLUT1 synthesis in lymphocytes is induced by HIF-1α and Myc at the transcriptional level [Osthus et al., 2000, Ferrer et al., 2014]). However, it has to be considered that the intracellular GLUT concentrations have no relevance for GLUT-mediated glucose uptake *per se*. GLUTs only affect glucose uptake if they are incorporated into the cell membrane.

Besides the level of surface expression of the transporter, glucose uptake is also affected by the transport kinetic of GLUT1, which is regulated by glycosylation and phosphorylation. Glycosylation is reported to decrease GLUT1 K_M 2.5-fold [Asano et al., 1991, Ahmed and Berridge, 1999]. GLUT1 phosphorylation by PKC increases glucose transport velocity about twofold [Lee et al., 2015]. GLUT3- and GLUT4-mediated glucose uptake, in contrast, seem to be primarily regulated by the surface expression of the transporters.

In addition to GLUTs, there are also sodium-glucose-linked transporters (SGLTs) in mammalian cells, which transport glucose by using the energy of the sodium gradient across the cell membrane. However, much less is known about SGLT expression and relevance in immune cells. There is evidence of SGLT1 expression in cytotoxic T cells [Bhavsar et al., 2016] but it is controlled by JAK3, which is not involved in IL-1 signaling (reviewed in [Pei et al., 2018]).

1.6 Mechanisms of GLUT surface expression

Although the surface expression of GLUTs is a key factor for cellular energy homeostasis in lymphocytes, the underlying mechanisms are not well explored. Much of the knowledge about the regulation of GLUT-trafficking was obtained in studies of insulin-sensitive GLUT4 in adipocytes and muscle cells. Interestingly, there are many parallels in the molecular mechanisms between regulation of GLUT4 in insulin-sensitive cells and GLUT1 in lymphocytes.

The amount of GLUT1 in the cell membrane is a steady state, which is determined by the rate of GLUT1-vesicle delivery to the membrane and GLUT1 internalization. The processes that are involved are the initial surface localization, internalization, recycling, and degradation of the transporter (Figure 3).

For surface localization, freshly produced GLUT1 vesicles are secreted from the Golgi apparatus and transported to the cell membrane. Ras-associated binding (Rab) proteins, which are necessary for membrane fusion are, however, blocked by the GTPase-activating proteins (GAP) TBC1 domain family member 1 (TBC1D1) or TBC1 domain family member 4 (TBC1D4). TBC1D4 is frequently also termed AKT substrate of 160 kDa (AS160). Upon phosphorylation by AKT or AMPK, TBC1D1/4 is transferred to a 14-3-3 protein and the GLUT1-containing vesicles are able to fuse with the cell membrane [Chen et al., 2008, Treebak et al., 2010].

Internalization of GLUT1 is induced by binding of thioredoxin-interacting protein (TXNIP). The GLUT1-TXNIP-complex is subsequently internalized through clathrin-coated pits and results in the formation of GLUT1 vesicles. AKT and AMPK control the internalization of GLUT1 by phosphorylation of TXNIP, which is inactive in its phosphorylated form [Waldhart et al., 2017, Wu et al., 2013]. Once GLUT1 is internalized, there are two possibilities for its further processing. Either it is recycled and transferred back to the cell surface, or it is degraded.

The recycling process of GLUT1 vesicles is controlled by mTOR [Buller et al., 2008]. The mTOR complex integrates signals from upstream pathways, such as cytokines

and growth factors depending on cellular amino acid, oxygen and energy levels. The most prominent inputs of intracellular signaling to mTor are AKT, AMPK, GSK3 and MAPKs [Saxton and Sabatini, 2017]. Notably, all of them are activated or suppressed by IL-1 signaling (see Section 1.1.3). The degradation of GLUT1 is initiated by the ubiquitin conjugating enzyme 9 (Ubc9). It transfers sentrin, a small ubiquitin-like protein also known as SUMO1 to GLUT1. Sentrin then directs GLUT1 trafficking to lysosomes [Giorgino et al., 2000, Wieman et al., 2009].
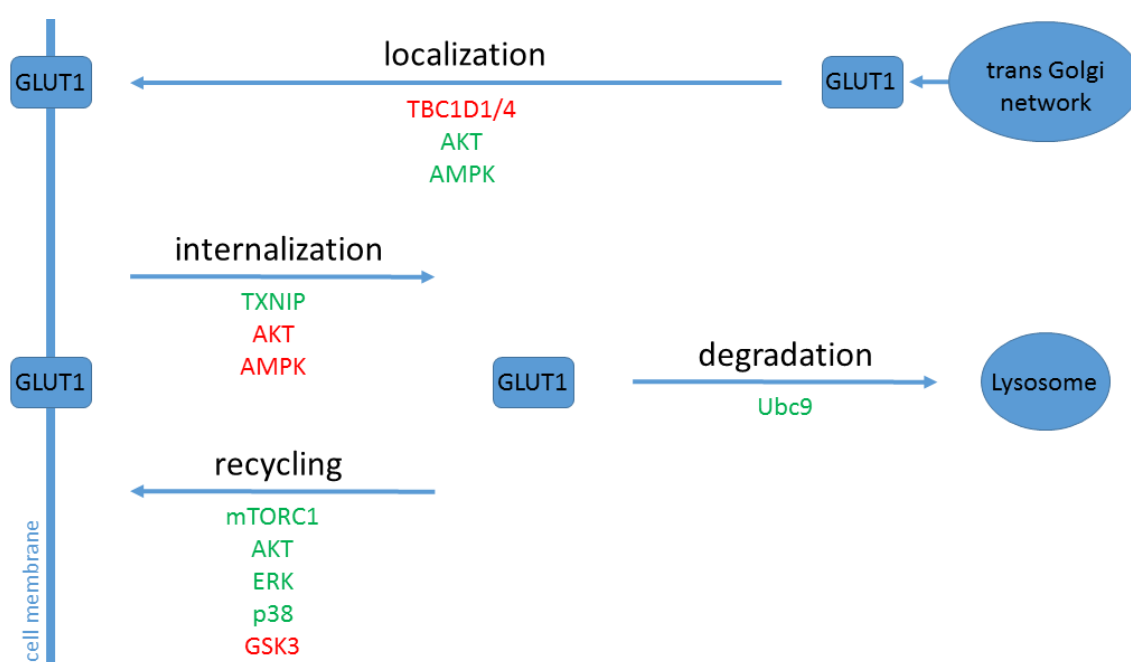
Figure 3. Regulatory mechanisms of GLUT1 surface expression.

Localization: GLUT1 vesicles are budding from the trans-Golgi network and are transported along microtubuli to the cortical actin filaments. Fusion with the cell membrane is prevented until TBC1D1/4 is inactivated by AKT or AMPK [Chen et al., 2008, Treebak et al., 2010].

Internalization: If TXNIP is not kept phosphorylated by AKT and AMPK, it associates with GLUT1 and induces internalization through clathrin-coated-pits [Waldhart et al., 2017, Wu et al., 2013].

Recycling: The internalized GLUT1 protein can be recycled back to the cell membrane. This process is controlled by mTOR, which in turn is activated by signals from AKT, AMPK, ERK, p38 and inhibited by GSK3 [Buller et al., 2008, Saxton and Sabatini, 2017].

Degradation: Alternatively to recycling, internalized GLUT1 can also be sumoylated by Ubc9, thus inducing transport to lysosomes and degradation [Giorgino et al., 2000, Wieman et al., 2009].

1.7 Putative key-molecules of IL-1-mediated glucose uptake

AKT, MyD88, and the inward-rectifier potassium channel 6.2 ($K_{ir}6.2$) are putative key-molecules that could be involved in IL-1-mediated glucose uptake.

AKT

AKT, which has been described in Section 1.4, integrates signals from the IL-1R1 and other TLRs [Troutman et al., 2012], and it is involved in the regulation of GLUT1 localization in lymphocytes [Wofford et al., 2008]. Therefore, it is possible that AKT transduces IL-1β-mediated effects on glucose uptake.

MyD88

As described in chapter 1.1.3, MyD88 is an essential adapter protein for IL-1R and TLR signaling. Without functional MyD88, IL-1β cannot activate its transcription factors. It has been shown, for example in human fibroblasts lacking functional MyD88, that IL-1β is not able to induce any transcription compared to 1451 transcripts induced in wildtype (WT) cells [von Bernuth et al., 2008]. Concerning glucose regulation, it has been shown that MyD88 is necessary for the development of IL-1β-induced hypoglycemia. In contrast to the WT animals, administration of IL-1β to MyD88 knockout (KO) mice does not affect glucose blood levels, neither when the cytokine is injected i.p. nor intracerebroventricular [del Rey et al., 2016].

$K_{ir}6.2$

The open probability of $K_{ir}6.2$ is influenced by the ATP/ADP ratio and thus connects the membrane potential to the metabolic condition of the cell. If the cell is adequately supplied with nutrients, the ATP/ADP ratio is high and the channels are closed, allowing membrane depolarization. If nutrients are scarce, the ATP/ADP ratio becomes low and the channels open, hyperpolarizing the membrane. This mechanism is utilized for example by insulin-secreting β-cells in the pancreas to couple insulin exocytosis to glucose blood

levels. Also, the firing behavior of hypothalamic glucose-excited neurons is regulated by $K_{ir}6.2$. These neurons act as a brain-sensor of blood glucose and their signals are integrated in a network that monitors the energy status of the organism. This hypothalamic network is therefore able to sense the need to raise blood glucose levels and can induce central counter-regulatory responses to hypoglycemia, such as stimulation of gluconeogenesis or food seeking behavior [Miki et al., 2001, Sherwin, 2008]. In addition to these specialized sensory cells, $K_{ir}6.2$ is expressed in a broad spectrum of tissues, where it is thought to play an important protective role in response to hypoglycemia, ischemia, and hypoxia [Seino and Miki, 2003]. Interestingly, $K_{ir}6.2$ has been shown to be involved in the regulation of glucose uptake by skeletal muscles cells [Miki and Seino, 2005] and is also expressed in lymphocytes [Papatheodorou et al., 2018]. We have previously shown that the hypoglycemia induced by IL-1β *in vivo* is significantly more pronounced in $K_{ir}6.2$ KO mice than in the WT controls [del Rey et al., 2016], suggesting that $K_{ir}6.2$ might be involved in IL-1-mediated glucose uptake.

1.8 Aims of this work

IL-1β, a cytokine mainly produced by immune cells, induces insulin-independent and long lasting hypoglycemia [del Rey et al., 2006]. IL-1β-induced hypoglycemia is caused by both peripheral and central effects [Besedovsky and del Rey, 2010]. It has already been shown that exogenous IL-1β facilitates glucose uptake by adipocytes, fibroblasts and chondrocytes [Bird et al., 1990, Garcia-Welsh et al., 1990, Shikhman et al., 2001]. In addition, we recently found an inhibitory effect of exogenous administered IL-1Ra on glucose uptake and metabolism in astrocytes and neurons [del Rey et al., 2016]. A subject of current research is the interdependency between glucose uptake, metabolism, and function of lymphocytes [Jacobs et al., 2008, Caro-Maldonado et al., 2014, Donnelly and Finlay, 2015, Slack et al., 2015]. Glucose is required by B and T cells for an adequate immune response, in order to meet the high energetic demands of activation-dependent growth and proliferation [Jacobs et al., 2008, Caro-Maldonado et al., 2014]. However, an

unphysiologically increase of glucose metabolism in lymphocytes can result in elevated levels of activation and an autoimmune-like phenotype [Maciver et al., 2008]. Therefore, glucose uptake by lymphocytes needs to be tightly regulated to maintain a healthy immune homeostasis. It was found that cell extrinsic signals, such as co-receptors and cytokines, are critical for the regulation of glucose uptake by lymphocytes [Frauwirth et al., 2002, Wieman et al., 2007, Wofford et al., 2008].

We hypothesize that IL-1β plays an important role in fueling immune responses. The main aim of this work was to investigate the influence of endogenously produced IL-1 on lymphocyte glucose uptake and energetic metabolism in resting and LPS-stimulated lymphocytes.

An additional aim was to start investigating the intracellular signaling pathways responsible for putative effects of IL-1 on these parameters, focusing on the IL-1R1 adapter protein MyD88, a well-described transducer of IL-1 signaling, the protein kinase AKT, a key regulator of GLUT surface expression, and the $K_{ir}6.2$ ion channel, which connects the cell membrane potential to the availability of intracellular energy in the form of ATP and has also been implicated in the regulation of glucose uptake.

21

2 Materials and Methods

2.1 Materials

Materials, instruments, reagents, and the software used for the experiments performed in this work are listed in Tables 1-5.

Table 1. **Materials used for this work**

Materials	Product name	Producer
96 well plate	Greiner Cellstar flat bottom	Sigma-Aldrich; Germany
96 well plate	Seahorse XF96 cell culture microplate	Agilent; Germany
Balance	Mettler PM3000	Mettler Toledo; Germany
Centrifuge	Hettich Universal 30 RF	Hettich Zentrifugen; Germany
Centrifuge	Biofuge Fresco	Hearus; Germany
Direct light microscope	Wilovert (20x/0.25)	Will; Germany
Flow cytometer	FACScan	Becton Dickinson; USA
Flow cytometer	LSRII	Becton Dickinson; USA
Flow cytometry tubes	5 ml, 75x12 mm tube	Sarstedt; Germany
Haemocytometer	Neubauer Improved 0.0025 mm^2	Kobe Marburg; Germany
Hood	Nuaire class II type A/B3	Integra Biosciences; Germany
Incubator	Heraeus	Heraeus; Germany
Inverse microscope	Leica type 020-518.500 DMLS (40x /0.65)	Leica Microsystems; Germany
Microtube 0.5 ml	Microtube 0.5 ml	Sarstedt; Germany
Microtube 1.5 ml	Microtube 1.5 ml	Sarstedt; Germany
Precision balance	Mettler AJ150	Mettler Toledo; Germany
Seahorse apparatus	Seahorse XF96	Agilent; Germany
Single use serological pipette	Cellstar serological pipette, sterile 10 ml	Greiner Bio-One; Germany
Single use syringe	1 ml Norm-Ject	Henke Sass Wolf; Germany
Surgical blade	Sterile carbon steel blade	Heinz Herenz; Germany
Tissue culture flask 25 cm^2	Cellstar tissue culture flask 25 cm^2 50 ml PS	Greiner Bio-One; Germany
Tube 15 ml and 50 ml	Cellstar PP-tube, 15 ml / 50 ml sterile	Greiner Bio-One; Germany

Table 2. Reagents

Reagent	Product name	Producer
2-NBDG	2-(N-(7-nitrobenz-2-oxa-1.3-diazol-4-yl)amino)-6-deoxyglucose	Cayman Chemical; USA
7-AAD	7-aminoactinomycin D	Sigma-Aldrich; Germany
AKTi8	AKT inhibitor VIII	Santa Cruz; USA
Annexin V	FITC	BD Pharmingen; Germany
Antimycin-A	Antimycin-A	Santa Cruz; USA
DMEM without glucose	DMEM without L-glutamine, without glucose	PAA; Germany
FCCP	Carbonyl cyanide-4-(trifluoro-methoxy)phenylhydrazone	Santa Cruz; USA
FCS	FBS Gold, fetal bovine serum	PAA; Germany
Flow cytometry buffer	BD FACS sheath solution with surfactant	BD Bioscience; Germany
HEPES	HEPES buffer 1 M	Capricorn; USA
IL-1β	Human recombinant IL-1β	Glaxo Institute for Molecular Biology; Switzerland
IL-1Ra	Human recombinant IL-1Ra	Dr. Daniel E. Tracey; Upjohn Laboratories; USA
Kineret	Human recombinant IL-1Ra	Swedish Orphan Biovitrum; Sweden. Kindly provided by Prof. Dr. R. Straub; Germany
L-glutamine	L-glutamine 100x (200 mM)	PAA; Germany
Low-buffered DMEM	D5030 DMEM	Sigma-Aldrich; Germany
LPS	LPS L4391 from Escherichia coli O111:B4	Sigma-Aldrich; Germany
Oligomycin	Oligomycin	Sigma-Aldrich; Germany
PBS	Phosphate-buffered saline 1x without Ca^{2+} and mg^{2+}	PAA; Germany
Pen-Strep	Penicillin-Streptomycin (100x)	PAA; Germany
Phloretin	Phloretin $\geq 99\%$	Sigma-Aldrich; Germany
Polylysine	Poly-L-lysine solution (0.01 %)	Merck; Germany
Rotenone	Rotenone	VWR International; Germany
RPMI 1640	RPMI 1640 without glutamine	Capricorn; USA
Trypan blue	Trypan blue solution (0.4 %)	Sigma-Aldrich; Germany

Table 3. Antibodies

Antibody	Label	Clone	Producer
Anti-B220	PE	RA3-6B2	Biolegend; Germany
Anti-B220	PE-Cy5	RA3-6B2	Tonbo Biosciences; USA
Anti-CD3ϵ	PE	145-2C11	Biolegend; Germany
Anti-CD3ϵ	PE-Cy5	145-2C11	Biolegend; Germany

Table 4. Composition of buffers and media

Buffer or Medium	Composition
ACK lysis buffer	160 mM NH$_4$Cl 170 mM TRIS
Annexin binding buffer	140 mM NaCl 2,5 mM CaCl$_2$ 10 mM HEPES/NaOH pH 7.4
Culture medium	RPMI 1640 (11.1 mM glucose) 5 % FCS 1 % Pen/Strep (100x) 2 mM L-glutamine 10 mM HEPES
Low-buffered DMEM	D5030 DMEM 25 mM Glucose 1.85 g/l NaCl pH 7.35 $\pm$ 0.05 pH
Low glucose medium (40 mg/dl glucose)	20 % RPMI 80 % DMEM without glucose

Table 5. Software

Software	Product name	Source
FACS evaluation	FlowJo 10	FlowJo LLC; USA
FACS evaluation	WinMDI 2.9	Joe Trotter
Image processing	Fiji	Open source
Seahorse evaluation	Wave 2.6	Agilent; Germany
Statistical analysis	Prism 7	Graphpad, USA
Statistical analysis	SPSS 24	IBM; Germany

2.2 Animals

Mice were permanently housed in temperature-, humidity-, and light-cycle (12 h) controlled rooms. Food and water were provided *ad libitum*. To avoid fluctuations in parameters that could be caused by hormonal changes due to the female cycle, only male animals were used in the experiments. Mice were individually caged for at least one week before starting an experiment. The experiments were performed with mice that were at least 12 week-old.

C57Bl/6J mice were obtained from Harlan Winkelmann, Germany, and bred at the animal facilities of the Philipps University, Marburg.

K$_{ir}$6.2 KO breeding pairs on C57Bl/6J background were kindly provided by Dr. B. Liss, Institut für Angewandte Physiologie, University Ulm, following the agreement of Dr. S. Seino, Division of Cellular and Molecular Medicine, Department of Physiology and Cell Biology, Kobe University Graduate School of Medicine, Japan. The mice used in the experiments reported here were bred at the animal facilities of the Philipps University, Marburg.

MyD88 KO breeding pairs on C57Bl/6J background were kindly provided by Prof. Dr. Axel Pagenstecher, Institute of Neuropathology, Medical Faculty, University Marburg, following the agreement of Dr. Shizuo Akira, Immunology Frontier Research Center, University Osaka, Japan, and further bred at the animal facilities of the Philipps University, Marburg.

The use of these animals was granted in the permissions EX-15-2013 and EX-17-2016.

2.3 Spleen cell culture

Mice were sacrificed by cervical dislocation in the operating room of the animal facility. After weighing, the fur was soaked with alcoholic disinfectant and cut open on the left side. The skin was pulled back, so that the left side of the ribcage and stomach was accessible. With another set of sterile scissors, the muscle layers over the spleen were cut and the spleen was removed from the peritoneal cavity. Adherent fat and blood vessels were trimmed off and the spleen was transferred to a sterile 15 ml tube containing 10 ml ice-cold PBS and kept on ice until further processing in the laboratory.

The spleen was transferred to a petri dish containing a $100\,\mu m$ metal mesh cell strainer under sterile conditions. The spleen capsule was incised twice, and cells were collected by gently rubbing the tissue through the mesh with the stamp of a syringe. Throughout the procedure, the mesh and the tissue were always covered with PBS. The resulting cell suspension was transferred to a 15 ml centrifuge tube with a fresh syringe and centrifuged at 300 g for 10 min, at $4\,°C$. The supernatant was discarded and the cell pellet was resuspended in 5 ml ice-cold ACK (ammonium-chloride-potassium) buffer to lyse red blood cells. The cell suspension was kept on ice for 5 minutes and gently shaken several times during this period. The reaction was stopped by transferring the suspension to a fresh 15 ml centrifuge tube containing 5 ml ice-cold PBS, centrifuged for 10 minutes at 300 g, $4\,°C$, and washed with 10 ml ice-cold PBS.

After one final centrifugation of 10 minutes at 300 g at $4\,°C$, the supernatant was discarded and the cells were resuspended in 5 ml culture medium. The culture medium was RPMI 1640 containing 11.1 mM D-glucose, 5 % fetal calf serum (FCS), 2 mM L-glutamine, 10 mM HEPES buffer and penicillin/streptomycin. Cell concentration and viability were determined by counting an aliquot of the cells stained with trypan blue in a Neubauer chamber. Cell concentration was adjusted to 1 x 10^6 cells/ml and $200\,\mu l$ per well were seeded in a 96-well flat bottom plate. The plates were incubated at $37\,°C$ with a 5 % CO_2 atmosphere in a humidified incubator.

2.4 Stimulation of spleen cells

LPS-stimulated samples were prepared by addition of LPS to the medium (final concentration 50 µg/ml), prior to seeding the cells into 96 well plates.

2.5 Methods to evaluate glucose uptake

Since its introduction more than 50 years ago, radiolabeled glucose and its derivates such as 2-deoxy-D-glucose were the main tools to evaluate cellular glucose uptake. This method allowed the characterization of the kinetics of glucose transport in many cell types, including the determination of GLUT substrate specificity and the initial description of GLUT regulation [Barros et al., 2009]. The advantages of radiolabeled glucose derivates are a high signal-to-noise ratio and their chemical similarity to unlabeled glucose derivates, which results in almost unchanged affinities to the binding sites of the transporters and the kinetics of the transport. However, glucose uptake assays using radiolabeled glucose also have disadvantages. The spatial resolution is too low for single cell analysis and a comparably large number of cells has to be purified and evaluated. Further, commonly used radiolabels only have a relatively short half-life and also have the disadvantage of handling and disposal of radioactive substances. In the last decades, powerful optical systems were developed and the radioactive method to evaluate glucose uptake was complemented and partially replaced by the use of fluorescent glucose analogs that were first described in the 1980s [Speizer et al., 1985].

Fluorescence-labeled glucose analogs

At present, two well-described fluorescence-labeled glucose analogs (FLGAs) are commercially available: 2-deoxy-2-[(7-nitro-2,1,3-benzoxadiazol-4-yl)amino]-D-glucose (2-NBDG) and 6-deoxy-6-[(7-nitro-2,1,3-benzoxadiazol-4-yl)amino]-D-glucose (6-NBDG). 2-NBDG and 6-NBDG differ in the carbon atom of glucose to which 7-nitrobenzo-2-oxa-1,3-diazol (NBD) is attached (Figure 4). NBD displays an excitation maximum of 465 nm and an emission maximum of 535 nm, and it can be measured in the standard 530/30 nm

27

fluorescein isothiocyanate (FITC) channel. It should be mentioned that the affinity of FLGAs to the GLUTs binding sites is altered by the fluorescent label and the overall transport velocity is severely decreased. It has been reported that the affinity of 6-NBDG to GLUT1 is increased about 300-fold and that the transport velocity via GLUT1 is decreased 50 to 100 times compared to glucose [Barros et al., 2009]. Nevertheless, FLGAs are taken up by facilitated diffusion into the cells via the same glucose transporters as physiological D-glucose, and the uptake and cytoplasmic concentration of FLGA correlate with those of glucose within reasonable limits. Although the transport kinetic differs from glucose, FLGAs have an important advantage over the radioactive counterparts. FLGAs can be used with standard optical laboratory equipment designed for single cell analysis like fluorescence microscopes or flow cytometers. These instruments make it possible to analyze glucose uptake at the single cell level. Additionally, it is possible to simultaneously identify the cell types by using fluorescence-conjugated antibodies to distinctive antigens.

The position of the fluorescence label is decisive for the intracellular fate of the FLGA. 6-NBDG cannot be phosphorylated by glucose hexokinase and the kinetic of its accumulation in the cytoplasm is affected by a declining concentration gradient across the cell membrane. This differs from the kinetic of glucose transport, since glucose is constantly phosphorylated in the cytoplasm and therefore removed from the concentration gradient. However, this property of 6-NBDG has only a limited significance if sufficiently high concentrations are used and the incubation time is kept short. On the other hand, the feature of not being metabolized has the advantage that it is not degraded within the cell, which would eventually result in the loss of fluorescence.

2-NBDG, in turn, can be phosphorylated by hexokinase as glucose, and its concentration gradient across the cell membrane is maintained stable, which mimics the kinetics of glucose uptake much better. Unfortunately, even though the phosphorylated form of 2-NBDG is still fluorescent and well measurable, phosphorylated 2-NBDG is further metabolized and quenched over time. Thus, at least theoretically, it would not be possible to distinguish a cell that takes up a small amount of 2-NBDG and has a slow metabolism from a cell that takes up a large amount of 2-NBDG and has a fast metabolism.

Taken together, radiolabeled glucose, 6-NBDG, and 2-NBDG have advantages and disadvantages. In summary, the kinetics of incorporation of radiolabeled glucose is more comparable to that of normal glucose but the method does not allow single cell measurements. 6-NBDG uptake is disturbed by a declining driving force caused by intracellular accumulation but is not degraded. Finally, 2-NBDG has a more stable, glucose-like kinetic, but might be degraded over time.
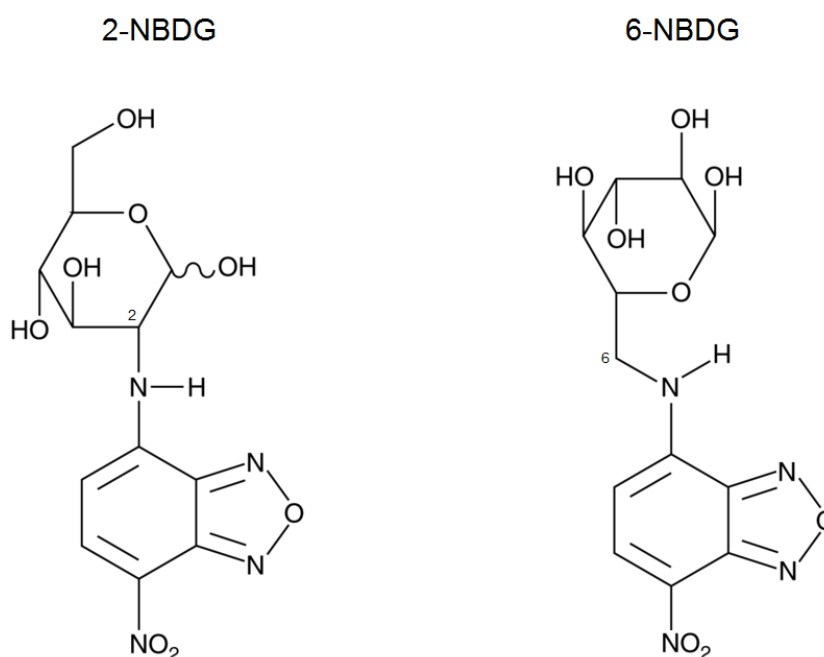

Figure 4. Chemical structure of the fluorescence-labeled glucose analogs 2-NBDG and 6-NBDG. In 2-NBDG, the fluorescent label 7-nitrobenzo-2-oxa-1,3-diazol (NBD) is attached by an amino group to the second carbon atom of glucose. Although the overall structure is significantly larger than glucose alone, glucose hexokinase is able to phosphorylate 2-NBDG at the sixth carbon molecule, as it does with glucose. This phosphorylation removes intracellular 2-NBDG from the concentration gradient across the cell membrane and resembles the kinetic of unlabeled glucose. 2-NBDG-phosphate can be further metabolized and will finally lose its fluorescence. However, this process is very slow, probably because the additional NBD residue interferes with enzyme binding. The fluorescent NBD label of 6-NBDG is attached to the sixth carbon atom of glucose. Hexokinase is not able to process 6-NBDG and the transport across the cell membrane is slowed down by 6-NBDG accumulation within the cell gradually over time. The intracellular concentration is, however, not altered by degradation since 6-NBDG cannot be converted to 6-NBDG-phosphate and, therefore, the glycolytic pathway cannot proceed.

Because of the possibility of additional labeling and high throughput in flow cytometry, a FLGA was chosen for the experiments planned for this work. No significant differences between 2-NBDG and 6-NBDG were detected in preliminary experiments. In particular, no relevant intracellular degradation of 2-NBDG was detected. Therefore, 2-NBDG was used for further experimentation. In both flow cytometers used in this work (FACScan and LSRII), a 488 nm argon laser was used for excitation and the 530/30 nm FITC filter was used for detection of the NBD fluorescence.

2.6 General experimental protocol to evaluate glucose uptake

After a series of preliminary experiments to determine the optimal conditions, all experiments designed for the evaluation of glucose uptake followed the same experimental protocol (Figure 5). Spleen cell suspensions were prepared as described above and incubated in the absence or presence of LPS for 3 or 23 h. For reasons of simplicity, the cells cultured in the absence of LPS are termed in the rest of this work as "non-stimulated".
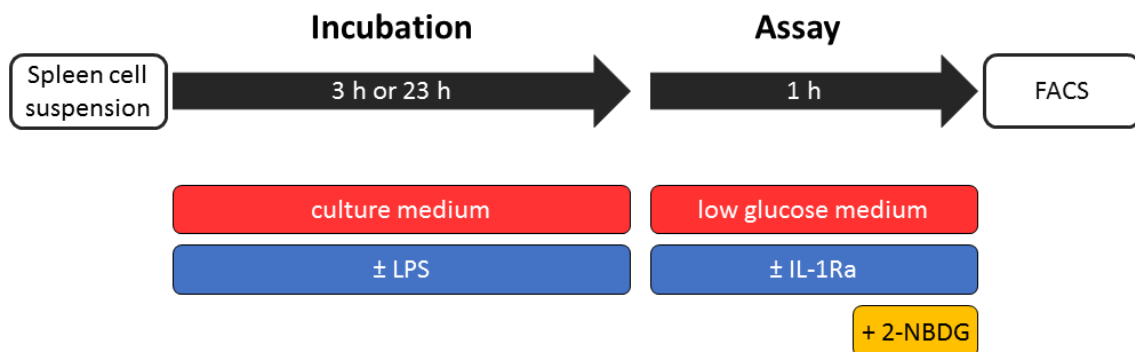

Figure 5. General experimental protocol to evaluate IL-1Ra/IL-1-mediated changes in 2-NBDG uptake. After spleen preparation, the cells were incubated for 3 h or 23 h in the presence or absence of LPS. Then, the medium was changed to the low glucose assay medium. In order to evaluate the effect of IL-1Ra, pairs of corresponding samples were incubated with and without IL-1Ra. 2-NBDG was present in the medium during the last 7 min of the incubation time. Cells then were prepared for flow cytometry by washing and, if appropriate, by additional staining. The assay was only slightly modified for the determination of the effects of phloretin and AKT inhibition. The modifications are described in the respective sections.

After this culture period, the medium was changed to low glucose medium and the cells were incubated one more hour (thus, 4 or 24 h in total). All other reagents were added at defined time points within the last hour of incubation. IL-1Ra or the corresponding vehicle was added to the cultures one hour before harvesting, and 2-NBDG, the fluorescent glucose analogue used to evaluate glucose uptake, was always present in the medium during the last 7 minutes of the incubation period.

2.7 2-NBDG uptake assay

2-NBDG is difficult to dissolve in aqueous solutions and tends to precipitate when thawed. Although it is suggested not to prepare frozen aliquots [Yamada et al., 2007], it is practically not possible to prepare fresh solutions daily because of the hygroscopic nature of 2-NBDG. Unfortunately, there is no commercially available packaging size that would provide reasonable low amounts. We were able to solve the problem of precipitation by keeping frozen aliquots at a comparatively low concentration of 1 mM.

After incubation in culture medium for 3 h or 23 h, cells were transferred to flow cytometry tubes, centrifuged 5 min at 300 g, and the supernatant was discarded. The cell pellet was resuspended in low glucose medium and incubated with or without the substances to be tested. The incubation in low glucose medium always lasted a total time of 1 h. The substances to be tested were added during this incubation period, at the time indicated in the corresponding figures (see Results). 2-NBDG was added 7 minutes before harvesting at a final concentration of 100 μM. The reaction was stopped by addition of 500 μl ice-cold PBS and the cells were centrifuged for 5 minutes at 300 g at 4 °C. The supernatant was discarded and the cells were washed twice with 500 μl cold PBS to remove extracellular 2-NBDG.

2.8 Annexin V apoptosis assay

The annexin V apoptosis assay has found widespread application and acceptance since its introduction in 1994 [Koopman et al., 1994]. It is based on the fact that healthy cells actively keep phosphatidylserine molecules in the inner leaflet of the membrane by the

enzyme flippase. When the cell undergoes apoptosis, phosphatidylserine is transferred to the membrane outer leaflet either by diffusion or by the enzyme scramblase, where it is accessible to extracellular FITC-labeled annexin V. Combined with a viability dye such as 7-AAD, which is efficiently excluded by intact cells, it is possible to distinguish three populations (Figure 6): unstained cells that are healthy, annexin-FITC-stained cells that are undergoing apoptosis, and annexin-FITC+7-AAD double stained cells that are dead [van Engeland et al., 1998].

The experiments were performed as described above for the 2-NBDG assay and the preparation for flow cytometry was done as described in Section 2.9, except that annexin-binding buffer was used instead of PBS for the washing and incubation steps. Annexin-binding buffer contains elevated Ca^{2+} concentrations compared to PBS, but does not contain phosphate and is designed to facilitate Annexin V binding to phosphatidylserine. Annexin V-FITC was applied at a final concentration of 200 ng/ml. After the last centrifugation, cells were also resuspended in annexin binding buffer and not in flow cytometry buffer in order to keep the annexin V-FITC binding stable. A positive control for apoptosis was generated by incubating cells of the respective experiment for 15 min at 55 °C.
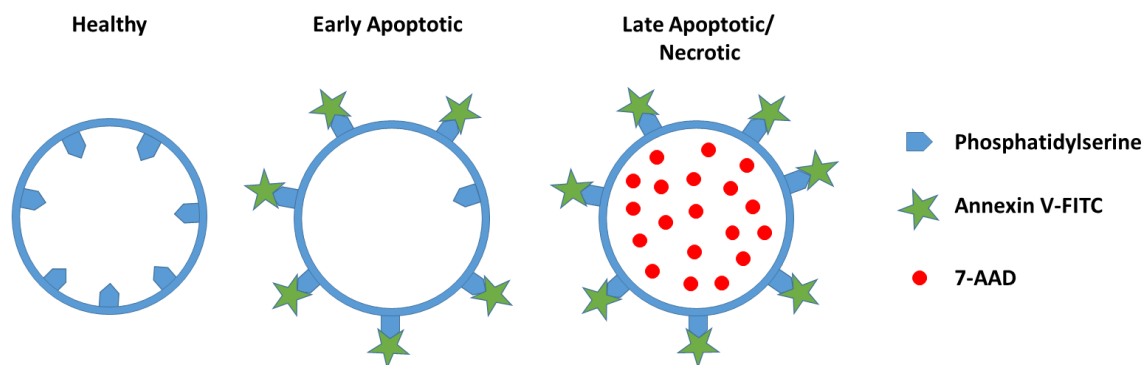

Figure 6. Principle of the apoptosis detection assay. In healthy cells, phosphatidylserine is not present on the cell surface as the enzyme flippase is constantly turning it towards the cytoplasm. In apoptotic cells however, flippase is inactivated and, additionally, the enzyme scramblase transfers phosphatidylserine outwards where it is accessible to FITC-labeled annexin V. Combination of annexin V with a viability dye makes is possible to identify cells that are at an early stage of apoptosis, in which they are not yet stained by the viability dye.

2.9 Sample preparation and staining for flow cytometry

After the 2-NBDG assay, the samples were prepared for flow cytometry by staining with 7-AAD, by antibody-staining for identification of B and T cells in the respective experiments, and by resuspension in FACS buffer. Cells were washed with 500 µl ice-cold PBS, centrifuged 5 minutes at 300 g at 4 °C, and the supernatant was discarded. The cell pellet was resuspended in 100 µl cold PBS, and the appropriate staining was performed. The CD3 and B220 antibodies were applied at a concentration of 2 µg/ml and the vitality dye 7-AAD at a concentration of 5 µg/ml. After 10 minutes of incubation on ice, cells were centrifuged 5 minutes at 300 g, 4 °C, and washed once with 500 µl cold PBS. After a final centrifugation step the pellet was resuspended in 250 µl cold FACS buffer and kept on ice until analyzed by flow cytometry.

2.10 Analysis of flow cytometry data

For appropriate evaluation, clumps and dead cells were excluded, and the recorded events categorized as T or B cells in the respective experiments, so that the mean 2-NBDG fluorescence of these populations can be determined. The example shown in Figure 7 illustrates the gating strategy of data acquired with an LSRII cytometer (Core Facility Flow Cytometry, University Marburg). Except for the exclusion of cell clumps by pulse height to pulse width ratio of side scatter (SSC), which is possible with the LSRII flow cytometer but not with the FACScan, the procedure was the same for both flow cytometers.

In flow cytometry, forward scatter (FSC), SSC and the fluorescence intensities are measured in arbitrary units (AU). Figure 7 A gives an example of raw data depicted as FSC/SSC diagram. In addition to the living single cells, the raw data still includes dead cells and cell clumps. Flow cytometric data are usually presented by the signal area composed of pulse height and pulse width. A single cell requires a defined time to be carried through the laser by the sheath fluid, which depends on the characteristics of a given cell population and on the cytometer setting. While the cell moves through the laser beam, it generates a signal. The magnitude of this signal is termed pulse height. If the

duration of the signal, termed pulse width, is longer than the typical duration and does not have an appropriate ratio to the pulse height, it is most likely not derived from a single cell. Most of the doublets and cell clumps can be excluded from the analysis by gating reasonable ratios of SSC pulse height (SSC-H) and SSC pulse width (SSC-W) for single cells (Figure 7 B).

After SSC-H/SSC-W gating, dead cells are excluded from the analysis by only gating cells that are not positive for 7-AAD (Figure 7 C). The identification of T cells by CD3-PE fluorescence plotted on the x-axis can also be observed in this figure. The selection of living, single CD3-PE positive cells is used to determine the 2-NBDG mean fluorescence (MFI) of the T lymphocyte population. The MFI of a given population is the essential readout of the 2-NBDG assay. This value is subsequently used to compare the 2-NBDG fluorescence of different samples, and to calculate ratios between the MFI of controls and experimental groups to evaluate the effect of a substance on glucose uptake. Since the fluorescence is acquired as logarithmic data in flow cytometry, the MFI in this work is calculated using the geometrical mean. Thus, the data is converted to a linear scale for better comparability. A PE-labelled anti B220 was additionally used to identify B cells. Double staining experiments showed that there were only few double negative or double positive cells for both the T cell marker CD3 and the B cell marker B220 in the spleen cell suspensions used in this work. Therefore, most samples were only stained with anti-CD3 and it was assumed that the CD3 negative cells are B cells. For the comparison to the initial FSC/SSC raw data, the result of the gating process that removed cell clumps and dead cells is shown in Figure 7 D. An example of 2-NBDG fluorescence data and MFI calculation is illustrated in Figure 8.
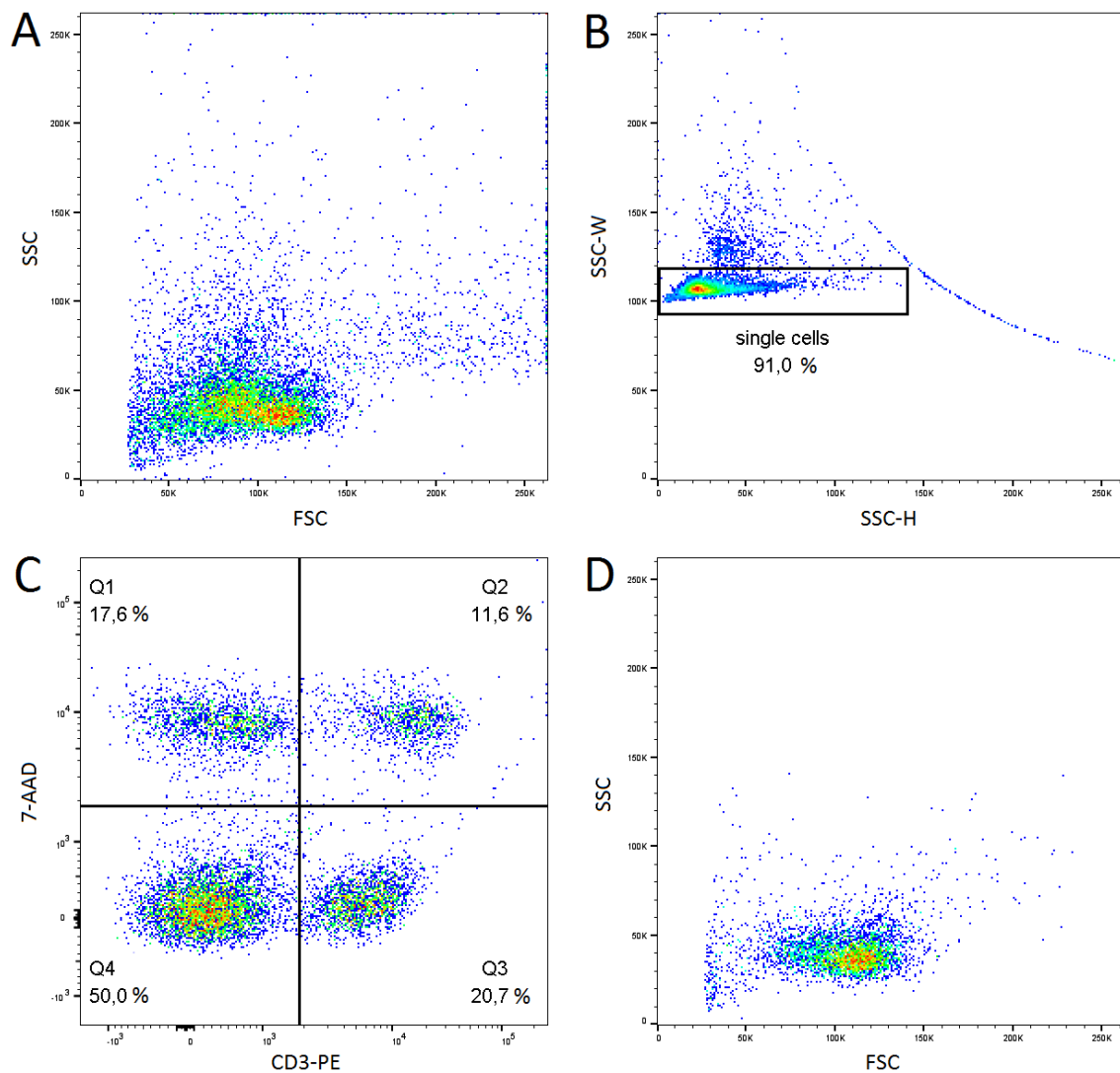
Figure 7. Example of the procedure used to analyze flow cytometric data. Density dot plots showing low event density in blue and high density in red. Green and yellow indicate intermediate densities. **A)** Forward scatter/side scatter graph of the raw data including cell clumps and dead cells. **B)** The region labelled "single cells" displays a given SSC pulse height (H) to pulse width ratio (W). This area is selected to exclude cell doublets and clumps and contains 91 % of all events. **C)** 7-AAD, as marker of dead cells, is depicted on the y-axis and the T cell marker (PE-labelled anti CD3) on the x-axis. This results in 4 populations, namely Q1: dead non-T cells, Q2: dead T cells, Q3: alive T cells and Q4: alive non-T cells. These gates are used to calculate the 2-NBDG MFI of the cells within the respective gate. **D)** The same data set as shown in A after the gating procedure, showing only events from Q3 and Q4. The graph displays alive single cells in the large cloud and a few 7-AAD negative sub-cellular particles to the left, near the origin of the axis.
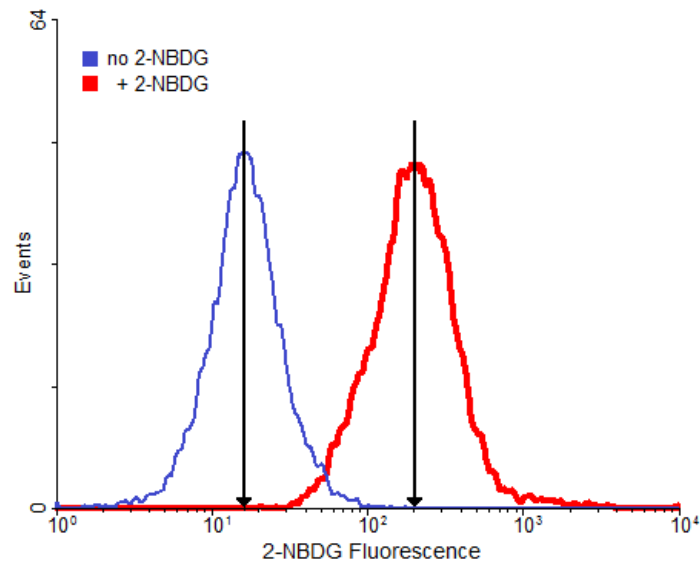
35

Figure 8. An example of 2-NBDG uptake. After exclusion of dead cells and doublets, the 2-NBDG fluorescence of given populations is depicted as histogram. Overlay histograms, as shown here, can be used to visualize the 2-NBDG uptake of different samples. Since the data is depicted on a logarithmic scale, the mean intensity of the fluorescence is represented by the geometrical mean, indicated by arrows. The value of the 2-NBDG geometrical mean fluorescence intensity (MFI) is used for the statistical comparison of 2-NBDG uptake by different samples and populations.

2.11 Laser scanning microscopy

Confocal imaging was performed with an upright LSM 710-Axio Examiner.Z1 microscope equipped with a W-Plan-Apochromat 63x/1.0 M27 water immersion objective (Carl Zeiss, Jena, Germany). 2-NBDG was excited at 488 nm with an argon laser and fluorescence emission was detected at 493-556 nm. Spleen cells from C57Bl/6J mice were incubated for 23 h on polylysine-coated cover slips in culture medium and 1h with 100 µM 2-NBDG in low glucose medium prior to the analysis. After discarding the low glucose medium containing 2-NBDG, cells were gently rinsed with PBS and kept in PBS for imaging. Confocal images were processed using the Fiji software [Schindelin et al., 2012].

2.12 Principles of the live-cell metabolic flux analysis

A live-cell metabolic flux analysis, as performed using the Seahorse system, provides an appropriate way to evaluate the metabolic activity of cell populations. It can simultaneously detect the oxygen consumption rate (OCR) and the extracellular acidification rate (ECAR). The measurement of both OCR and ECAR is based on the use of fluorophores embedded in plungers that descend into the wells of the microplate during data acquisition (Figure 9).
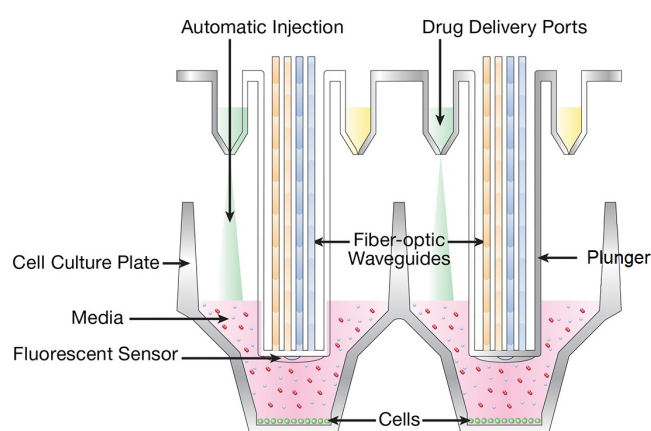

Figure 9. Technical principle of the live-cell metabolic flux assay. The fiber optics and fluorophore containing plungers lower into each microplate well and form a transient microchamber. Activation of the oxygen and pH sensitive fluorophores and signal readout occur via optical fibers. The process is repeated periodically during an experiment to generate a time line of OCR and ECAR. Test reagents can be injected via 4 drug injection ports. [Agilent Technologies, 2014], reprinted with permission.

The transient microchamber that is formed by plunger and well has a very small volume (less than 3 µl) and is therefore much more sensitive to analyte changes than the whole medium of the well. The Seahorse apparatus transmits stimulating light via optical fibers through the plungers to the fluorophores and receives a fluorescence signal. The plungers contain two types of fluorophores. One reacts to oxygen tension and the other to pH. To avoid detrimental effects of oxygen depletion and acidification due to the small volume of the microchamber, the plungers rise after each reading cycle and allow

reperfusion of the cells. For the addition of test reagents, every well has 4 drug injection ports that can be individually loaded with different substances. Depending on the scope of the experiments, the frequency of readouts and points in time of the injections can be programmed prior to the experiment.

Evaluated parameters

Generally, oxygen is mainly consumed by cellular respiration, and medium acidification is primarily generated by glycolysis if glucose is available in the medium [Divakaruni et al., 2014]. The Seahorse system allows to determine the speed at which changes in these parameters occur, and the results are expressed as OCR and ECAR. Several other metabolic variables can be calculated from these two directly detected parameters by selectively inhibiting key molecules of a particular energetic pathway. Figure 10 describes how details of oxygen consumption are evaluated.

During OCR measurements, oligomycin is used to inhibit the ATP-producing enzyme ATP synthase. Carbonyl cyanide-4-(trifluoromethoxy)phenylhydrazone (FCCP) is a decoupling ionophore that makes the mitochondrial membrane permeable for hydrogen ions, which permits to evaluate the maximal mitochondrial respiration rate. Rotenone and antimycin-A block the respiratory chain, thus terminating mitochondrial oxygen consumption. By administering oligomycin, FCCP and rotenone/antimycin-A sequentially, the rate of oxygen consumption for basal respiration, ATP production, proton leak, maximal respiration, spare capacity and non-mitochondrial oxygen consumption can be determined.

Interferences in mitochondrial function affect the overall energy homeostasis of the cell. The inhibition of mitochondrial ATP-synthase by oligomycin results in an insufficient ATP production rate and subsequently in a shortage of energy within the cell. As a compensatory mechanism to cope with the loss of mitochondrial energy production, glycolysis is enhanced and the ECAR raises (Figure 11).
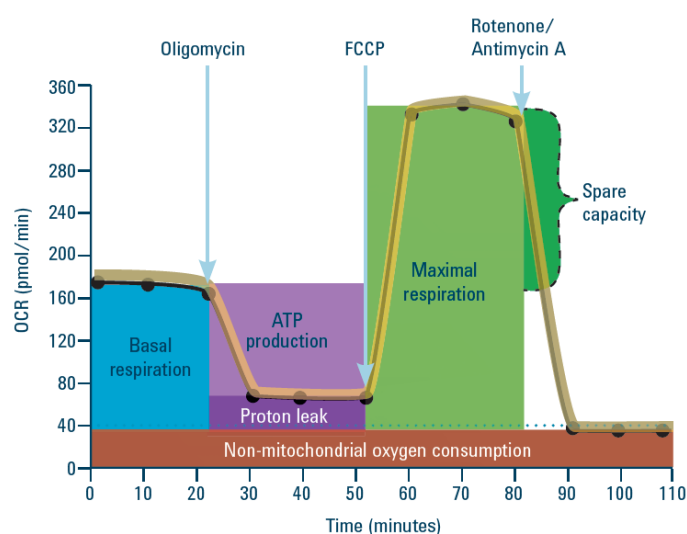
Figure 10. Evaluation of respiratory parameters. By selectively inhibiting key steps of the respiratory energetic pathway, it is possible to evaluate the composition of the overall oxygen consumption. Oligomycin inhibits the ATP synthase, thus indicating the percentage of oxygen that is actually used for ATP synthesis. The ionophore FCCP transports hydrogen ions across the mitochondrial membrane and, therefore, uncouples the respiratory chain from ATP synthesis. As the cells try to re-establish the mitochondrial ion gradient, the respiratory chain runs at maximum load, indicating the maximal respiratory capacity of the cells. The respiratory spare capacity can be derived from the values corresponding to the basal and maximal respiratory capacities. Proton leak in the mitochondria and non-mitochondrial oxygen consumption can be calculated from the OCR determined after complete blockade of the mitochondrial respiratory chain by rotenone and antimycin A. [Agilent Technologies, 2017], reprinted with permission.

2.13 Live-cell metabolic flux analysis

The conditions for the real-time live-cell metabolic flux assays were kept as similar as possible to those used for the determination of glucose uptake to achieve a potential comparability. Cell suspensions were prepared in the same way, except that the cells were not plated on standard cell culture 96-well plates but on the corresponding polylysine-coated 96-well plates used in the Seahorse assay system. The appropriate cell density was determined in preliminary experiments. Unstimulated cells were seeded at a concentration of 4.5 x 10^5/well and LPS-stimulated cells were seeded at 3 x 10^5/well. After 23 h incubation at 37 °C with a 5 % CO_2 atmosphere in a humidified incubator, plates were

transferred to an incubator without additional CO_2 supply for one hour to avoid effects of the atmosphere on the readout of the assays. Prior to insertion into the Seahorse apparatus, the plates were centrifuged at room temperature for 5 min at 200 g and the medium was replaced by low buffered Seahorse assay medium. The initial volume was 180 µl. After medium renewal, the plates were centrifuged again for better and homogeneous cell adherence. The plate was first centrifuged at mild acceleration until 50 g were reached and stopped by mild brake. The plate was turned 180° and accelerated again up to 300 g.
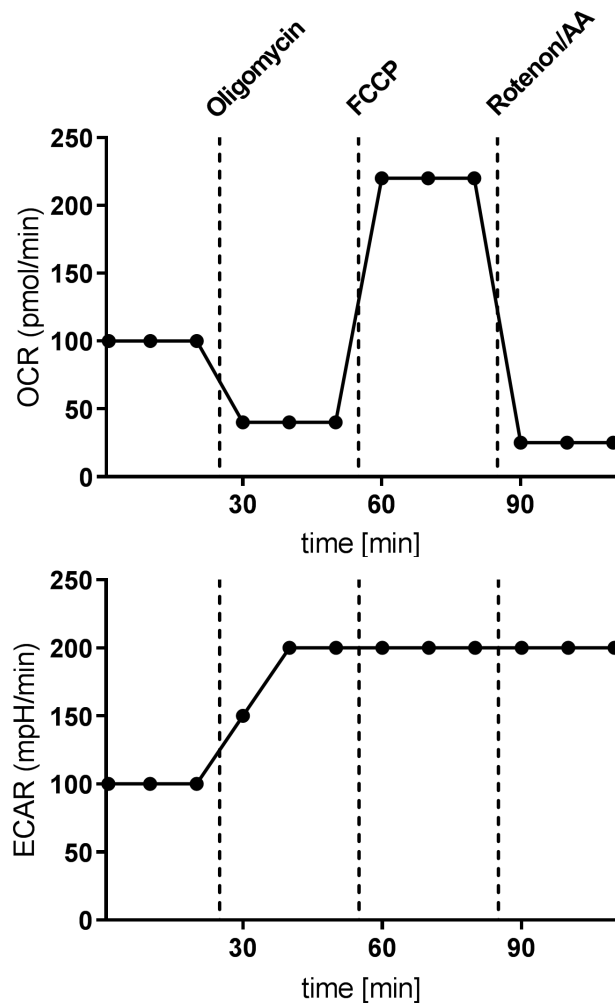

Figure 11. Compensatory increase of glycolysis after blockade of mitochondrial ATP production. Complementary to the manipulations described in Figure 10, the parallel response of ECAR is depicted in this figure. After the inhibition of mitochondrial ATP production by oligomycin, glycolysis is enhanced as compensation to satisfy cellular ATP demand.

40

The plate was then inserted into the Seahorse system and the measurements began after an equilibration phase of 10 min. The protocol was set so that there are alternating mixing and measurement cycles of 3 minutes each. Thus, each data point represents the average of the values recorded during the last 3 minutes. Substances were always injected immediately before a mixing cycle.

A baseline of OCR and ECAR was recorded during 3 measurement cycles, followed by the first injection at 20 min. Before the end of the experiment, usually after 4.5 h, 2 μM oligomycin, 1.8 μM FCCP and 1 μM rotenone/antimycin-A were injected in this sequence. OCR and ECAR were determined during 3 cycles after each injection. The values recorded after injection of these substances are used to calculate non-mitochondrial oxygen consumption, maximal respiratory capacity and the proton leak (Table 6).

Table 6. **Calculation of respiratory parameters**

Parameter	Calculation
Proton leak	Minimum OCR after oligomycin injection **-** Minimum OCR after rotenone/antimycin-A injection
Maximal respiratory capacity	Maximum OCR after FCCP injection **-** Minimum OCR after rotenone/antimycin-A injection
Non-mitochondrial oxygen consumption	Minimum OCR after rotenone/antimycin-A injection

2.14 Statistical analysis

The experimental design for the flow cytometric 2-NBDG uptake measurements in this work is a block design. Thus, a whole data set is composed by independent blocks of experiments, each of them performed with cells obtained from a single mouse spleen and exposed to different treatments. The advantage of a block design is that it controls the variability between subjects, similar to a repeated measure design. The statistical significance of comparisons between the different experimental groups was determined using

the appropriate tests indicated in the legend to each figure. All p-values are two tailed. Gaussian distribution of the data was confirmed using the Shapiro-Wilk normality test and homogeneity of variances was assessed by the Brown-Forsythe test. Student's t-test was used to compare two groups of data with normal distribution and homogeneous variances, and Student's t-test with Welch's correction if variances were not homogeneous. Mann-Whitney U-test was used when data were not normally distributed. For results obtained from paired samples with normal distribution, the paired t-test was used. When the data did not follow a normal distribution in results obtained from paired samples, they were compared with the Wilcoxon matched-pairs signed rank test. To determine if the results of a group are statistically different from a hypothetical value, e.g. 100 % of the control, the one sample t-test was used for normally distributed data, and the Wilcoxon signed-rank test when this condition was not fulfilled.

One-way analysis of variance (ANOVA) was used when multiple comparisons of normally distributed data with homogeneous variances were needed. Repeated measures were analyzed with repeated measure ANOVA (RM ANOVA). If significant, ANOVA and RM ANOVA was followed by a post hoc test. Dunnett's multiple comparisons test was used to compare several groups with a single group taken as control. Sidak's post hoc test was performed to compare multiple groups with more than one group. If the criteria of homogeneity of variance or Gaussian distribution were not fulfilled, the non-parametric Kruskal-Wallis test followed by Dunn's test was performed for independent samples, and the Friedman test followed by Dunn's post hoc test for paired samples. For comparison of two variables that changed with time, two-way ANOVA followed by Fisher's LSD post hoc test was used. Differences were considered statistically significant if p was less than 0.05.

3 Results

3.1 Effect of endogenous IL-1 on spleen cell glucose uptake

After establishing the method to be used with splenocytes, the main question of the project was addressed, namely whether glucose uptake by lymphocytes is affected by endogenously produced IL-1. The effect of exogenous IL-1β administration was also tested. Furthermore, to start studying the possible mechanisms of IL-1β-mediated glucose uptake, the contribution of the ATP sensing potassium channel $K_{ir}6.2$, the IL-1R1 adapter protein MyD88, and AKT were examined.

3.1.1 Intracellular distribution of 2-NBDG fluorescence in splenocytes

As a general validation of the method, it was analyzed if 2-NBDG fluorescence is located evenly distributed in the cytoplasm as expected. Laser scanning microscopy (LSM) evaluation shows that 2-NBDG is taken up by the cells and results in a relatively homogeneous intracellular signal with no visible unspecific staining of the plasma membrane. For LSM evaluations, the standard protocol for FACS had to be modified. Since LSM is less sensitive than flow cytometry, 2-NBDG incubation time was prolonged to 1 h in order to intensify the signal. Representative LSM sections of a lymphocyte showing 2-NBDG incorporation are shown in Figure 12.

3.1.2 2-NBDG uptake by LPS-stimulated splenocytes

It is known that stimulation leads to increased glucose incorporation in lymphocytes, and exposure to LPS is frequently used as immune cell stimulus, particularly for B cells and macrophages [Vogel et al., 1983, Caro-Maldonado et al., 2014]. 2-NBDG uptake was evaluated in LPS-stimulated mouse spleen cells and compared to the results of unstimulated cells (Figure 13). The culture conditions and LPS stimulation are described in Material and Methods. Only a marginal (about 6 %) increase in 2-NBDG uptake was
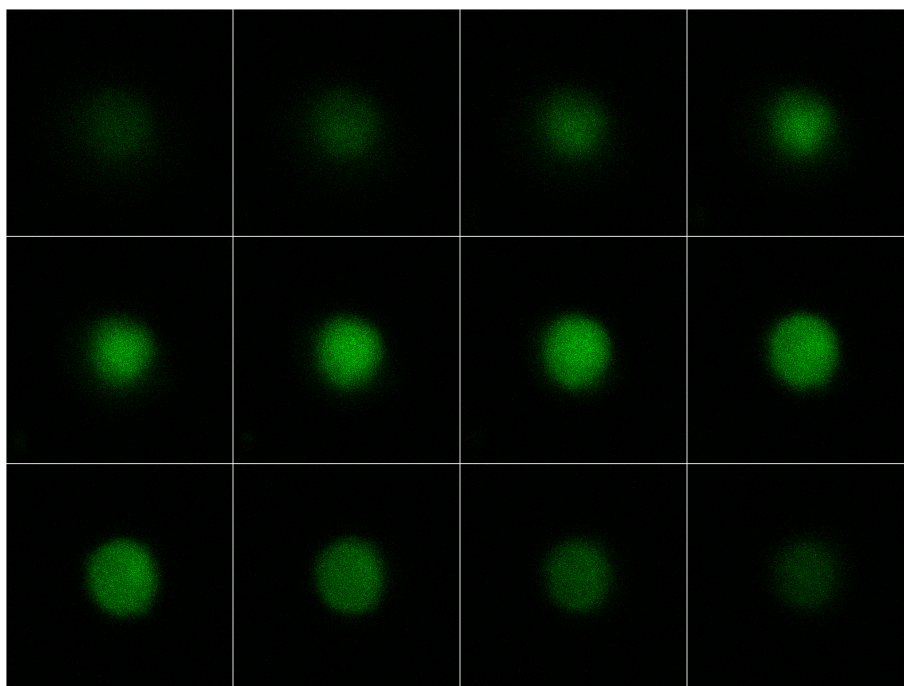
Figure 12. LSM images of cellular 2-NBDG fluorescence distribution. The panel shows a z-stack of sections through one representative lymphocyte from a spleen suspension that was incubated with 100 μM 2-NBDG for 1 h. The series begins at the upper left corner of the panel. The first image shows a section of the downwards-facing side of the cell, adjacent to the object carrier. The following images were generated by incrementally stepping upwards through the sample. The middle row of the panel shows the largest section area, with the fluorescence evenly distributed intracellularly and not sticking to the cell membrane. Confocal microscopy was performed with the kind help of Dr. Kirstin Hobiger, AG Neurophysiology.

observed in LPS-stimulated cells as compared to control samples 4 h after incubation. However, this increase was consistently observed in all experiments and the difference is statistically significant (Figure 14A). A larger increase in 2-NBDG uptake (approximately 60 %) was observed 24 hours after LPS stimulation (Figure 14B). Interestingly, prolonging the time of incubation under "basal" culture conditions only (e.g. no overt stimulation) also results in a significant increase in 2-NBDG incorporation (Figure 14).
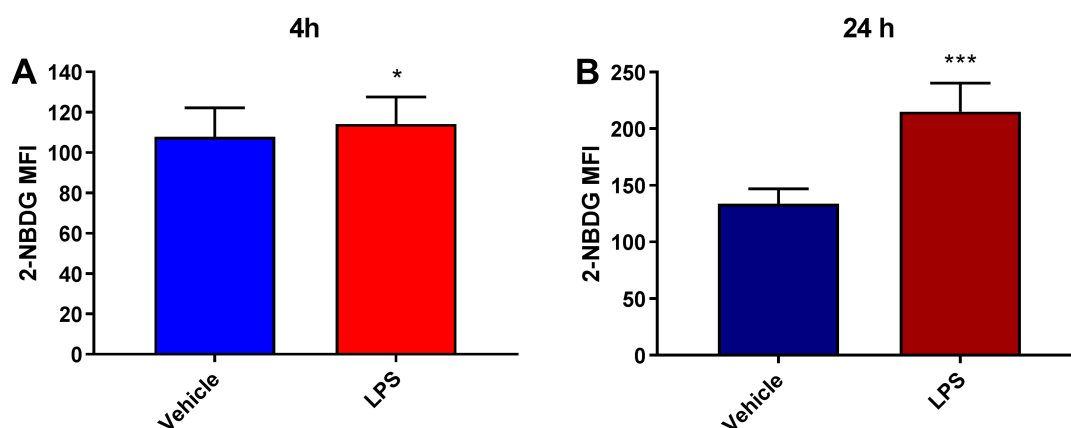
Figure 13. LPS stimulation increases 2-NBDG uptake by splenocytes. After 3 h (n=6 per group) or 23 h (n=12 per group) incubation with or without LPS, the medium was replaced by low glucose medium for the last hour of incubation and the 2-NBDG assay was performed as described in Material and Methods. Results are shown as mean ± SEM of 2-NBDG MFI. Data were analyzed by paired t-test: * p<0.02 (4h); *** p<0.001 (24 h) vs. vehicle.

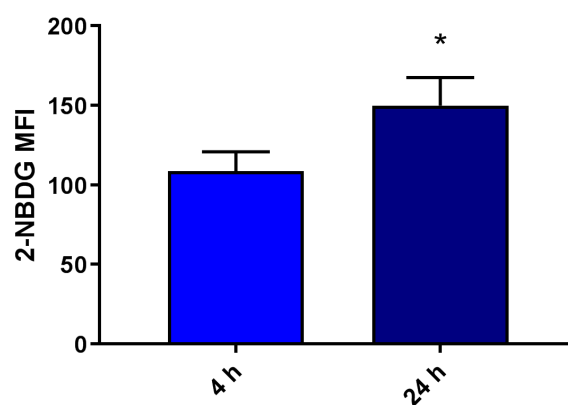**Figure 14. Prolonging the incubation time under basal conditions results in increased 2-NBDG uptake.** After 3 h or 23 h incubation, the medium was replaced by low glucose medium for the last hour of incubation and the 2-NBDG assay was performed as described in Material and Methods. Results are shown as mean ± SEM of 2-NBDG MFI from 7 individual experiments. Data were analyzed by paired t-test: * p<0.025 vs 4 h.

3.1.3 Inhibition of splenocyte 2-NBDG uptake by phloretin

To assess the specificity of the method and to be able to appreciate the magnitude of eventual changes in 2-NBDG uptake in subsequent experiments, the effect of blocking glucose transport by the GLUT inhibitor phloretin was determined.

Since phloretin can be toxic when used at high concentrations, the maximum phloretin concentration that would not affect cell survival under the culture conditions used in this work was evaluated. As shown in Figure 15, concentrations up to $250\,\mu$M phloretin did not induce cell death. Thus, in the following experiments phloretin was applied at this concentration.
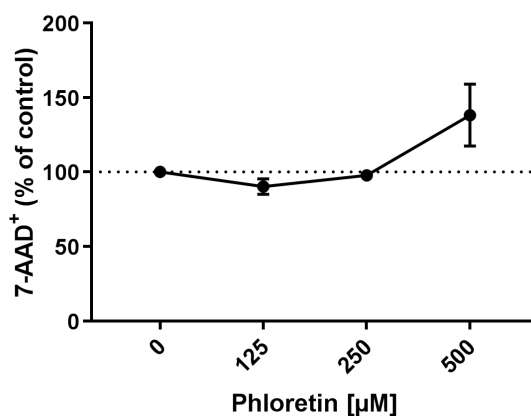

Figure 15. Titration of the GLUT inhibitor phloretin. Spleen cell suspensions were prepared as described in Material and Methods. After 3 h in culture, the medium was replaced by low glucose medium. Phloretin was added 48 min later and further incubated for 12 min. As in previous experiments, 2-NBDG was added to the cultures 7 minutes before harvesting. Between 10 % and 15 % cells were dead in the controls (no phloretin) after 4 h incubation. Results are shown as mean ± SEM of the percentage of 7-AAD+ cells detected in the samples containing phloretin normalized to the respective simultaneous control (no phloretin) in each individual experiment (n=3).

As in the experiments shown above (Figure 13), 2-NBDG uptake was increased in non-stimulated cells (vehicle) after 24 h incubation, and the increase was even more marked in LPS-stimulated cells (Figure 16). Under the conditions used in these experiments, phloretin inhibited 2-NBDG uptake by around 20 %. The magnitude of the inhibition was relatively constant, independently of whether the GLUT blocker was added to the cultures at 4 or 24 h, and of whether cells were stimulated with LPS or not (Figure 17).

Figure 16. Effect of phloretin on 2-NBDG uptake by splenic cells. After 3 h (n=3 per group) or 23 h (vehicle n=6 per group; LPS n=5 per group) incubation with or without LPS, the medium was replaced by low glucose medium for the last hour of incubation and the 2-NBDG assay was performed as described in Material and Methods. Phloretin was added 5 min before the 2-NBDG assay. The total incubation time was 4 h or 24 h. Results are shown as mean ± SEM of 2-NBDG MFI. **4 h)** Paired t-test: ** $p < 0.01$ vs. vehicle; + $p < 0.02$ vs. LPS. **24 h)** Wilcoxon test: * $p < 0.035$ vs. vehicle; Paired t-test: + $p < 0.02$ vs. LPS.

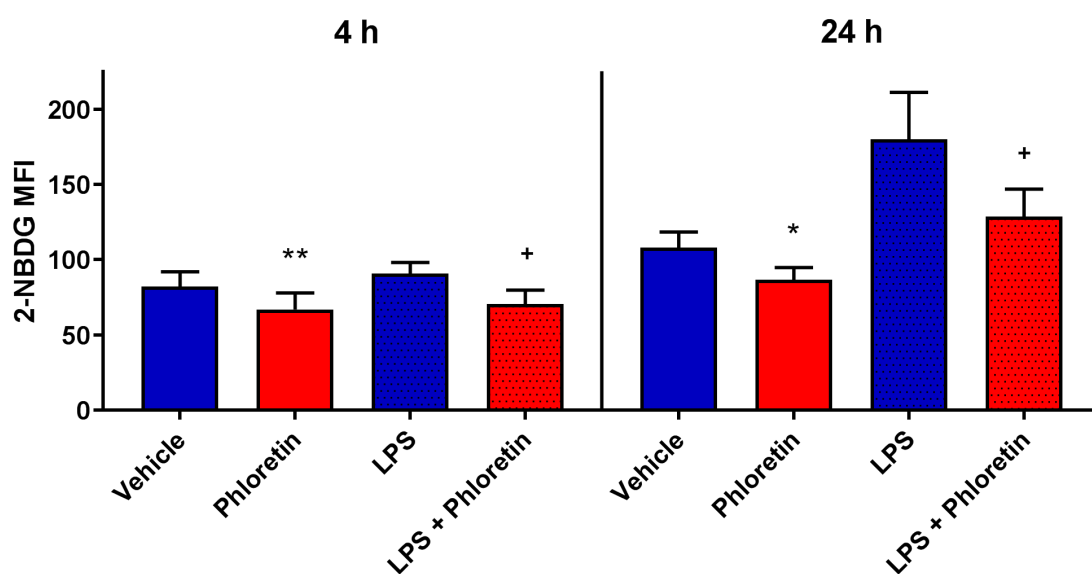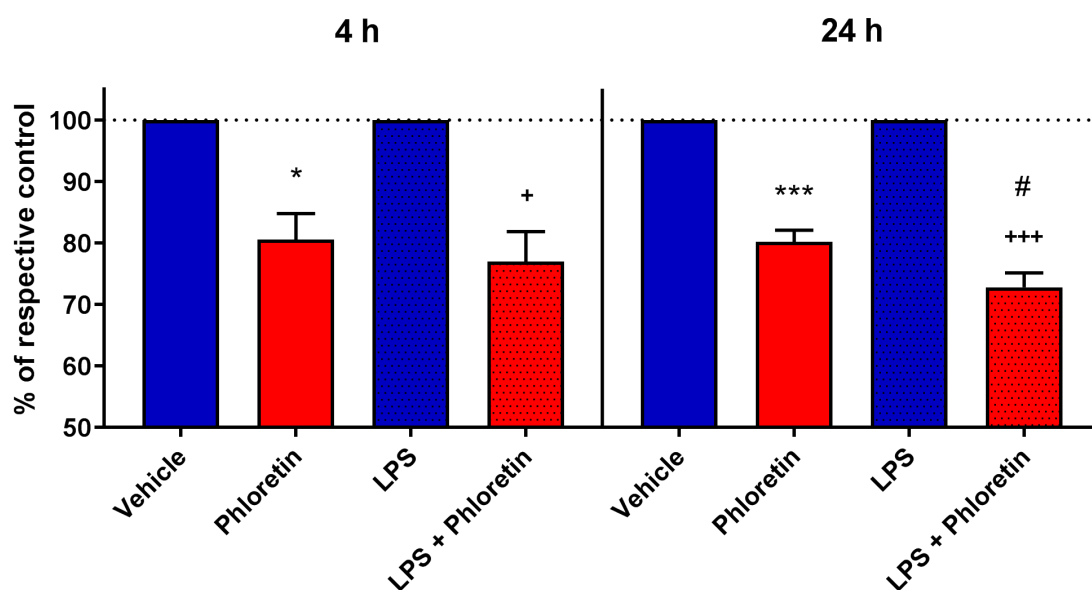**Figure 17. Normalized effect of phloretin on 2-NBDG uptake by splenocytes.** After 3 h (n=3 per group) or 23 h (vehicle n=6 per group; LPS n=5 per group) incubation with or without LPS, the medium was replaced by low glucose medium for the last hour of incubation and the 2-NBDG assay was performed as described in Material and Methods. Phloretin was added 5 min before the 2-NBDG assay. The total incubation time was 4 h or 24 h. The results were normalized to the simultaneously performed cultures that received vehicle or LPS, and shown as mean 2-NBDG MFI percentage $\pm$ SEM of the corresponding group. **4 h)** One sample t-test: * p<0.045 vs. vehicle; + p<0.045 vs. LPS. **24 h)** One sample t-test: *** p<0.001 vs. vehicle; +++ p<0.001 vs. LPS. Students t-test: # p=0.032 vs. phloretin.

3.1.4 Effect of IL-1 signaling on apoptosis and cell death

The strategy chosen to study if endogenously produced IL-1 affects glucose uptake by lymphocytes was to block its signaling by addition of IL-1Ra. Thus, it was essential to evaluate the effect of the antagonist on cell survival.

As can be seen in Figure 18A, treatment with 3 mg/ml IL-1Ra decreases the number of dead cells present in the samples. Independently of whether the cells were stimulated with LPS or not, this treatment resulted in 21 % less 7-AAD positive (dead) cells than in the corresponding control.

Also, a series of experiments containing both the apoptosis marker annexin V and the viability dye 7-AAD was performed to exclude the possibility that cells that are undergoing apoptosis but are not yet 7-AAD positive at the time point analyzed affect 2-NBDG uptake by IL-1Ra-treated samples. Figure 18B shows that the percentage of apoptotic cells is not higher in IL-1Ra-treated samples and that there is even a tendency to less apoptosis. The percentage of 7-AAD positive cells of the experiments with annexin V is shown for comparison. It does not differ from the series of experiments that contained only 7-AAD staining.
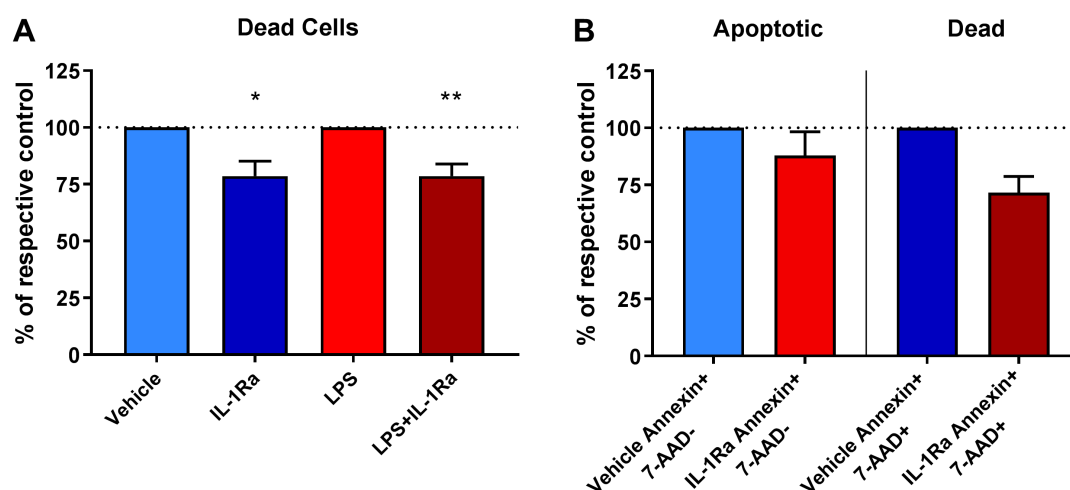
Figure 18. Effect of IL-1Ra on spleen cell survival. A) After 23 h incubation with (n=8 per group) or without (n=7 per group) LPS, the medium was replaced by low glucose medium and IL-1Ra or the corresponding vehicle was added for the last hour of incubation. Cells were stained with 7-AAD to detect dead cells. One sample t-test: * p<0.02 vs. vehicle; ** p<0.005 vs. LPS. Results are shown as mean percentage ± SEM of the respective control vehicle or LPS. **B)** Cells were incubated for 4 h (n=3 per group). After 3 h the medium was replaced by low glucose medium and IL-1Ra or the corresponding vehicle was added for the last hour of incubation. Annexin V and 7-AAD were used to detect apoptotic and dead cells respectively. Results are shown as mean percentage ± SEM of respective control cell count. Bars indicating 100 % in both panels are included for better appreciation of the differences.

3.1.5 Effect of blocking endogenous IL-1 on glucose uptake by splenocytes

For this and the following sections, it is important to remark that in most published reports the IL-1 antagonist has been added to the cells shortly before or at the same time as the immune stimulus (for example [Park et al., 2015]). As described in Material and Methods, in the studies shown here, IL-1Ra was always added 3 h or 23 h after LPS. Thus, IL-1 receptors were not already occupied by IL-1Ra before endogenous IL-1 started to be produced in the cultures. Instead, there was rather either a competition between the amount of IL-1 already produced during this time and the IL-1Ra added, or a displacement by IL-1Ra of already bound IL-1, which does not strictly mean a "blockade" in the usual sense. The expression "blockade of IL-1 receptors" is used below for reasons of simplicity. Since in preliminary experiments the antagonist showed only a small effect on 2-NBDG uptake by cells that were incubated for 4 h, the lower concentration (1 mg/ml) was omitted in experiments with the short incubation time.

Accordingly, IL-1Ra inhibition of 2-NBDG uptake after 4 h was also relatively small as can be seen in Figure 19. Both vehicle and LPS groups show about the same level of inhibition after 4 h of incubation and the addition of 3 mg/ml IL-1Ra. This is consistent with the fact that LPS exerts only a marginal effect on 2-NBDG uptake within 4 h. After 24 h of incubation, IL-1Ra exhibited a more pronounced and dose-dependent inhibition of 2-NBDG uptake by untreated and LPS-incubated cells.

The percentage of 2-NBDG uptake inhibition by IL-1Ra is shown in Figure 20. The IL-1Ra-treated groups differ significantly from the 100 % value of their respective control after 24 h incubation, and the inhibition correlates with cell stimulation. No effect of IL-1Ra is observed in vehicle-treated cells at 4 h, but it is detectable after 24 h. The maximal effect of IL-1Ra on 2-NBDG uptake is observed in LPS-stimulated cells after 24 h incubation. In these cultures, 1 mg/ml IL-1Ra has almost the same effect as 3 mg/ml in the vehicle-treated cells.

The percentual changes of 2-NBDG uptake in response to 3 mg/ml IL-1Ra are not significantly different between vehicle- and LPS-treated samples after 4 h of incubation.

After 24 h, however, IL-1Ra addition induced a significantly larger percentual decrease of 2-NBDG uptake by LPS-treated samples compared to vehicle-treated samples. To investigate if the effect of 3 mg/ml IL-1Ra on glucose uptake is elicited by an unspecific elevation of the protein concentration, we tested whether 3 mg/ml of the unrelated protein human serum albumin (HSA) would also induce changes in glucose uptake. The experiments were conducted the same way as described above, except that IL-1Ra was replaced by 3 mg/ml HSA. As shown in Figure 20, HSA has no effect on splenocyte 2-NBDG uptake.
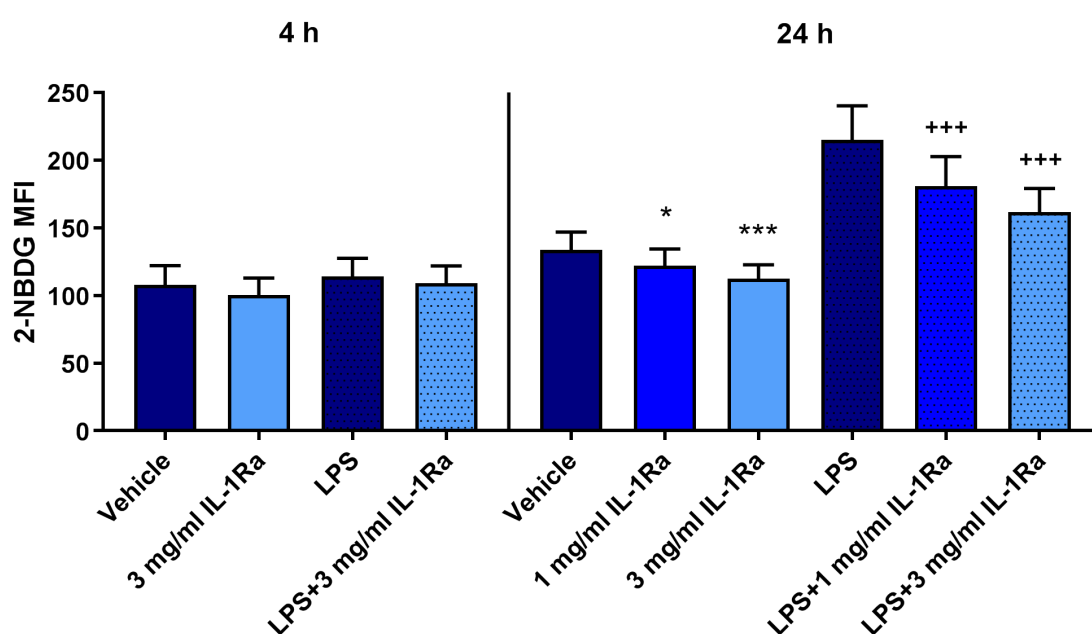
Figure 19. Blockade of IL-1 receptors decreases 2-NBDG uptake by splenocytes. After 3 h (n=6 per group) or 23 h (n=12 per group) incubation with or without LPS, the medium was replaced by low glucose medium and IL-1Ra or the corresponding vehicle was added for the last hour of incubation. The 2-NBDG assay were performed as described in Material and Methods. Results are shown as mean $\pm$ SEM of 2-NBDG MFI. **24 h**) Friedman Test and Dunn's multiple comparisons test: * $p<0.05$ and *** $p<0.001$ vs. vehicle. RM one-way ANOVA and Dunnett's multiple comparisons test: +++ $p<0.001$ vs. LPS.
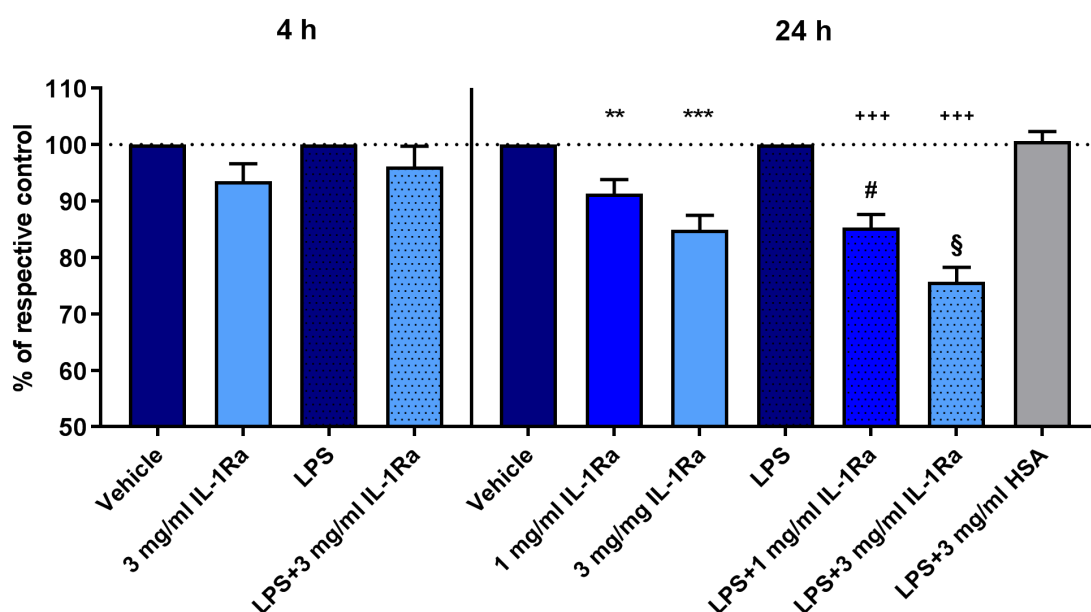
Figure 20. Blockade of IL-1 signaling decreases 2-NBDG uptake by spleen cells in a stimulation- and dose-dependent manner. After 3 h (n=6 per group) or 23 h (n=12 per group; HSA n=5 per group) incubation with or without LPS, the medium was replaced by low glucose medium and IL-1Ra or the corresponding vehicle was added for the last hour of incubation. The 2-NBDG assay were performed as described in Material and Methods. An additional group to test the effect of increased protein concentration on 2-NBDG uptake is also included here (LPS+3 mg/ml HSA). The results were normalized to the simultaneously performed cultures that received vehicle or LPS, and shown as mean 2-NBDG MFI percentage $\pm$ SEM of the corresponding group. **24 h)** One sample t-test: ** $p<0.01$ vs. vehicle; *** $p<0.001$ vs. vehicle; +++ $p<0.001$ vs. LPS. Bars indicating 100 % are included for better appreciation of the differences. Paired t-test for the other comparisons indicated in the figure: # $p<0.05$ vs. 1 mg/ml IL-1Ra; § $p<0.015$ vs. 3 mg/ml IL-1Ra.

3.1.6 Comparison of the effect of IL-1Ra and phloretin on glucose uptake by splenocytes

Phloretin, an inhibitor of GLUT- and SGLT-mediated glucose transport, served as a reference to evaluate the magnitude of the decreased 2-NBDG uptake caused by IL-1 blockade (Figure 21). The decrease in 2-NBDG uptake by phloretin was between 20 and 27 % depending on the time of incubation and whether the cells were stimulated with LPS or not.

As in the experiments described above, IL-1Ra did not induce a significant inhibition of 2-NBDG uptake after 4 h. However, the effects of IL-1Ra and phloretin were comparable after 24 h culture in stimulated and non-stimulated cells. This supports the observation that the percentage of 2-NBDG uptake that can be inhibited by IL-1Ra (thus IL-1-mediated 2-NBDG uptake) depends on the state of activation of the cells.
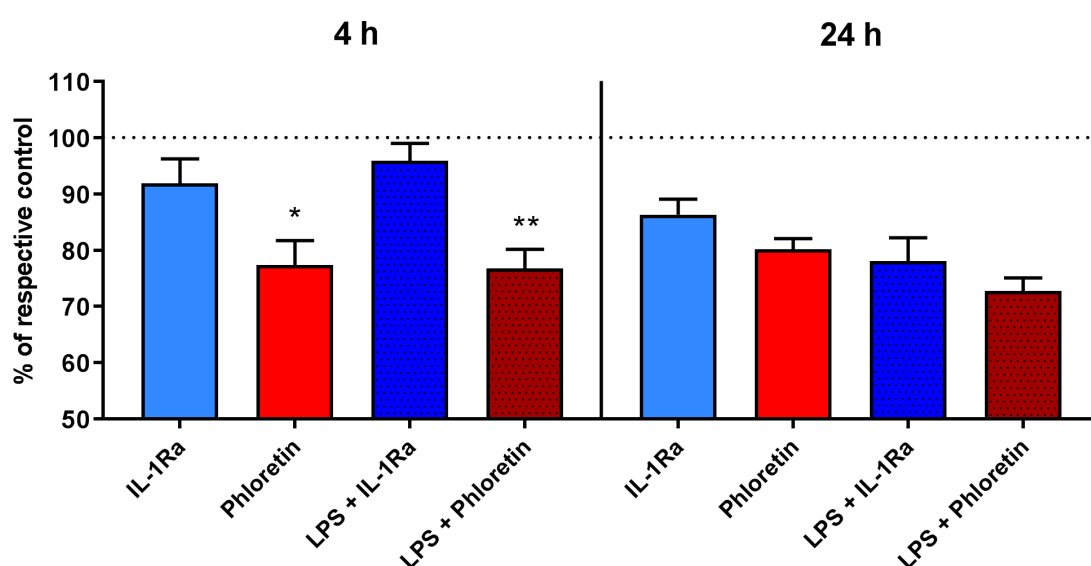
Figure 21. Comparison of IL-1Ra and phloretin effects on 2-NBDG uptake.
After 3 h (n=4 per group) or 23 h (groups without LPS n=6 per group, LPS groups n=5 per group) incubation with or without LPS, the medium was replaced by low glucose medium and IL-1Ra, or the corresponding vehicle was added for the last hour of incubation. Incubation with phloretin and the 2-NBDG assay were performed as described in Material and Methods. Results are shown as mean percentage $\pm$ SEM of the respective control 2-NBDG MFI. **4 h)** RM one-way ANOVA followed by Sidak's multiple comparisons test: * p<0.035 vs. 3 mg/ml IL-1Ra; ++ p<0.01 vs. LPS+3 mg/ml IL-1Ra.

3.2 Effect of IL-1 signaling on glucose uptake by B and T cells

As a next step, it was investigated whether there are differential effects of endogenously produced IL-1 on glucose uptake by T and B cells, the two main splenic immune cell populations. Essentially the same protocol as for the studies described above was followed, with the addition that specific markers to identify these cell populations were included. B cells were tagged with an antibody against the surface antigen B220 (CD45R) and T cells with an antibody against CD3, an accessory protein of the T cell receptor. First, glucose uptake by B and T cells with and without LPS stimulation and under the experimental conditions used in this work was investigated. In the experiments in which the effect of IL-1Ra on 2-NBDG uptake by the two cell types was tested, the antagonist was used at a concentration of 3 mg/ml.

3.2.1 2-NBDG uptake by B and T cells following LPS stimulation

Figure 22 shows the results of 2-NBDG uptake by T and B cells after 4 and 24 h in culture with and without LPS addition. The results are expressed as mean percentage of MFI relative to the corresponding simultaneous control. While no significant effect of LPS stimulation was observed in T cells after 4 h of incubation, B cells showed a modest (around 10 %) but statistically significant increased 2-NBDG uptake. These results were consistent with those reported in Section 3.1.2. Even after 24 h, 2-NBDG incorporation was not significantly changed in T cells that were incubated in the presence of LPS. B cells, in contrast, markedly enhanced 2-NBDG uptake to 247 % as compared to the corresponding non-stimulated controls.
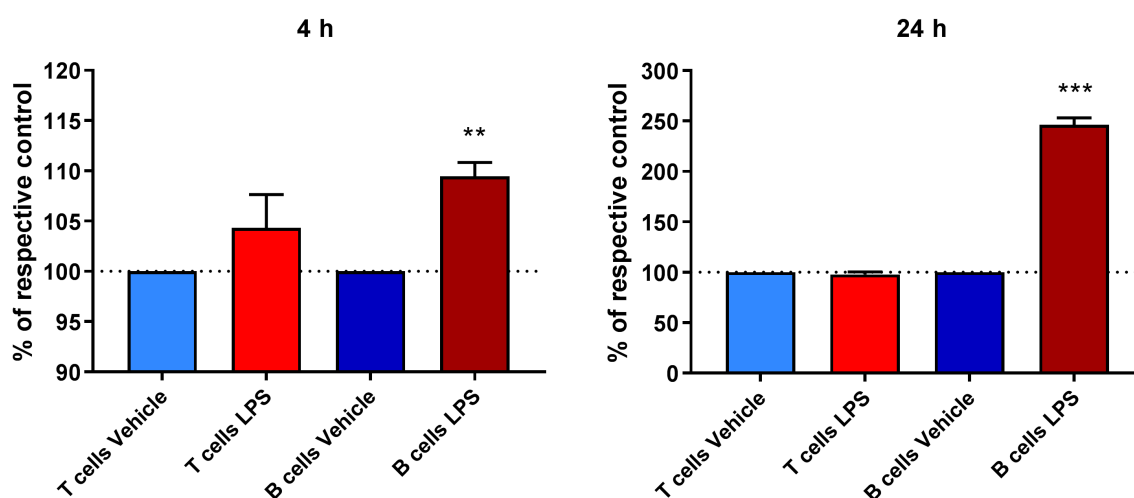
Figure 22. Effect of LPS on 2-NBDG uptake by B and T cells.

After 3 h (n=6 per group) or 23 h (n=10 per group) incubation with or without LPS, the medium was replaced by low glucose medium for the last hour of incubation and the 2-NBDG assay was performed as described in Material and Methods. T and B cells were discriminated by staining with antibodies to the surface antigens CD3 and B220, respectively. Results are shown as mean percentage $\pm$ SEM of the respective control 2-NBDG MFI. **4 h)** one sample t-test: ** $p<0.005$ vs. B cells+vehicle. **24 h)** One sample t-test: *** $p<0.001$ vs. B cells+vehicle. Bars indicating 100 % are included for better appreciation of the differences.

3.2.2 Effect of IL-1 blockade on glucose uptake by B cells

As described in Section 3.1.5 showing the effect of IL-1Ra on 2-NBDG uptake by whole spleen cell suspensions, there is a time-dependent increase of 2-NBDG uptake due to *in vitro* conditions (Figure 23). B cells display a notable increase of 2-NBDG uptake after 24 h in the vehicle-treated group. The 2-NBDG uptake of B cells exhibited a very low variability after 4 h, and there was no difference in the effect of IL-1Ra between cells that were incubated or not with LPS at this time point. The variability of the results was larger after 24 h of incubation, presumably due to inter-individual differences in the degree of activation. The inhibition of 2-NBDG incorporation in B cells by IL-1Ra was clearly larger after 24 h than after 4 h, and was more profound in LPS-treated cells than

in those that received the vehicle alone. B cells showed a pattern in response to IL-1Ra that was similar to the results of the whole spleen cell suspension, evaluated without the discrimination of individual cell types by fluorescent antibodies (Section 3.1.5). These results clearly indicate that the effect of blocking IL-1 receptors is larger when B cells are stimulated and incorporate more 2-NBDG than under basal conditions.

Figure 23. IL-1 blockade reduces B cell glucose uptake. After 3 h (n=6 per group) or 23 h (n=10 per group) incubation with or without LPS, the medium was replaced by low glucose medium and IL-1Ra or the corresponding vehicle was added for the last hour of incubation. B cells were tagged with an anti-B220 antibody. The 2-NBDG assay was performed as described in Material and Methods. **A)** Results are shown as mean $\pm$ SEM of 2-NBDG MFI. 4 h) Wilcoxon matched-pairs signed rank test: * p<0.035 vs. vehicle; 24 h) Paired t-test: ** p<0.005 vs. vehicle; +++ p<0.001 vs. LPS; Mann-Whitney test: ## p<0.003 vs. 4 h vehicle; **B)** Results are shown as mean percentage $\pm$ SEM of the respective control 2-NBDG MFI. 4 h) One sample t-test: *** p<0.001 vs. vehicle; 24 h) One sample t-test: *** p<0.001 vs. vehicle; +++ p<0.001 vs. LPS; Student's t-test: # p<0.05 vs. 24 h IL-1Ra.

3.2.3 Effect of IL-1 blockade on glucose uptake by T cells

Basal 2-NBDG uptake after 4 h incubation was almost threefold higher in T cells than in B cells (159 AU and 54 AU, respectively; Figures 23 and 24). However, 2-NBDG uptake by T cells did not increase over time, nor following LPS addition. There was no difference in the response to IL-1Ra by untreated and LPS-treated T cells. In contrast to B cells, the incorporation of the glucose analogue in T cells was markedly inhibited by IL-1Ra after 4 h incubation. There is even a tendency towards more inhibition by IL-1Ra after 4 h than after 24 h (Figure 24). Percentually, T cells showed a similar degree of 2-NBDG uptake inhibition in response to IL-1Ra as LPS-stimulated B cells after 24 h (24 % in T cells and 22 % in B cells).
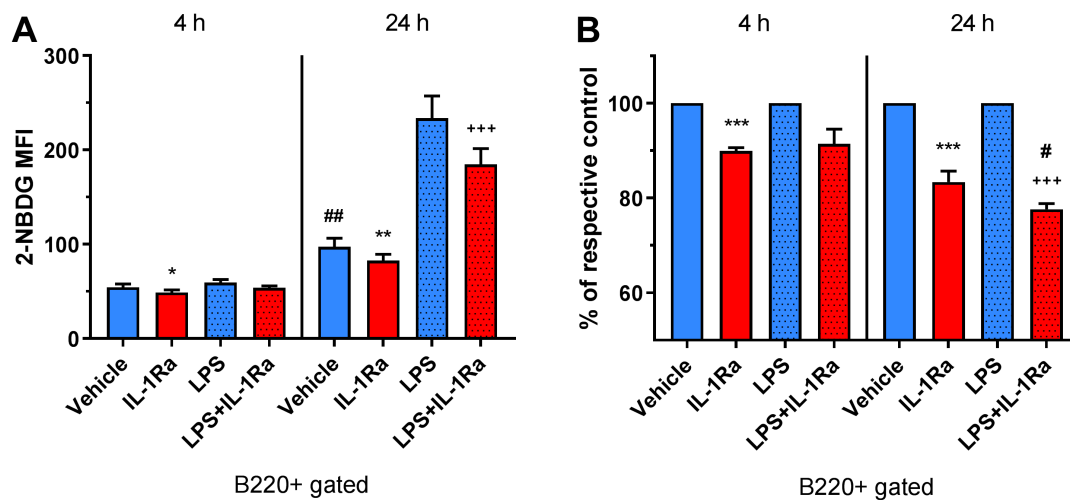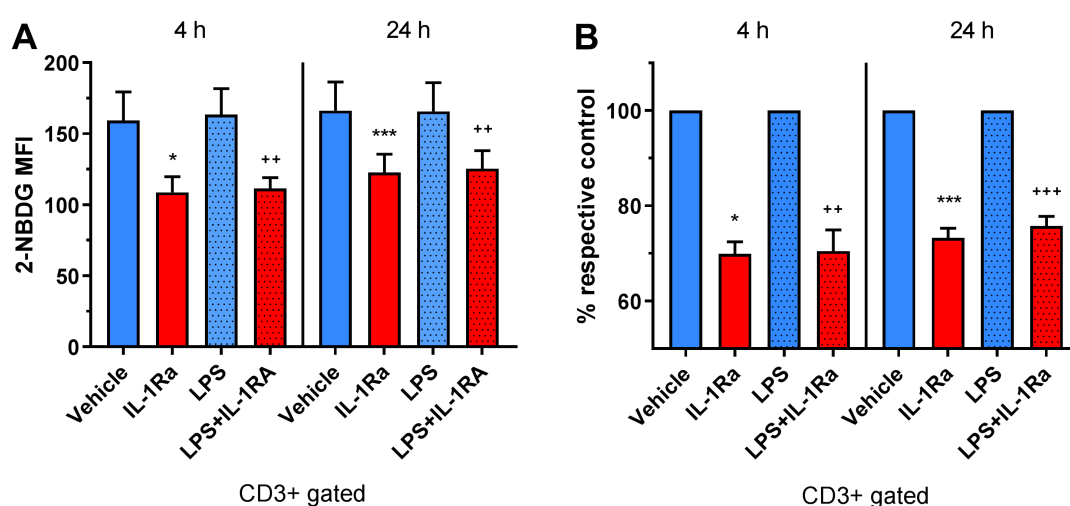

Figure 24. IL-1 blockade reduces T cell glucose uptake. After 3 h (n=6 per group) or 23 h (n=10 per group) incubation with or without LPS, the medium was replaced by low glucose medium and IL-1Ra or the corresponding vehicle was added for the last hour of incubation. T cells were tagged with an anti-CD3 antibody. The 2-NBDG assay was performed as described in Material and Methods. **A)** Results are shown as mean ± SEM of 2-NBDG MFI. 4 h) Wilcoxon matched-pairs signed rank test: * $p < 0.035$ vs. vehicle; Paired t-test: ++ $p < 0.01$ vs. LPS; 24 h); Paired t-test: *** $p < 0.001$ vs. vehicle; ++ $p < 0.005$ vs. LPS; **B)** Results are shown as mean percentage ± SEM of the respective control 2-NBDG MFI. 4 h) Wilcoxon Signed Rank Test: * $p < 0.035$ vs. vehicle; One sample t-test: ++ $p < 0.005$ vs. LPS; 24 h) One sample t-test: *** $p < 0.001$ vs. vehicle; +++ $p < 0.001$ vs. LPS.

3.3 Mechanisms involved in IL-1-mediated glucose uptake

The experiments described in this section were performed to investigate the contribution of three key pathways that could potentially be involved in IL-1-mediated glucose uptake by splenic cells, namely those mediated by MyD88, Kir6.2 and AKT/PKB. For this purpose, cells were obtained from MyD88 and $K_{ir}6.2$ KO mice, and AKT was inhibited pharmacologically. In each experimental round in which cells from KO mice were studied, cells derived from the corresponding WT mice were processed in parallel.

3.3.1 The effect of IL-1 on glucose uptake is not dependent on $K_{ir}6.2$ in splenocytes

To evaluate the role of $K_{ir}6.2$ in IL-1β-mediated glucose uptake, spleen cells from mice in which this ATP-sensitive K channel was knocked out were treated with IL-1Ra following a protocol comparable to the experiments described in the previous section. As depicted in Figure 25, cells from both $K_{ir}6.2$ KO and WT mice show a comparable, dose-dependent effect of IL-1Ra on 2-NBDG uptake. These results indicate that the inward-rectifier potassium channel is dispensable for the effect of IL-1 on glucose incorporation into immune cells.

3.3.2 The effect of IL-1 on glucose uptake by spleen cells is MyD88-independent

As described in Section 1.1.3, IL-1R1 signaling via the receptor adapter protein MyD88 is well described, and, although other alternatives are known at present, it is considered a major pathway of IL-1 signal transduction. Therefore, MyD88 was a candidate to study the pathway by which IL-1 may affect glucose uptake. As expected, MyD88-deficient spleen cells did not increase 2-NBDG uptake in response to LPS, because the LPS-sensing TLR4 is also dependent on MyD88 [Kawai et al., 1999]. However, spleen cells obtained from MyD88 KO mice did not show an altered response to IL-1Ra in their 2-NBDG uptake compared to the WT (Figure 26).

Figure 25. Effect of IL-1 blockade on 2-NBDG uptake by K_{ir}6.2 knockout splenocytes.
Spleen cell suspensions were obtained from K_{ir}6.2 KO and C57Bl/6J (WT) mice (n=3 per genotype) and incubated with or without LPS. The total incubation time was 24 h. Incubation with IL-1Ra and the 2-NBDG uptake were performed as described in Material and Methods. Results are shown as mean $\pm$ SEM of 2-NBDG MFI. K_{ir}6.2 KO: RM one-way ANOVA followed by Sidak's multiple comparison test: * p<0.015 vs. vehicle; + p<0.04 vs. LPS. WT: RM one-way ANOVA followed by Sidak's multiple comparison test: * p<0.035 vs. vehicle; + p<0.035 vs. LPS.
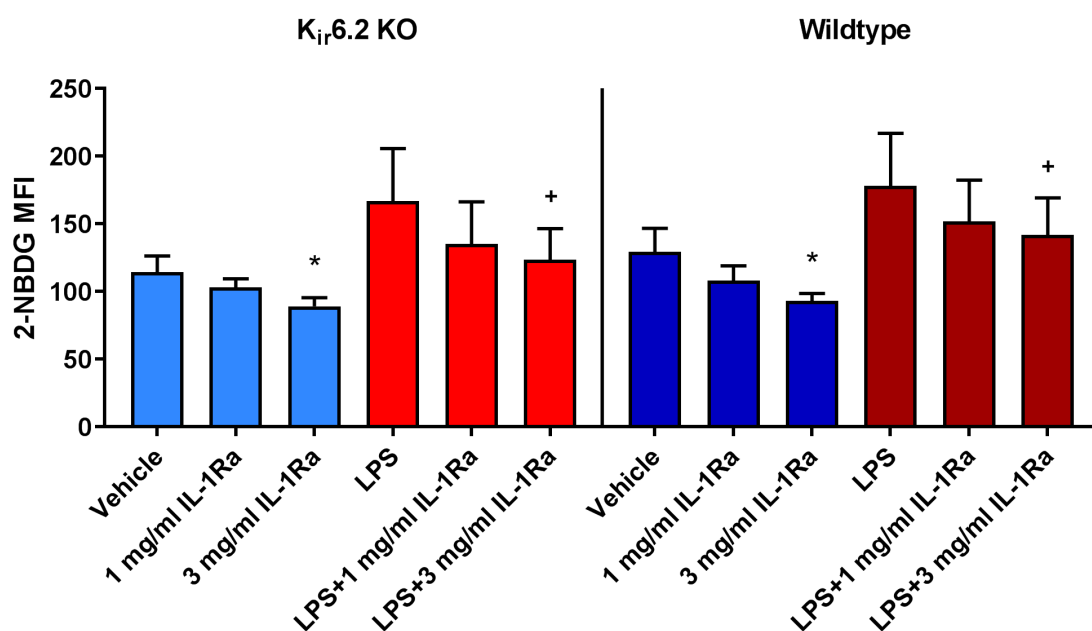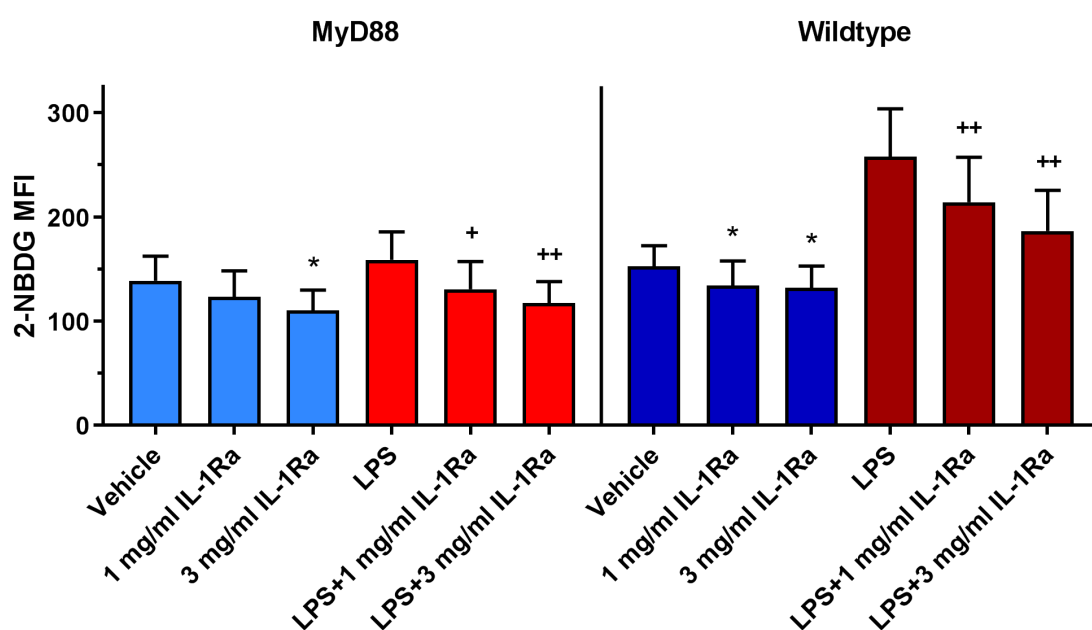
Figure 26. Effect of IL-1 blockade on 2-NBDG uptake by MyD88 knockout splenocytes. Spleen cell suspensions were obtained from MyD88 KO and C57Bl/6J (WT) mice (n=3 per genotype) and incubated with or without LPS. The total incubation time was 24 h. Incubation with IL-1Ra and the 2-NBDG uptake were performed as described in Material and Methods. Results are shown as mean $\pm$ SEM of 2-NBDG MFI. MyD88 KO: RM one-way ANOVA followed by Sidak's multiple comparison test: * p<0.015 vs. vehicle; + p<0.02 vs. LPS; ++ p<0.005 vs. LPS. WT: RM one-way ANOVA followed by Sidak's multiple comparison test: * p<0.03 vs. vehicle; ++ p<0.01 vs. LPS; ++ p<0.002 vs. LPS.

3.3.3 The effect of IL-1 on glucose uptake is not dependent on AKT

To further explore the signaling pathway by which IL-1 leads to stimulation of 2-NBDG uptake, experiments with an inhibitor of AKT/PKB were performed. It has been reported that AKT enhances the expression of glucose transporters [Frauwirth et al., 2002, Doughty et al., 2006, Caro-Maldonado et al., 2014], and the potent PH-domain AKT inhibitor VIII (AKTi8) decreased 2-NBDG uptake by T cells as expected. The decrease was comparable in magnitude to the effect caused by addition of IL-1Ra (Figure 27). The effect of the simultaneous addition of IL-1Ra and the AKT inhibitor on 2-NBDG uptake by T cells was not significantly different from the effect exerted by each substance alone, but

tended to be additive. Surprisingly, addition of the AKT inhibitor resulted in the opposite effect on B cells, namely it increased 2-NBDG incorporation in this cell type. IL-1Ra was still capable of decreasing 2-NBDG uptake by B cells in which AKT activity was inhibited (Figure 27). Comparable results were consistently obtained in 4 independent experimental rounds. These results indicate that AKT is not involved in IL-1Ra-mediated decrease of 2-NBDG uptake by B cells.
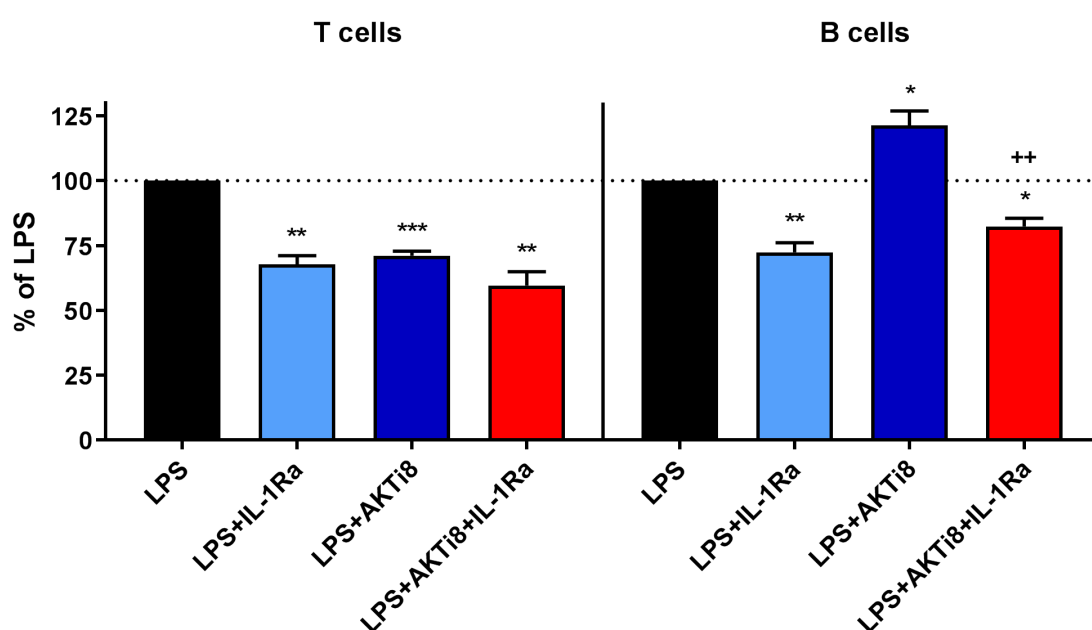
Figure 27. Effect of AKT inhibition on IL-1Ra-induced decrease of 2-NBDG uptake. After incubating spleen cells for 23 h with LPS (n=4 per group), the culture medium was replaced by low glucose medium, as in previous experiments. The AKT inhibitor AKTi8 (final concentration 25 μM) was added to the indicated cultures 30 minutes before the incubation was terminated after 24 h. IL-1Ra (3 mg/ml) was added to the corresponding cultures 5 minutes after AKTi8. 2-NBDG was added 7 minutes before harvesting the cells for flow cytometric analysis, as in the previous experiments. Results are shown as mean percentage $\pm$ SEM of LPS 2-NBDG MFI. T cells: One sample t-test: ** $p<0.005$ vs. LPS; *** $p<0.001$ vs. LPS; B cells: One sample t-test: ** $p<0.005$ vs. LPS; * $p<0.03$ vs. LPS; RM one-way ANOVA followed by Sidak's multiple comparison test: ++ $p<0.002$ vs. LPS+AKTi8.

3.4 Effect of exogenous IL-1β on 2-NBDG uptake by splenocytes

The results described above showing that 2-NBDG uptake decreases when IL-1 receptors are blocked demonstrate that endogenously produced IL-1 can affect glucose incorporation in immune cells. The question addressed in this section was whether exogenous administration of the cytokine can increase glucose uptake. As shown in Figure 28, addition of IL-1β resulted in increased 2-NBDG uptake after 1 h of incubation. Although modest, such increase was statistically significant in B cells. The same tendency was observed in T cells, but the response showed larger variability than in B cells. In fact, in one experimental round the uptake of the glucose analogue by T cells doubled the increase induced in B cells when IL-1 was added to the cultures. The response of B cells to IL-1β was more homogenous and statistically significant differences were detected with the higher doses used when compared to the corresponding control group.
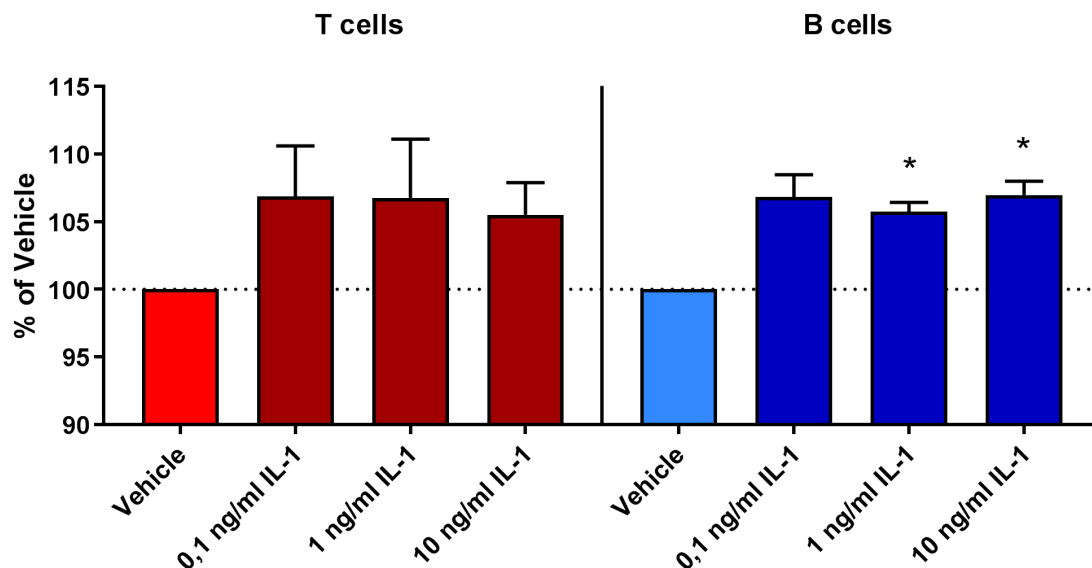

Figure 28. 2-NBDG uptake by splenocytes in the presence of IL-1β. After 3 h incubation (n=3 per group), spleen cell suspensions received the indicated doses of human recombinant IL-1β or the vehicle alone, and the cultures were further incubated for one hour. Results are shown as mean percentage ± SEM of LPS 2-NBDG MFI. One sample t-test: * p<0.025 vs. vehicle.

It should be remarked that the different concentrations of IL-1β did not elicit a dose-dependent increase neither in T nor in B cells. It seems that the receptors are already saturated at the lowest concentration used in these studies.

3.5 Effects of endogenous IL-1 on splenic cell energetic metabolism

In the previous sections, the contribution of IL-1 to affect the dynamic capacity of glucose transport across the cell membrane of immune cells was investigated. The experiments described in this section were designed to study if IL-1 can also affect energetic metabolism in spleen cells. For this purpose, OCR and ECAR, two parameters that allow conclusions about oxidative phosphorylation in the mitochondria and glycolysis, were evaluated by an assay that allows to perform a live-cell metabolic flux analysis. For reasons of brevity, this methodology is termed "Seahorse assay" in the following sections.

The Seahorse assay displays very dynamic signals, with a fast reaction to injections. Even injection of medium alone can result in perturbations of these signals. An example is provided in Figure 32F, where medium injection led to an increase of ECAR in the LPS group. To reduce disturbances, cells were seeded directly in the assay plates 24 h before the actual measurements, and manipulations were kept to a minimum on the day of the Seahorse run.

Although after the plate was inserted in the Seahorse apparatus, there was an equilibration phase of 10 min, in some experiments the baseline of OCR and ECAR was not yet established when measurements began. It is not clear to what extent this phenomenon is caused by reactions of the fluorophores to medium change or an increase in metabolism. Nevertheless, in all experiments a baseline was established after further 20 min, before injections were made. Similar to the flow cytometric experiments, cell suspensions of different mice showed a variation of the absolute values, as can be seen in the left columns of Figures 29 and 30. Thus, for better comparability, the results are first presented as absolute OCR and EACR and subsequently as relative values normalized to their respective control.

3.5.1 Effect of endogenous IL-1 on mitochondrial respiration in splenocytes

After 24 h of incubation and replacement of the medium, 3 cycles of measurements were performed to record a stable baseline (for detailed protocol 2.13). Considering the different cell numbers (4.5×10^5 per vehicle sample and 3×10^5 per LPS sample) OCR was about double in LPS-stimulated cells as compared to cells that did not received LPS. IL-1Ra (3 mg/ml) was injected 20 minutes after starting the recording and a sharp and marked reduction (about 50 %) in OCR was observed in both non-LPS (Figure 29 A, C) and LPS-incubated cells (Figure 30 A, C, E). This indicates that IL-1Ra injection led to a decreased mitochondrial function. The OCR values in the non-LPS-stimulated samples that received IL-1Ra started to recover and returned to the basal levels 1 to 1.5 h later. In contrast, the OCR of the LPS-treated samples did not completely recover and remained low for at least 4 and a half hour, until the following mitochondrial function test was performed.

The subsequent injection of oligomycin, FCCP, and antimycin-A/rotenone allows to determine the proton leak, maximal respiratory capacity and the non-mitochondrial oxygen consumption, as described in Section 2.12. The effect of these substances on the rate of oxygen consumption is dependent on the activation and metabolic activity of the spleen cells. In some experiments, the basal OCR was already at the maximal respiratory capacity, while cells of other experiments displayed a lower basal OCR. These results are shown in the right columns of Figures 29 (B,D) and 30 (B,D,F), which correspond to the respective determinations done at earlier time points in the same cells after injection of vehicle or IL-1Ra (A and C in Fig. 29, and A, C and E In Figure 30). It seems that the effect of IL-1Ra on the maximal respiratory capacity after FCCP injection is also dependent on the metabolic activity of the cells. IL-1Ra only reduced the maximal respiratory capacity when the OCR was comparably low at the beginning of the experiment. Since IL-1Ra induced changes in proton leak and non-mitochondrial respiration cannot be seen as clear as the maximal respiratory capacity in the raw data, they will be presented as bar diagrams in Section 3.5.3 and will be discussed there.

Figure 29. Effect of IL-1 blockade on the OCR of spleen cells. The Seahorse assay was started 24 h after incubation of the spleen cells. After 3 initial measurements performed in 20 min, 3 mg/ml IL-1Ra or the vehicle alone were injected to the indicated samples. Each pair of graphs (A+B; C+D) represents one experiment with n=6 samples per group. The graphs on the left depict the OCR during the first 180 minutes after injection of IL-1Ra or vehicle. The graphs on the right show the continuation of the recordings after the consecutive injection of oligomycin, FCCP and rotenone/antimycin-A (R/AA). Results are shown as mean OCR $\pm$ SEM. Two-way ANOVA followed by Fisher's LSD test was performed to compare the results of the groups treated with IL-1Ra with those that received the vehicle alone. * $p<0.05$; ** $p<0.01$; *** $p<0.001$.
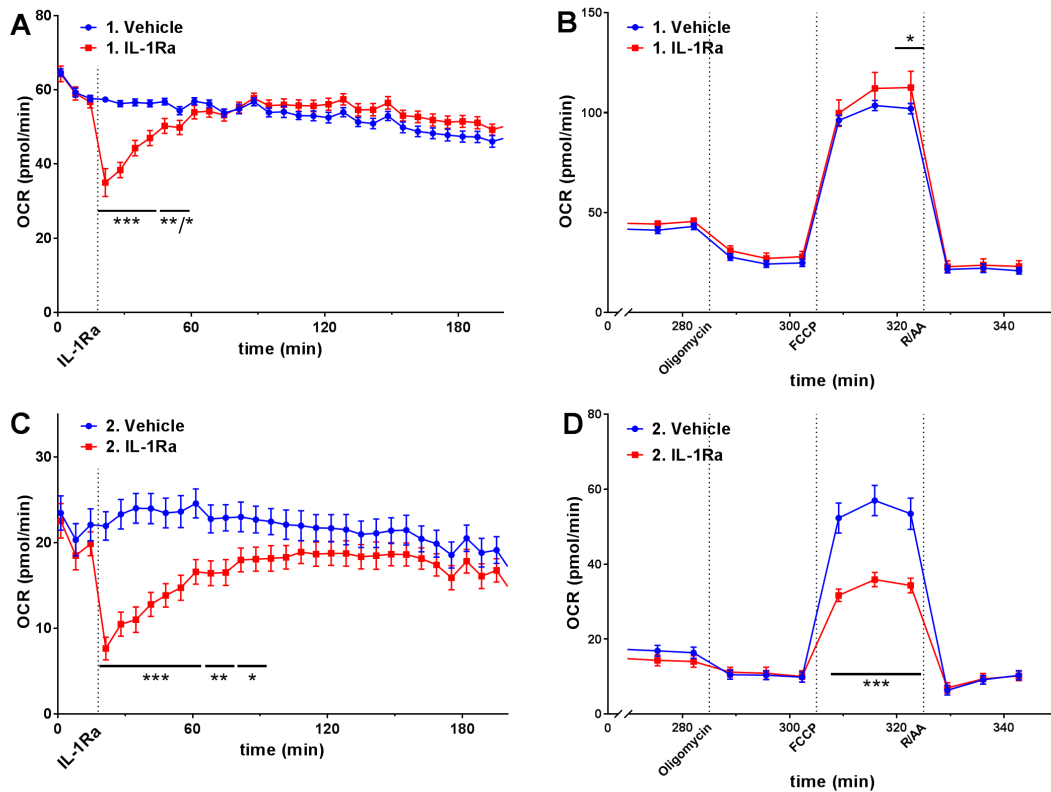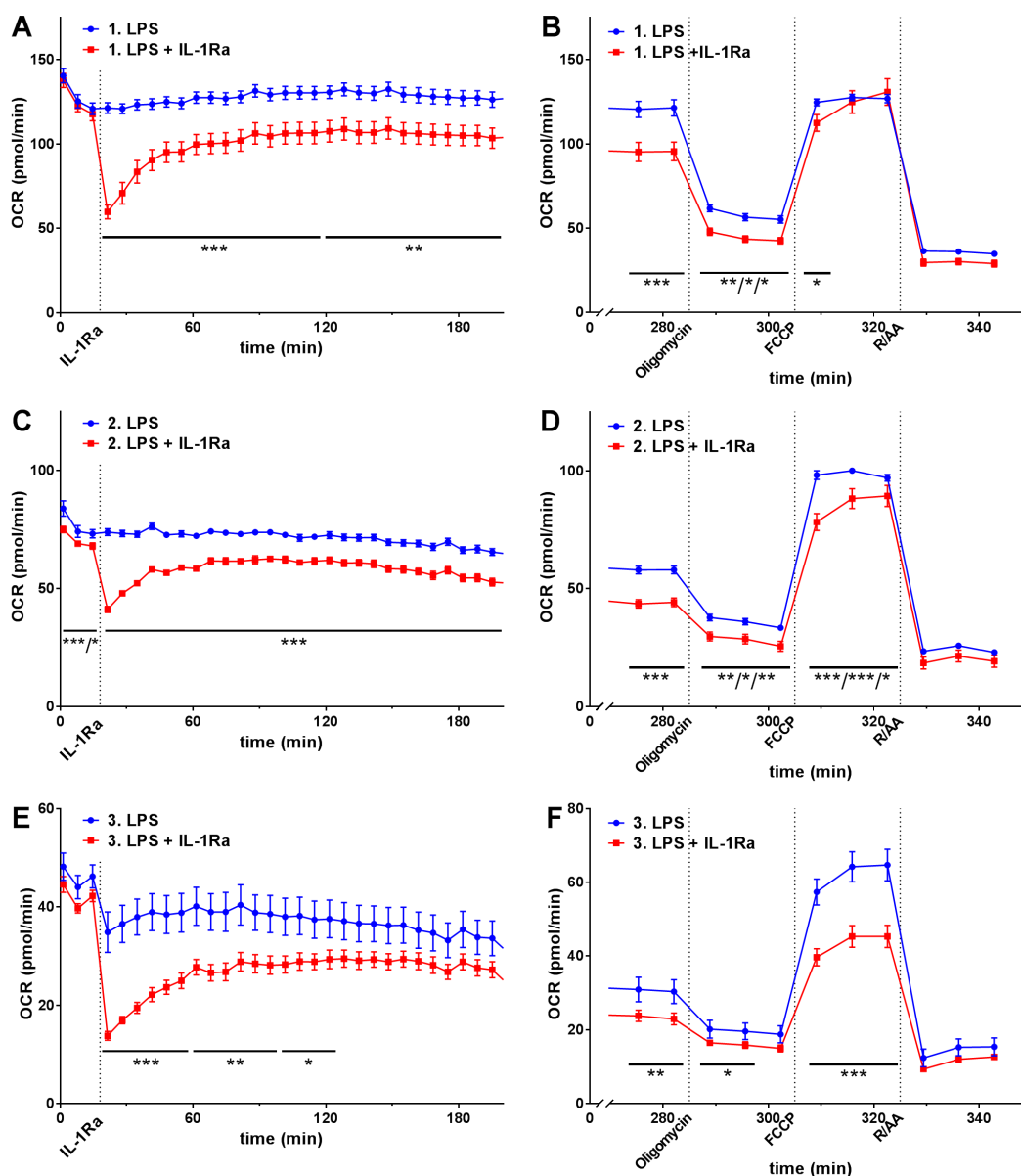
Figure 30. Effect of IL-1 blockade on the OCR of LPS-stimulated spleen cells. The Seahorse assay was started 24 h after incubation of the spleen cells with LPS. After 3 initial measurements performed in 20 min, 3 mg/ml IL-1Ra or the vehicle alone were injected to the indicated samples. Each pair of graphs (A+B; C+D; E+F) represents one experiment with n=6 samples per group. The graphs on the left depict the OCR during the first 180 minutes after injection of IL-1Ra or vehicle. The graphs on the right show the continuation of the recordings after the consecutive injection of oligomycin, FCCP and rotenone/antimycin-A (R/AA). Results are shown as mean OCR $\pm$ SEM. Two-way ANOVA followed by Fisher's LSD test was performed to compare the results of the groups treated with IL-1Ra with those that received the vehicle alone. * p<0.05; ** p<0.01; *** p<0.001.

Figure 31 shows the OCR of the groups that received IL-1Ra as mean percentage of the corresponding group without the antagonist. The proton leak and non-mitochondrial oxygen consumption indicated in the figure were calculated from the corresponding values in the right panels of Figures 29 and 30. The fraction of oxygen consumption that is specific for ATP production was almost completely abolished in response to IL-1Ra. The OCR recovered to the initial level in the IL-1Ra-treated vehicle samples but not in the LPS-incubated samples that received IL-1Ra.
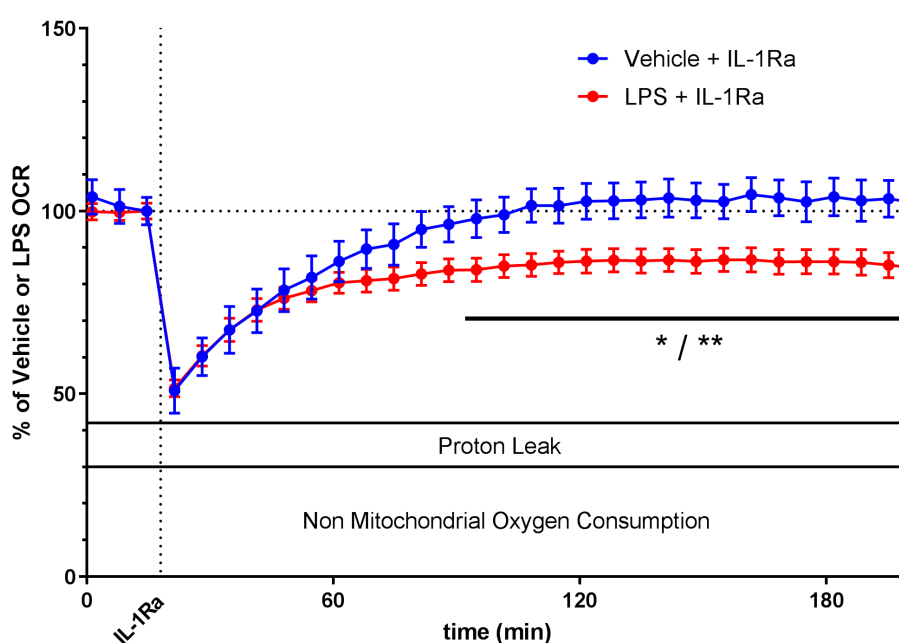
Figure 31. Normalized effect of IL-1 blockade on the OCR of stimulated and non-stimulated spleen cells. After 24 h in culture with or without LPS and 3 initial measurements to determine the base line, IL-1Ra (3 mg/ml) or the vehicle alone were added to the samples. The results shown in Figures 29 and 30 are depicted here as mean percentage of the corresponding control group (no IL-1Ra injection). Results are shown as mean percentage OCR $\pm$ SEM of 12 samples (vehicle) and 18 (LPS) samples from 2, respectively 3 independent, experiments. Two-way ANOVA followed by Fisher's LSD test was performed to compare the effect of IL-1Ra on cells that were cultured with LPS (LPS+IL-1Ra) with those that received the vehicle alone (Vehicle +IL-1Ra): * p<0.05; ** p<0.01.

It has to be considered that although non-LPS-stimulated and LPS-stimulated cells show a comparable relative OCR decrease in response to IL-1Ra, the initial absolute values of the LPS-treated samples were much higher than in the non-LPS-stimulated samples. It is worth noting that the effect of blocking IL-1 receptors on OCR is comparable in magnitude to the effect of completely blocking ATP synthesis by oligomycin.

3.5.2 Effect of endogenous IL-1 on the rate of extracellular acidification in LPS-stimulated splenocytes

Addition of IL-1Ra to non-LPS-stimulated spleen cells resulted in a marked increase (about 5-fold) in the ECAR, followed by a relatively rapid decline and a prolonged plateau phase of elevated EACR, with a tendency to drop below the basal value after around 2 h (Figure 32, panels A, C, E). Interestingly, the response to IL-1Ra of LPS-incubated cells was clearly different (Figure 32, panels B, D, F). First, a small but distinct reduction to a lower ECAR occurred that was followed by a further slow decrease, similar to the plateau phase in non-LPS-incubated groups. Figure 32 F shows a probably unspecific perturbation after medium injection in the LPS group. Therefore, the ECAR values shown in Figure 32 F were excluded from the calculation of percentage values in Figure 33.
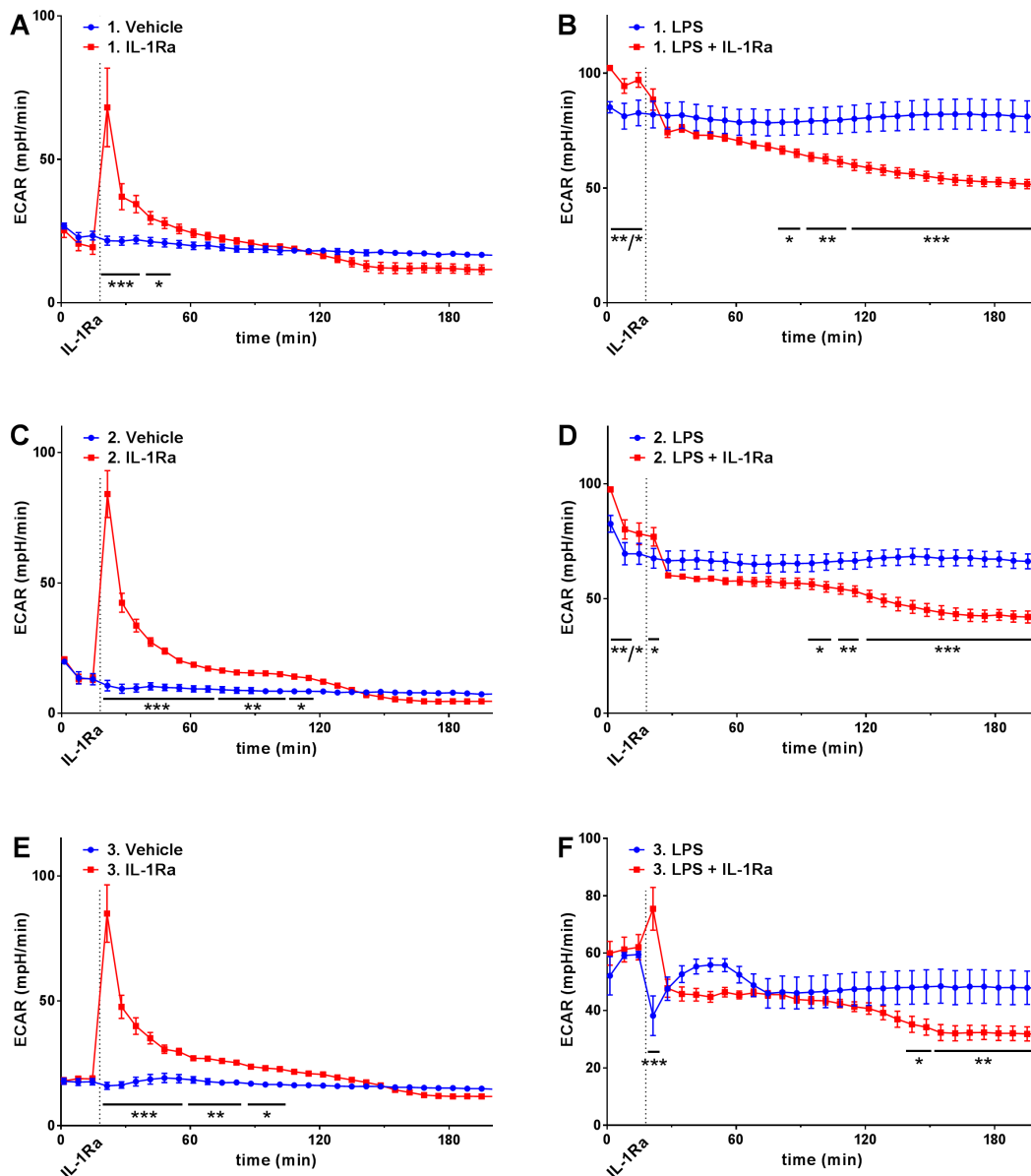
Figure 32. Effect of IL-1 blockade on the ECAR of spleen cells. The Seahorse assay was started 24 h after incubation of the spleen cells with or without addition of LPS. After 3 initial measurements performed in 20 min, 3 mg/ml IL-1Ra or the vehicle alone were injected to the indicated samples. Each pair of graphs (A+B; C+D; E+F) represents one experiment with n=6 samples per group. The graphs on the left depict the samples that were not incubated with LPS, and the graphs on the right side depict the LPS-stimulated samples of the corresponding experiment. Results are shown as mean ECAR ± SEM. Two-way ANOVA followed by Fisher's LSD test was performed to compare LPS and LPS+IL-1Ra data. * $p<0.05$; ** $p<0.01$; *** $p<0.001$.

Because of the variability in absolute values between the individual experiments, the data of the IL-1Ra-injected groups shown in Figure 32 are presented in Figure 33 as percentage of the respective control (no IL-1Ra injection) for a more comprehensive summary.
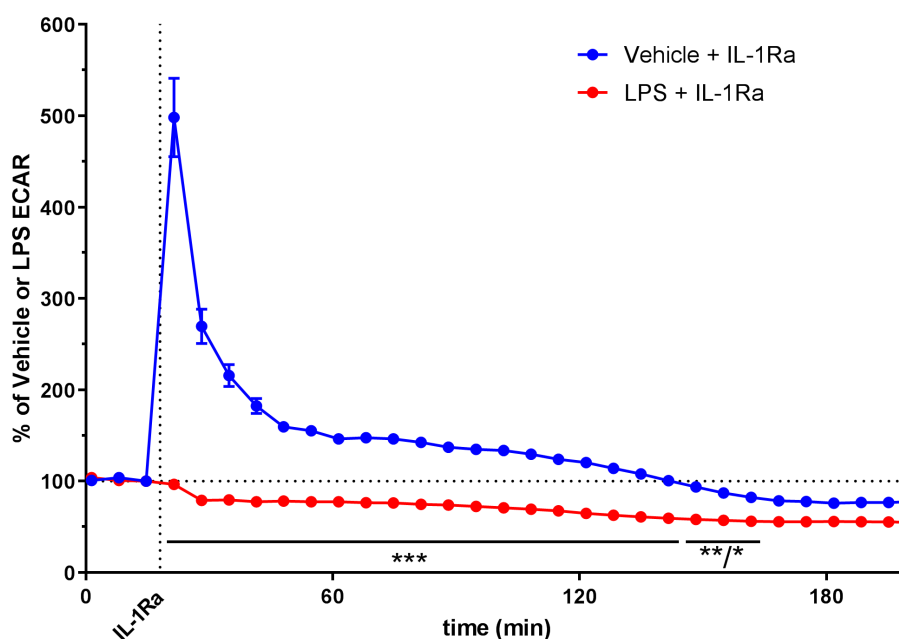
Figure 33. Normalized effect of IL-1 blockade on the ECAR of stimulated and non-stimulated spleen cells. After 24 h in culture with or without LPS addition and 3 initial measurements to determine the base line, IL-1Ra (3 mg/ml) or the vehicle alone were added to the samples. The results shown in Figure 32 are depicted here as mean percentage of the corresponding control group (no IL-1Ra injection). Results are shown as mean percentage $\pm$ SEM of 18 samples (vehicle) and 12 (LPS) samples from 3, respectively 2, independent experiments. Two-way ANOVA followed by Fisher's LSD test was performed to compare the effect of IL-1Ra on LPS-treated cultures with those that did not received LPS (vehicle). * $p<0.05$; ** $p<0.01$; *** $p<0.001$.

The ECAR of the non-LPS-stimulated groups raised about 5-fold immediately after IL-1Ra injection. This steep increase dropped sharply, but remained elevated for 2 h before returning to the basal level and stabilized even below. In LPS-stimulated cells, the

first ECAR data point after IL-1Ra injection persisted almost at the basal level, followed by a subsequent decrease. Analogous to the non-LPS-stimulated samples, there was also a plateau phase, and the basal ECAR was not recovered in any of the two groups.

3.5.3 Parameters derived from the OCR determinations

The parameters proton leak, maximal respiratory capacity, and non-mitochondrial respiration derive from the measurements of the OCR performed after addition of the ATP-synthase blocker oligomycin, the ionophore FCCP and the respiratory chain blockers rotenone/antimycin-A. No statistically significant differences were detected in the mentioned parameters between cultures that received IL-1Ra and the vehicle alone when cells were not overtly stimulated (Figure 34 A). No changes in proton leak, maximal respiratory capacity and non-mitochondrial respiration are evidence for a transient action of IL-1-blockade in nonovertly stimulated cells.

In the LPS-stimulated cells, however, IL-1Ra treatment resulted in significantly reduced proton leak and non-mitochondrial respiration, while the maximal respiratory capacity of the mitochondria was not affected (Figure 34 B). The stability of the maximal respiratory capacity is especially noteworthy, because a decrease in the OCR in response to IL-1Ra, as seen in Figures 30 and 31, could also have been the result of a reduced number of viable cells. In contrast, a decrease in proton leak, which indicates a lower mitochondrial membrane-potential, combined with a stable maximal respiratory capacity, indicates that the cells downregulate mitochondrial activity, but are able to increase it again to the same maximal level as the vehicle-injected group when energetically challenged.

71
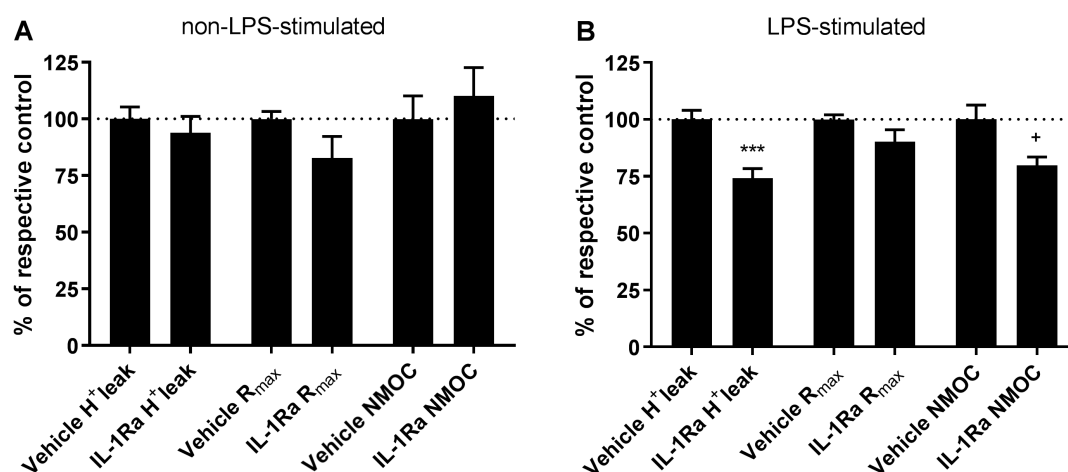
Figure 34. Effects of IL-1 blockade on spleen cell proton leak, maximal respiratory capacity and non-mitochondrial oxygen consumption. The Seahorse assay was started 24 h after incubation of spleen cells with or without LPS. After 3 initial measurements performed in 20 min, 3 mg/ml IL-1Ra or the vehicle alone were injected into the indicated samples. After another 4.5 h the sequence of oligomycin, FCCP and rotenone/antimycin-A was injected for measurement of mitochondrial proton leak, maximal respiration, and non-mitochondrial respiration, as described in Material and Methods. Results are shown as mean percentage $\pm$ SEM of the group that received the vehicle alone. Non-LPS-stimulated (n=12 per group) and LPS-stimulated (n=18 per group) samples were obtained from 2, respectively 3, independent experiments. **A)** No statistical significant differences were found in non-LPS-stimulated cells. **B)** Results of LPS-stimulated cells were analysis by Students t-test, *** p<0.001 vs. vehicle H^+ leak, and Students t-test with Welch's correction + p<0.015 vs. vehicle NMOC. H^+ leak: proton leak; R_{max}: maximal respiratory capacity; NMOC: non-mitochondrial oxygen consumption.

3.5.4 IL-1Ra effect on OCR and ECAR of spleen cells from MyD88 knockout mice

As in the experiments designed to explore the effect of endogenously produced IL-1 on glucose uptake, spleen cells from MyD88 KO mice reacted to IL-1Ra in the metabolic flux analysis with a response similar to WT cells (Figure 35). Interestingly, although there was no upregulation of metabolism by LPS, MyD88 KO cells that were incubated in the presence of the endotoxin resembled the response of the LPS-stimulated WT cells

to IL-1Ra. In both LPS-incubated MyD88 KO and WT cells, the OCR did not return to the baseline after IL-1Ra injection, as non-LPS-incubated cells did, but remained below 90 % of the basal value (Figure 35B).
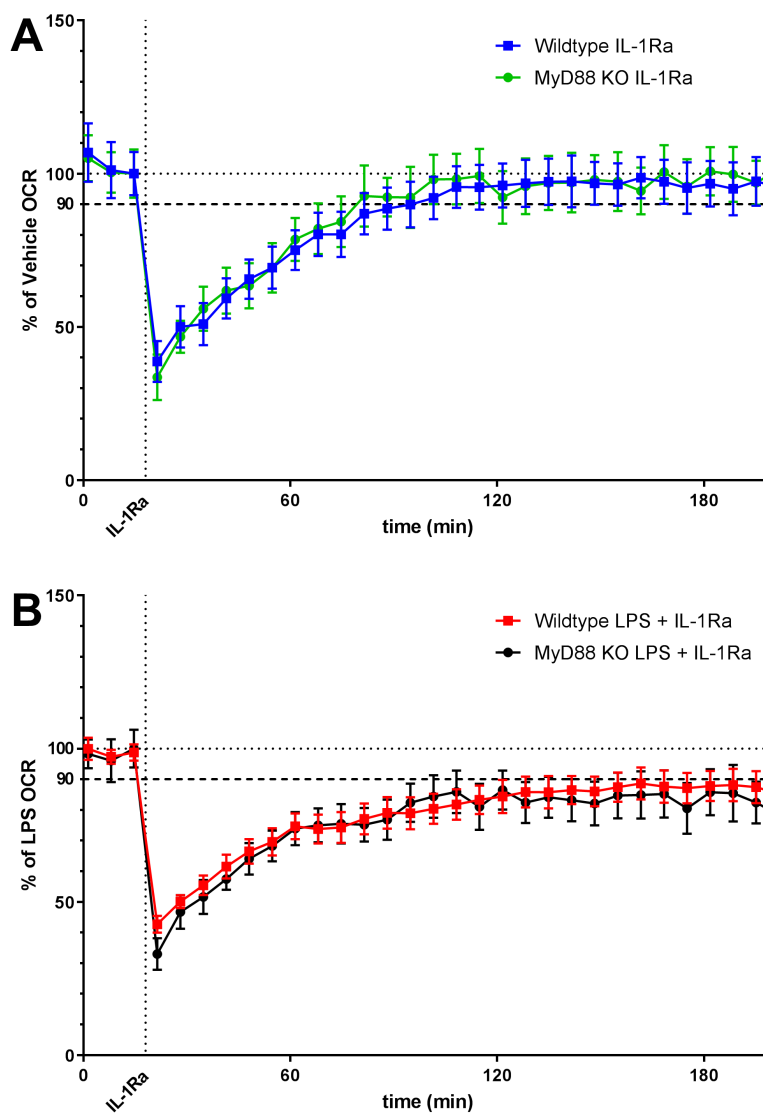
Figure 35. Effects of IL-1 blockade on MyD88 knockout spleen cell OCR. The experiments were performed as described in the legend to figure 31. MyD88 KO and WT cells were incubated without (A) or with LPS (B). The metabolic assay was performed 24 h later. Vehicle or IL-1Ra (3 mg/ml) were added after establishing a basal value. Results are expressed as percentage of the simultaneous group that received the vehicle alone (mean ± SEM; n=6 per group). No statistically significant differences between the response of MyD88 KO and WT cells to IL-1Ra was found.

However, the difference between non-LPS and LPS-incubated MyD88 KO spleen cells in their response to IL-1Ra was not statistically significant, probably because of the relatively low number of samples. The ECAR response of MyD88 KO spleen cells to IL-1Ra was also comparable to that of the corresponding WT cells (Figure 36A). LPS-incubated MyD88 KO cells showed a significantly different ECAR after the injection of IL-1Ra when compared to the response of the LPS-stimulated WT cells, because the endotoxin did not affect ECAR in MyD88 KO cells (Figure 36B). Taken together, these results indicate that MyD88 is not indispensable for the effect of IL-1-blockade on OCR and ECAR.

3.5.5 Effect of exogenous IL-1β on spleen cell metabolism

As opposed to the effect of IL-1 on glucose analogue uptake, no immediate effect of the cytokine was detected in the metabolic flux analysis. No significant changes in OCR or ECAR were detected within 3 h, the time frame in which these measurements are usually performed (Figure 37). However, it has to be considered that in contrast to the flow cytometric experiments with IL-1β, which were performed after 4 h of incubation, the metabolic assays were performed after 24 h of incubation. Nevertheless, OCR began to significantly increase in IL-1β-treated samples after 8-9 h of incubation (Figure 38). Although the cells did not respond with a short term upregulation of metabolism to IL-1β, the long term increase in OCR indicates that the injected cytokine exerted a biological effect. The oxygen consumption might be elevated by gene expression via IL-1 signaling. The corresponding ECAR measurements dropped below a level that allows a reliable evaluation after a few hours and are therefore not shown.
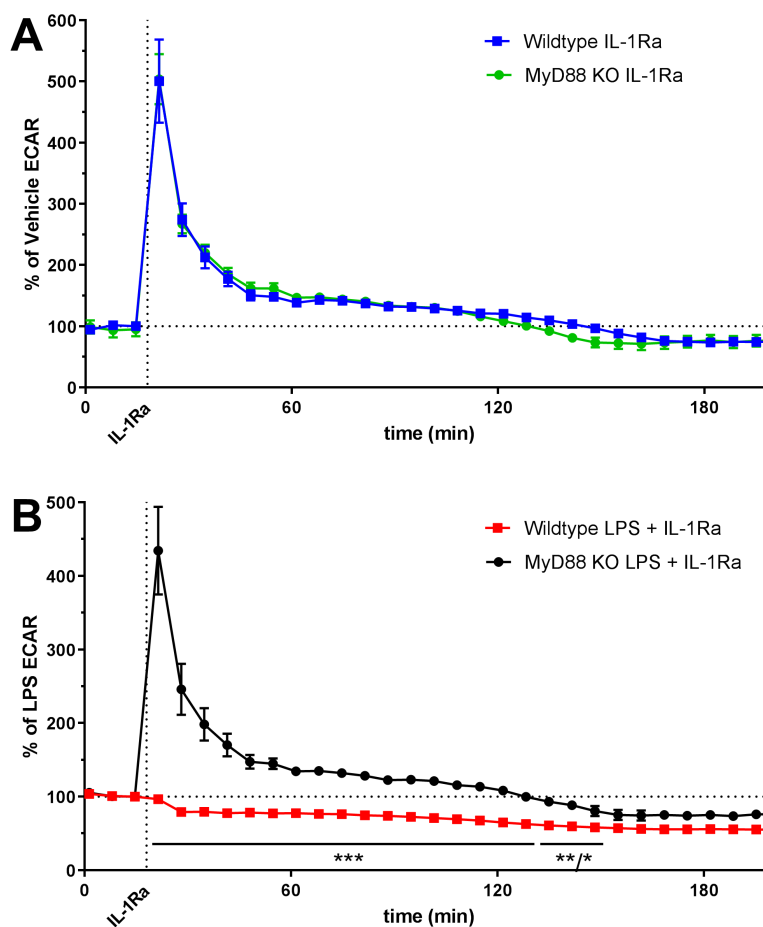
Figure 36. Effects of IL-1 blockade on MyD88 knockout spleen cell ECAR. The results of the ECAR determinations that correspond to the OCR results shown in Figure 35 are depicted in this figure. The experiments were performed as described in the legend to figure 31. MyD88 KO and WT cells were incubated without (A) or with LPS (B). The metabolic assay was performed 24 h later. Vehicle or IL-1Ra (3 mg/ml) were added after establishing a basal value. **A)** Results are expressed as percentage of the simultaneous group that received the vehicle alone (mean $\pm$ SEM; n=6 per group). No statistically significant differences between the response of MyD88 KO and WT cells to IL-1Ra was found. **B)** Unfortunately, there was a technical problem in the ECAR determination of the LPS-stimulated WT samples in the simultaneously done experiment. Thus, the results shown in the figure include equivalent samples from 2 different experiments. Results are expressed as percentage of the group that received the vehicle alone (mean $\pm$ SEM; MyD88 n=6, WT n=11). Two-way ANOVA followed by Fisher's LSD test were performed to compare WT+IL-1Ra and MyD88+IL-1Ra data. * $p<0.05$, ** $p<0.01$, *** $p<0.001$.
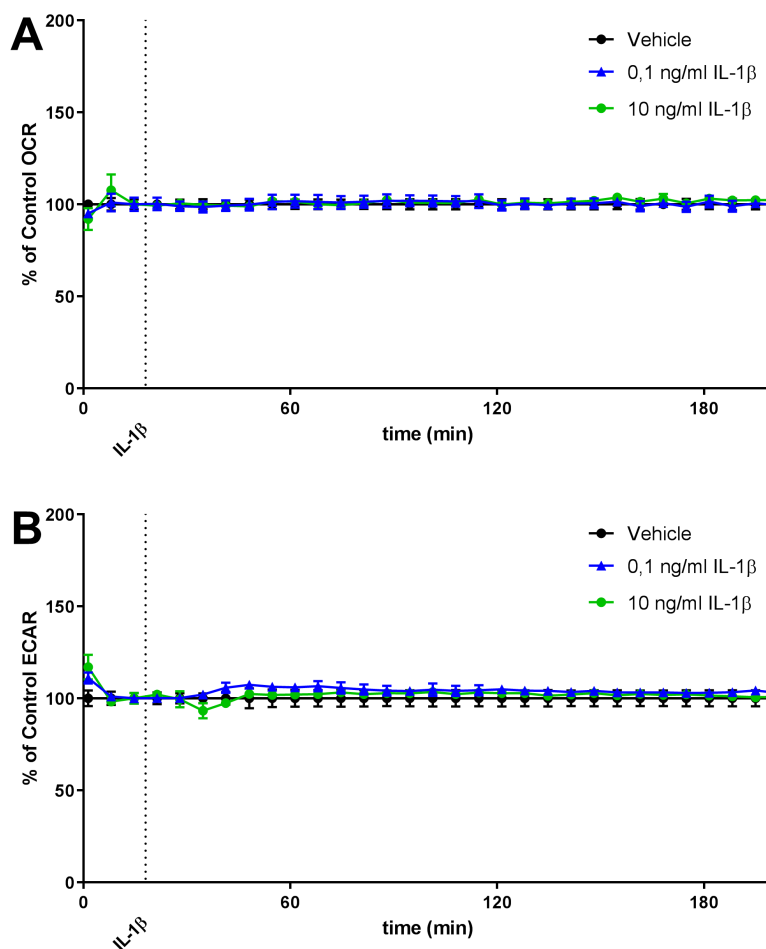
Figure 37. Spleen cell OCR and ECAR in IL-1β-treated samples. The cells were cultured for 24 h before the assay was conducted. After a stable base line was established, IL-1β (0.1 ng/ml or 10 ng/ml) or the vehicle alone were added to the samples. The IL-1β-treated groups are depicted as mean percentage of the corresponding control groups (vehicle). Results are shown as mean OCR and ECAR ± SEM of 3 samples per IL-1β concentration, and 11 samples in the vehicle group. No significant differences were found between the groups.

76
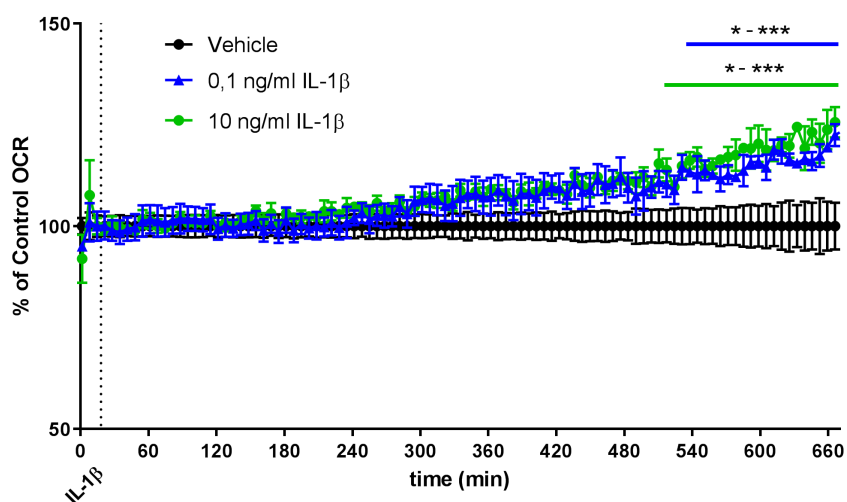
Figure 38. Long term effects of IL-1β on spleen cell OCR. Cells were cultured for 24 h before the assay was conducted. After a stable base line was established, IL-1β (0.1 ng/ml or 10 ng/ml) or the vehicle alone were added to the samples. The results of the groups that received IL-1β (n=3 per concentration) are shown as percentage ($\pm$ SEM) of the control group (vehicle; n=11). Results were analyzed by two-way ANOVA followed by Fisher's LSD test. * $p<0.05$; ** $p<0.01$; *** $p<0.001$.

4 Discussion

It has been shown that IL-1 is able to induce hypoglycemia and profound changes in energetic metabolism *in vivo* [del Rey and Besedovsky, 1987, del Rey and Besedovsky, 1989], and subsequent efforts have been undertaken to elucidate the biological relevance of these effects. It has been found that IL-1 induces changes in the regulation of glucose homeostasis at both central and peripheral levels (reviewed in [Besedovsky and del Rey, 2010]). This work addresses the effect of IL-1 on glucose uptake and energetic metabolism of immune cells. It has been hypothetized that an important function of IL-1 in peripheral glucose regulation is to deviate glucose to immune cells during the course of inflammatory and infectious diseases [Besedovsky and del Rey, 2010]. Although it has been shown that IL-1 directly promotes the expansion and differentiation of naïve and mature memory CD4+ and CD8+ T cells [Ben-Sasson et al., 2009, Ben-Sasson et al., 2013], there are no reports about the effect of endogenous IL-1 on lymphocyte glucose uptake. In this work, it is shown that IL-1 increases glucose uptake by lymphocytes and also supports energetic metabolism in immune cells.

4.1 The flow cytometric glucose uptake assay for lymphocytes

From the technical point of view, the flow cytometric 2-NBDG uptake assay for spleen cells had to be developed prior to the experiments of this work, since this assay had been described for other cell types but not for splenic lymphoid cells when this project started. Several caveats had to be overcome.

The procedure to prepare the suspensions for the cell cultures are likely to result in stressful conditions for the cells that result in an elevated glucose uptake. Although the preparation induced stress is mild in lymphocytes compared to other immune cell types, they needed several hours of rest before this stress-induced increase in glucose uptake stabilizes and experiments can be performed.

During the establishment of the glucose uptake test, attempts were made to improve the amount of 2-NBDG incorporation into cells to increase the fluorescence signal. A recommended procedure for this purpose is to culture cells in the absence of glucose. However, relevant lymphocyte functions, including IL-1 production, are dependent on glucose [Orlinska and Newton, 1993]. Thus, glucose concentration in the medium was lowered to 40 mg/dl, which is still sufficient to allow survival and proliferation [Maciver et al., 2008].

The results obtained with the 2-NBDG assay established in this work are comparable to those obtained in LPS-stimulated murine spleen cells using radioactive [³H] glucose as tracer [Monos et al., 1984]. Although ideally it would be better to compare the results obtained with the well-established method that uses radioactive 2-deoxyglucose as tracer, there are no data available in the literature using it under conditions similar to those used in this work.

4.1.1 LPS stimulation increases glucose uptake

The main reason to use LPS as stimulant in this work was that this endotoxin is one of the best inducers of IL-1 production. On the other hand, it has been reported long ago that glucose influx into murine peritoneal macrophages is stimulated by this endotoxin [Fukuzumi et al., 1996]. Considering only "classical" immune cells, probably macrophages and B cells were the first cell types to be described as targets of LPS [Hambleton et al., 1996, Melchers et al., 1975], but it has been described that also T cells can be either directly or indirectly be affected by LPS [Zanin-Zhorov et al., 2007, Xu et al., 2008].

The discovery of Toll-like receptors opened an important chapter in the field of immunology [O'Neill et al., 2013], leading to the identification of TLR4, the LPS receptor. However, recent studies have shown that there are non-canonical pathways of LPS recognition, since the endotoxin can activate several transient receptor potential (TRP) cation channels in a TLR4-independent manner [Boonen et al., 2018].

As expected, stimulation of spleen cells with LPS resulted in almost doubling 2-NBDG uptake after 24 h in culture. In experiments in which B and T cells were discriminated in LPS-stimulated spleen cell suspensions, no significant increased 2-NBDG

uptake was detected in T cells, while B cells, the most frequent cell type in spleen cell suspensions, increased 2-NBDG uptake to 245 % after 24 h in culture. The magnitude of LPS-induced glucose uptake by B cells after 24 h is comparable to previously reported results (e.g., [Caro-Maldonado et al., 2014]).

4.1.2 Phloretin inhibits glucose uptake

At present, there is only a limited number of glucose transport inhibitors available. Although there are highly specific synthetic GLUT inhibitors, it would be necessary to use a mixture of several inhibitors together with SGLT-inhibitors to completely block glucose uptake. There are naturally occurring GLUT inhibitors, such as cytochalasin B or phloretin, which have the advantage that they block both GLUTs and SGLTs, although they can also exert unspecific effects and may be toxic at high doses. Despite these disadvantages, phloretin is at present one of the most frequently used inhibitors of glucose transport. The concentration of phloretin used in this work (250 µM) is comparable to the concentrations described in the literature [McBrayer et al., 2012, Sasaki et al., 2016]. The short incubation time and the pyruvate contained in the culture medium, which can prevent cells from starving after GLUT blockade, might have contributed to the fact that 250 µM phloretin did not induce cell death under the experimental conditions used here. At this concentration and present in the medium for 12 minutes, the effect of this blocker was moderate. Phloretin inhibited 2-NBDG uptake by around 20 % under basal conditions, and by 27 % in cells that had been incubated with LPS for 24 h. Since phloretin exerted significantly more inhibition of 2-NBDG uptake by LPS-stimulated than by nonovertly stimulated cells, it can be concluded that phloretin-sensitive, most likely GLUT-mediated glucose uptake increases in response to LPS stimulation.

The degree of inhibition of 2-NBDG uptake caused by phloretin depends on the cell type. Although it can inhibit 2-NBDG uptake almost completely in certain cell types, for example in insulinoma cells [Sasaki et al., 2016], it only inhibits a comparably small fraction in B cells [McBrayer et al., 2012], the predominant cell type in whole spleen suspensions. Therefore, the results obtained in this work are in line with those reported in the literature.

It was excluded that 2-NBDG unspecifically stains the outer cell membrane because, as shown by laser scanning microscopy, the fluorescence was evenly distributed within the cell. Additionally, since the NBD loses its fluorescence when it is not linked to glucose, [Yamada, 2018], an unspecific staining by dye that dissociated from glucose can be discarded.

4.2 IL-1 increases glucose uptake by lymphocytes

It is known that several immune functions are supported by a co-stimulatory signal delivered by IL-1 (for example [Lichtman et al., 1988, Weaver et al., 1988, Huber et al., 1996, Brinster and Shevach, 2008, Ben-Sasson et al., 2009, Ben-Sasson et al., 2013]). It is possible that the capacity of IL-1 to increase glucose uptake by immune cells contributes to such co-stimulatory effects and therefore supports the metabolic reprogramming during the activation process.

4.2.1 Blockade of IL-1 receptors decreases glucose uptake

Blockade of IL-1 receptors by IL-1Ra resulted in decreased incorporation of the glucose analogue into splenic cells, and the effect was proportionally more pronounced when it was added to the cultures 24 h after stimulation with LPS. These results show that endogenously produced IL-1 can increase glucose uptake and indicate that the effect is more pronounced when cells are stimulated.

The magnitude of the IL-1Ra-induced inhibition of glucose uptake (24 % in 24 h-LPS-stimulated cells) was comparable to the decrease caused by phloretin (27 % in 24 h-LPS-stimulated cells), indicating that preventing IL-1 signaling has almost the same impact on glucose uptake as GLUT blockade. Glucose uptake by cells that were not exposed to LPS *in vitro* but were cultured for 24 h also incorporated more 2-NBDG than after 4 h, and such uptake was also reduced by addition of IL-1Ra. These findings suggest that these cultures cannot be strictly considered as representing "resting cells". In fact, spleen cell suspensions were not derived from germ-free mice and were also cultured in the presence of "foreign" proteins existing in the fetal calf serum. These results strengthen the hypothesis that IL-1-mediated glucose uptake develops in an activation-dependent manner.

4.2.2 IL-1 blockade reduces glucose uptake by T and B cells

The degree to which IL-1 blockade affected 2-NBDG uptake differed between T and B cells. The relatively quiescent B cells, which incorporated substantially less 2-NBDG than T cells after 4 h incubation, showed only a minor response to IL-1Ra at this time. On the second day, however, LPS-stimulated B cells incorporated more 2-NBDG than T cells. The percentage of IL-1-mediated 2-NBDG uptake raised from 10 % to 16 % in the non-LPS-stimulated, and significantly more (from 9 % to 22 %) in the LPS-stimulated B cells. These results indicate that IL-1-mediated glucose uptake by B lymphocytes is increased in response to stimulation. In contrast, 2-NBDG uptake by T cells was comparable when whole spleen cell suspensions were cultured during 4 or 24 h and with or without addition of LPS, and it could be inhibited to about the same extent by IL-1Ra. Therefore, it seems that IL-1-dependent glucose uptake by T cells under the conditions used in this work was already maximal after 4 h, and it could not be further increased when the suspensions were incubated with the endotoxin for additional 20 h. It has been described that purified T cells strongly increase glucose uptake when stimulated with anti-CD3 and CD28 [Wofford et al., 2008]. However, it has also been reported that, although cytokines could be important in supporting metabolism in activated T cells, they cannot replace the contribution of CD28 to this process at the initial stages of activation [Frauwirth et al., 2002].

4.2.3 Exogenous IL-1β enhances glucose uptake by T and B cells

Only a moderate increased 2-NBDG uptake was observed in B cells when they were exposed to exogenous IL-1β during 1 h. It is known that IL-1 can act as a co-stimulatory molecule for certain immune processes (see Section 4.2). It is therefore possible that a second signal is also needed for IL-1 to increase glucose uptake by immune cells, which was only present in a limited amount. Another explanation is that the amount of endogenous IL-1 already present in the samples was sufficient to elicit almost the maximal biological response.

4.3 IL-1 signaling and metabolism

As usual in studies using the live cell metabolic flux assay, it was necessary to perform preliminary experiments to determine the cell density needed to obtain values of OCR and ECAR within a certain reliable range. A substantial increase in both OCR and ECAR was observed when these parameters were measured immediately after cells were collected from the culture flasks, centrifuged, and re-suspended in the required low pH-buffered assay medium. This problem was overcome by seeding the cells directly into the assay plates, where they were also exposed to LPS, and by carefully replacing the medium to avoid cell disturbance, as much as possible. Furthermore, it should be remarked that the basal rates of oxygen consumption and extracellular acidification considerably differed between cell suspensions prepared from individual mice. When results were normalized to the original cell number seeded, ECAR and OCR increased fivefold, respectively threefold, in response to LPS stimulation. Although there were differences in the protocols used by other authors, the results obtained are comparable to previous reports (e.g., [Caro-Maldonado et al., 2014]).

4.3.1 IL-1Ra reduces lymphocyte OCR and affects ECAR in a stimulation-dependent manner

IL-1 blockade exerted profound effects on OCR and ECAR of spleen cell suspensions. The decrease in the rate of oxygen consumption in response to IL-1Ra indicates that mitochondrial oxidative phosphorylation was markedly reduced. These results strongly suggest that IL-1 exerts an important function in supporting energetic metabolism in immune cells.

Although there were differences in absolute OCR values between the different experimental rounds, and, as expected, between basal and LPS-stimulated cultures, the proportional reduction in response to IL-1Ra was approximately the same in both conditions. These findings show that there is an increase in IL-1-dependent oxygen consumption in response to LPS stimulation. The fact that the decrease in mitochondrial function after IL-1Ra injection was temporary and completely recovered after about 60 minutes in non-

stimulated cultures indicates that mitochondria were not damaged by this treatment. In LPS-stimulated cells, the initial mitochondrial activity was not re-established after IL-1 blockade during the following 4.5 h. However, after addition of FCCP, which induces maximum respiratory chain activity, the initial OCR before IL-1Ra application was even exceeded. It has been proposed that the maintenance of such spare respiratory capacity is a major factor defining the vitality and survival of cells [Pfleger et al., 2015].

There were significant effects of IL-1 blockade on respiratory parameters in several experiments. It should be considered that these parameters were calculated from measurements done during a relative long period (4.5 h) after IL-1Ra injection. The purpose of this design was to pursue the primary objective of these experiments; namely, to study the effect of blocking endogenously produced IL-1 on OCR and ECAR. A decreased mitochondrial proton leak paralleled by reduced maximal mitochondrial capacity was observed in some samples of different experiments still 4.5 h after IL-1Ra injection. A reduction in proton leak can indicate that the mitochondrial membrane voltage is decreased and that the mitochondria are less active. Additionally, a lower maximal respiratory capacity after IL-1Ra injection suggests that the maximal ability of mitochondria to produce energy was reduced by IL-1 blockade. Importantly, it is unlikely that these effects were caused by a reduction in the cell number due to cell death because a substantial decrease of OCR was also observed in non-stimulated, IL-1Ra-treated cells, which returned to the basal OCR within 1 h after IL-1Ra injection. Increased cell death, in contrast, would have most likely resulted in a decreased OCR compared to the control.

The reduction of glucose uptake by IL-1Ra, as observed in the flow cytometric experiments, is most likely not the cause of OCR reduction, because B and T cells can sustain the Krebs cycle with glutamine derived from the culture medium [Waters et al., 2018, Johnson et al., 2018]. Moreover, the initial ECAR peak in non-LPS-stimulated cells after IL-1 blockade indicates that, at this time, either there was not yet a restriction due to decreased glucose uptake or there was still sufficient fuel present in the cells to produce lactate.

It has been recently proposed that, as in other cells, pyruvate is converted to acetyl-CoA in stimulated B cells, which is then incorporated into fatty acids, a process that would also contribute to ECAR via the production of CO_2 and carbonic acid [Waters et al., 2018]. However, this process is associated with mitochondrial activity and oxygen consumption. In contrast, the studies reported here revealed a marked decrease in OCR in parallel to an increase in ECAR. Thus, the conversion of acetyl-CoA to fatty acids most likely did not contribute considerably to the ECAR peak after IL-1 blockade.

It is possible that a decrease in non-mitochondrial oxygen consumption participated in the IL-1Ra-mediated decrease of OCR. It has been reported that some cells with high glycolytic capacity have a high rate of cell surface oxygen consumption, and it was proposed that there is a mechanism to reoxidize NADH by oxygen consumption at the cell surface [Herst et al., 2004, Herst and Berridge, 2007]. However, it is unlikely that this is the primary cause by which IL-1Ra induced a reduction in OCR, because the effect of the antagonist on OCR was larger than all of the non-mitochondrial oxygen consumption. Therefore, the most plausible explanation seems to be that the effect of IL-1 blockade is primarily the result of reduced oxygen consumption by the mitochondria.

In addition to mitochondrial respiration, glycolysis is another important energetic pathway in LPS-activated B cells [Caro-Maldonado et al., 2014]. As shown here, IL-1 blockade promptly reduced ECAR in LPS-stimulated immune cells. This demonstrates that IL-1 signaling is also important in the maintenance of glycolysis in LPS-stimulated cells. ECAR reduction in LPS-stimulated cells can be divided into two phases. The first effect occurred immediately after IL-1 blockade and, therefore, it is likely mediated by a rapid signaling event. The second phase occurred between 1 h and 2 h after IL-1Ra injection, and it might involve an effect on gene expression. In cells that had not been stimulated with LPS, ECAR was first substantially elevated before falling below basal levels around 2 h after IL-1 blockade. An elevation of lactate production might be a compensatory mechanism in response to pyruvate accumulation, when oxidative phosphorylation is decreased in unstimulated cells. Stimulated lymphocytes in contrast, might not be able to further expand lactate production.

4.3.2 IL-1 effects on lymphocyte metabolism

The direct addition of IL-1β to the cells did not result in changes in OCR or ECAR within 5 h. Later, however, a tendency towards higher OCR was observed in cultures that received the cytokine as compared to those in which only the vehicle was injected. This difference reached statistical significance after 8.5 h of incubation, and it was maintained for at least another 3 h. It remains to be clarified whether the enhancing effect of the cytokine on oxygen consumption is the result of an effect on cell metabolism or on survival.

4.4 IL-1 signaling and cell death

IL-1Ra-treated samples showed 20 % less cell death than the controls, as evaluated by 7-AAD staining. Additionally, annexin V staining showed decreased levels of apoptotic cells in the IL-1Ra-treated samples. This suggests that IL-1 blockade may exert a protective effect in lymphocytes within the 1 h period of incubation, as it was described for several tissues in which IL-1Ra exhibits protective effects and reduces apoptosis [Friedlander et al., 1996, Sun et al., 2006]. Although no increased cell death after IL-1 blockade was observed in the studies reported here in the relatively short incubation time, the profound effects of IL-1 signaling on glucose uptake and metabolism make it likely that longer periods of IL-1 blockade would result in increased cell death in LPS stimulated cells. One of the mechanisms by which neutralization or absence of certain cytokines can cause cell death is a decrease in AKT signaling, which prevents apoptosis by suppressing pro-apoptotic Bad and Forkhead transcription factors (reviewed in [Rathmell and Thompson, 2002]). Because even an inhibition of AKT signaling by AKTi8 did not result in an increased number of dead cells in the timeframe of the experiments reported here, IL-1 signaling over AKT seems not to be essential for the inhibition of cell death. It should be remarked that the experimental conditions were chosen here so as to avoid excessive stress from starving by offering alternative fuels to the cells in the form of amino acids and pyruvate.

4.5 IL-1Ra efficiency

In the experiments reported here, a relatively high concentration of IL-1Ra was required to significantly decrease IL-1 effects on glucose uptake and energetic metabolism. Several lines of evidence may help to explain why such a large amount was needed. Other models required IL-1Ra concentrations ranging from 10 ng/ml to 100 ng/ml in astrocytes and neurons [Holliday and Gruol, 1993, del Rey et al., 2016] and up to 100 µg/ml in lymphocytes [Park et al., 2015] to reduce IL-1 effects. However, it has also been reported that a concentration of 200 µg/ml IL-1Ra was found to inhibit binding of IL-1α to proteose peptone-elicited peritoneal exudate cells or bone marrow cells only by 50% [McIntyre et al., 1991].

The lower concentrations of IL-1Ra cannot be compared to the experiments of this work, because either the cells used in the aforementioned experiments are not comparable to lymphocytes, or they were treated with IL-1Ra from the beginning of the incubation. The time point of IL-1Ra addition is particularly important. Addition of IL-1Ra before or at the time of immune stimulation would bind to IL-1 receptors before they can be occupied by newly synthetized IL-1. On the contrary, administration of the antagonist when IL-1 has already been produced, as done in this work, would require large amounts of IL-1Ra to displace IL-1 and prevent it from exerting its biological activity. In addition it is known that IL-1 can induce its own synthesis [Dinarello et al., 1987]. Cells treated with IL-1Ra from the beginning of the incubation will most likely produce less IL-1 and thus, lower concentrations of IL-1Ra would be sufficient to counteract IL-1 effects. The IL-1 signaling system is highly sensitive, and even very low concentrations of IL-1 can trigger biological responses [Ye et al., 1992]. Therefore, IL-1Ra must induce a receptor blockade by occupying all IL-1 receptors in order to eliminate IL-1 activity [Rosenwasser, 1998].

There are large differences between the amounts of IL-1Ra that is required to block IL-1 activity in different cell types. The IC$_{50}$ of IL-1Ra is 50.000 times higher in peritoneal cavity cells than in hepatocytes and 100.000 times higher in bone marrow cells

than in hepatocytes when given simultaneously [McIntyre et al., 1991].

The production of IL-1 by immune cells might also be relevant for the required amount of IL-1Ra. Even if the IL-1 present in the medium is removed, membrane bound IL-1α and freshly produced IL-1β are able to immediately act in an autocrine/paracrine manner. It has to be considered that the average IL-1 concentration in the medium is not necessarily decisive because the local concentration of the cytokine at the cell membrane would be much higher when IL-1 is secreted over the cell membrane where its target structure, the IL-1R1, is located.

In the circulation of healthy subjects, the amount of IL-1β is in the low picogram range per milliliter, and the concentration of IL-1Ra is around 100-300 ng/ml [Dinarello, 2011]. Thus, even under basal conditions, the amount of IL-1Ra exceeds the concentration of IL-1β by approximately a factor of 100,000. It has to be considered that even with this imbalance in favor of IL-1Ra, the organism is responsive to IL-1β, and that the amount of IL-1Ra would probably have to be increased in orders of magnitude to completely block IL-1 signaling.

It has been reported that LPS activation of monocytes causes a drastic reduction of IL-1R2 surface expression and an increase in IL-1R1 expression [Penton-Rol et al., 1999, Mantovani et al., 2001]. The decoy IL-1R2 acts in several ways to negatively regulate IL-1 signaling. It does not only bind IL-1, but also the IL-1RAcP, which in turn is no longer available for signaling via IL-1R1. Moreover, "shedded" soluble IL-1R2 neutralizes unbound IL-1 (reviewed in [Dinarello, 2011]). Therefore, a reduction of IL-1R2 results in the loss of several mechanisms attenuating IL-1 effects. If there is a similar mechanism in lymphocytes, this would drastically enhance IL-1 signaling and also the amount of IL-1Ra that would be needed to block it. Together, these mechanisms could result in the exponential elevation of the IL-1Ra concentration necessary to block IL-1 signaling.

There are different splice variants of the IL-1R1, which are in part induced by LPS activation [Penton-Rol et al., 1999]. However, it is not understood how these different splice variants affect IL-1 signaling. Of special interest in the context of the experiments

reported here is that alternative splicing can result in loss of the binding site for IL-1Ra. The resulting IL-1R is predicted to have a very low affinity to IL-1Ra [Qian et al., 2012]. The presence of such a splice variant with a very low affinity to IL-1Ra in splenic lymphocytes would contribute to explain the requirement of high IL-1Ra amounts.

Park et al. used up to 100 µg/ml IL-1Ra in their experiments with lymphocytes and only achieved partial inhibition of several IL-1-mediated effects [Park et al., 2015]. This evidence further supports the hypothesis that there are IL-1R1 in leucocytes with very low affinity to IL-1Ra, making it difficult to inhibit IL-1 effects in these cells with the antagonist.

The species difference between IL-1 derived from murine splenocytes and human IL-1Ra could also contribute to the low efficiency of the antagonist to block IL-1R1 or to displace already bound IL-1. For example, murine IL-1Ra is approximately seven times more efficient in competing with IL-1 for binding to the mouse pre-B cell line 70Z/3 than human IL-1Ra [Dripps et al., 1991]. Most likely, a combination of the factors mentioned above contributed to the high IL-1Ra concentration that was necessary to decrease IL-1 effects in the experiments reported here.

To exclude a loss of IL-1Ra potency due to the long storage time of the antagonist stock we had available, we compared the effect of the IL-1Ra used in this work with Kineret (Anakinra; Swedish Orphan Biovitrum AB, Sweden, kindly provided by Prof. Dr. R. Straub, Regensburg, Germany). Kineret is a recombinant, non-glycosylated human IL-1Ra protein that was first approved in 2001 in the United States to treat patients with rheumatoid arthritis and neonatal-onset multisystem inflammatory disease. No differences between both preparations were found in their efficiency to reduce 2-NBDG uptake by splenocytes.

A reduction of glucose uptake by elevation of osmotic pressure due to the amount of IL-1Ra applied was excluded since the same concentration of human serum albumin did not affect glucose uptake. Further, it has been reported that hyperosmotic stress induces activation and translocation of glucose transporters in mammalian cells, thus resulting in an elevated glucose uptake [Barros et al., 2001].

4.6 Connection of IL-1 signaling to pathways associated with glucose uptake

The discussion that follows is an attempt to summarize possible mechanisms that could link IL-1 signaling to pathways associated with glucose uptake and metabolism. In this work, signaling via IL-1R1 was inhibited when cells were already responsive to IL-1. In most of the work reported on this topic by other authors, the immediate effect of IL-1 blockade on glucose uptake was not explored, but rather which factors are necessary for the development of IL-1-mediated glucose uptake over a relatively long period, and in cells others than lymphocytes [Shikhman et al., 2001, Shikhman et al., 2004]. It is essential to discriminate between immediate and long-term effects of blocking IL-1 because they might be based on different mechanisms. Particularly because of this difference, the results shown here not only complement existing knowledge, but also have to be interpreted in the context of the different experimental approach when they are compared to previously published reports. An overview of the discussed signaling pathways is given in Figure 39.

4.6.1 Transcription

The results reported in this work indicate that some of the pathways known to regulate glucose uptake are most likely not involved in mediating the effects of IL-1 described here. In the real-time live cell metabolic assay, the effects of IL-1Ra were detected almost immediately after injection of the antagonist, and they were observed within 25 min in the flow cytometric experiments. Changes in the rate of *de novo* protein synthesis need in general more than 30 min to manifest in murine splenic B cells e.g. after LPS or BCR stimulation [Fowler et al., 2015]. Therefore, it is unlikely that the mechanisms involved are based on a decrease in the concentration of rate limiting metabolic enzymes, as it was observed when stimulated Th17 cells were incubated with IL-1Ra for 3 days [Park et al., 2015].

4.6.2 MyD88

The next question addressed was whether the observed effects on glucose uptake and metabolism are MyD88-dependent, since many IL-1 signals are mediated by this protein adapter. However, no significant difference between spleen cells obtained from WT and MyD88 KO mice was found in response to IL-1 blockade, neither in the glucose uptake tests nor in the real-time live cell metabolic assays.

As expected, LPS did not increase 2-NBDG uptake by spleen cell suspensions derived from MyD88 KO mice [Kawai et al., 1999]. However, MyD88 KO cells showed a clear reduction in glucose uptake in response to IL-1Ra that was comparable to the effect observed in WT spleen cells. In the Seahorse assays, the metabolism of MyD88 KO cells was also not activated by LPS, and both OCR and ECAR responded in the same way to IL-1Ra as non-stimulated WT cells. These results strongly suggest that MyD88 is not essential for the effects of IL-1 on glucose uptake and metabolism.

Interestingly, although energetic metabolism was not upregulated by LPS in MyD88 KO cells, they seemed to show a response to the endotoxin. One characteristic of LPS-stimulated WT cells was that the OCR did not recover to the initial level after the injection of IL-1Ra, as it happened in non-stimulated cells. Similar to the LPS-stimulated WT, the OCR of LPS-stimulated MyD88 KO cells showed a tendency not to fully recover after IL-1Ra injection. LPS signaling via TLR4 is not completely absent in MyD88 KO cells, but it is still partially active via TRIF and PI3K [Fitzgerald et al., 2003, Bagchi et al., 2007, Troutman et al., 2012]. Another possibility is the recently described TLR4-independent pathway mentioned above, which involves TRP cation channels [Boonen et al., 2018]. It is therefore likely that the permanent decrease in OCR observed in LPS-stimulated MyD88 KO cells treated with IL-1Ra was induced by the endotoxin via a MyD88-independent mechanism. However, the difference between the two groups is not statistically significant.

LPS-incubated MyD88 KO cells showed a marked increase in ECAR in response to IL-1Ra, similar to the non-LPS-stimulated WT cells. This ECAR response might, however, be a result of the missing MyD88-mediated LPS stimulation, rather than an involvement of MyD88 in the response to IL-1Ra.

4.6.3 MAPK

IL-1β stimulation results in increased expression and membrane incorporation of GLUT1 in chondrocytes [Shikhman et al., 2004]. Although IL-1 activates both ERK and p38 kinases in chondrocytes [Geng et al., 1996], only p38 is necessary for the enhancement of glucose uptake [Shikhman et al., 2001]. In lymphocytes, the enhancement of glucose uptake and metabolism can be activated by both ERK and p38 MAPKs [Marko et al., 2010], but it has not been investigated if they are involved in IL-1-mediated glucose uptake. Because ERK and p38 are not only downstream of MyD88, but also downstream of AMPK and PKC [Kim et al., 2010, Xi et al., 2001, Ueda et al., 1996], the results of our experimental approach indicate that MyD88-activation of ERK and p38 does not play a critical role in the IL-1 effects on glucose uptake and metabolism.

4.6.4 PI3K/AKT

It has been reported that inhibition of PI3K with Wortmannin in adipocytes results in suppression of GLUT1 exocytosis and a marked decrease in glucose uptake [Yang et al., 1996]. Comparable results were reported in monocytes [Dimitriadis et al., 2005]. It was also shown in the hematopoietic myeloid/lymphoid cell line FL5.12 that inhibition of PI3K with LY294002 in cytokine-stimulated cells reduces GLUT1 surface expression [Wieman et al., 2007]. However, Wortmannin and LY294002 are not specific PI3K inhibitors and affect several other proteins, such as GSK3 and mTOR [Gharbi et al., 2007]. In the context of glucose uptake studies, interactions of Wortmannin and LY294003 with GSK3 and mTOR are problematic because they are also key kinases for the regulation of glucose uptake. Even the specific inhibition of PI3K has a rather broad effect on downstream signaling. PI3K activates a large number of the 60 AGC kinase superfamily mem-

bers via the master kinase PDK1, including AKT itself, PKC, p70 ribosomal S6 kinase (S6K), and serum- and glucocorticoid-induced protein kinase (SGK) (reviewed in [Mora et al., 2004, Arencibia et al., 2013]). To achieve a higher specificity, in the approach followed in this work, AKT was directly inhibited. AKTi8 is specific for AKT and does not affect other PI3K targets, because it does not inhibit the production of PIP_3.

AKT directly controls metabolism by enhancing the catalytic activity of rate limiting glycolytic enzymes. AKT phosphorylates and stimulates hexokinase-II [Roberts et al., 2013] and isoforms of the phosphofructokinase [Lee et al., 2017], and induces the phosphorylation of pyruvate dehydrogenase (PDH) [Cerniglia et al., 2015]. In the context of our experiments, the control of PDH by AKT is especially interesting because PDH delivers fuel to the mitochondria in the form of acetyl-CoA, and inhibition of PDH results in decreased oxygen consumption [Cerniglia et al., 2015]. A decreased PDH activity after blocking IL-1R1-mediated PI3K/AKT signaling could have contributed to the reduced oxygen consumption in the live cell metabolic assay.

In this work, inhibition of AKT in T cells resulted in a decrease of 2-NBDG uptake, similar to that caused by IL-1 blockade. Addition of the antagonist to T cells in which AKT was inhibited, provoked only a non-significant tendency to further decrease the uptake of 2-NBDG. Because it is not possible to distinguish the effects of IL-1Ra and AKTi8 on 2-NBDG uptake, it is not possible to draw a conclusion regarding the involvement of AKT in IL-1-mediated glucose uptake by T cells.

In B cells, addition of the inhibitor AKTi8 resulted in an unexpected elevation of glucose uptake. There is evidence that inhibition of AKT with other AKT inhibitors results in decreased glucose uptake by splenic B cells [Doughty et al., 2006]. Overall, there are 206 PH domain-containing proteins in the human genome that could be potentially affected by unspecific binding of AKTi8 [Braschi et al., 2018], and there are at least 2 PH domain-containing proteins critically involved in the regulation of B cell activation. The 32 kDa B cell adapter molecule (Bam32) and tandem PH-domain containing protein (TAPP) provide a negative feedback to PI3K signaling, and the inactivation of these proteins results in chronic activation, elevated glycolysis, increased expression of

GLUT1, and a subsequently elevated glucose uptake by B cells [Marshall et al., 2000, Jayachandran et al., 2018]. Thus, one possibility is that the elevation of glucose uptake in response to AKTi8 in B cells is the result of an unspecific interaction of AKTi8 with the PH-domain of an unrelated protein.

Another possibility is that AKT promotes hexokinase II association with mitochondria in LPS-stimulated B cells. It has been observed that AKT inhibition results in hexokinase II dissociation from the mitochondria and a subsequent increase of glucose uptake by HeLa and MDA-MB-231 cancer cell lines [Neary and Pastorino, 2013].

Despite these unexpected effects of AKTi8, it can be assumed that AKT is also inhibited in B cells after the application of this inhibitor. Since addition of IL-1Ra still exerted a substantial effect on 2-NBDG uptake by AKTi8-treated B cells, it seems reasonable to conclude that IL-1-mediated glucose uptake is not critically dependent on AKT in B cells.

4.6.5 mTOR and GLUT glycosylation

Besides rising the number of GLUTs in the cell membrane, another possibility is that IL-1 would increase glucose uptake by lymphocytes by augmenting GLUT glycosylation, which enhances the affinity of GLUT1 for glucose [Asano et al., 1991]. A complete loss of GLUT1 glycosylation in chondrocytes [Shikhman et al., 2001] results in approximately the same percentage of inhibition of glucose uptake as observed here following IL-1 blockade. In rat adipocytes, IL-1β enhances glucose uptake by increasing the maximal transport velocity [Garcia-Welsh et al., 1990], and the incorporation of highly glycosylated forms of GLUT1 in chondrocytes [Shikhman et al., 2004].

It has been described that AKT activation of mTOR/RAPTOR in lymphocytes does not affect GLUT1 trafficking but regulates GLUT1 transporter activity [Wieman et al., 2007]. Furthermore, inhibition of mTOR in IL-1-stimulated Th17 cells decreases 2-NBDG uptake to the level of unstimulated controls [Deason et al., 2018]. However, the glycosylation status of GLUTs was not investigated. Therefore, it cannot be discriminated whether the reduction of glucose uptake was induced by attenuated GSK3 inhibition by

mTOR and subsequently less GLUT recycling, or by reduced GLUT activation due to less glycosylation.

The possible involvement of GLUT glycosylation in the effects reported in this work was not investigated, and it would be necessary to clarify this aspect. Concerning the results of the metabolic assays, it has to be considered that mTOR also regulates mitochondrial activity [Schieke et al., 2006], and that interruption of IL-1R1 signaling to mTOR might have contributed to the alterations in OCR.

4.6.6 PKCs

When IL-1 binds to its receptor, BCAP is recruited to the IL-1R1 and activates both PLCγ and PI3K [Halabi et al., 2017, Deason et al., 2018]. One of the IL-1-activated PKC isotypes is PKCβ [Halabi et al., 2017], and interestingly it has been shown that its activation increases glycolysis following B cell stimulation [Blair et al., 2012]. PKCs influence glucose uptake by activating ERK [Ueda et al., 1996], by inhibiting GSK3 [Jope and Johnson, 2004, Zhao et al., 2007], and by directly modifying GLUT1 transport velocity [Lee et al., 2015].

In T cells, there is a network of different PKC isoforms that are able to redundantly sustain the activation of ERK [Puente et al., 2006]. ERK activates mTOR [Mendoza et al., 2011] and also inhibits GSK3 [Wieman et al., 2007].

The development of IL-1-induced changes in glucose uptake over a period of 24 h requires PKC activity in chondrocytes [Shikhman et al., 2001, Shikhman et al., 2004]. Thus, it is conceivable that a similar mechanism, which results in enhanced glucose transport, operates in lymphoid cells.

4.6.7 Calcium

It has been shown that store-operated calcium entry (SOCE) and calcineurin control metabolic reprogramming in T cells by up-regulating the expression of glucose transporters and glycolytic enzymes, and by directly modulating glycolysis and oxidative phosphorylation (reviewed in [Trebak and Kinet, 2019]). Interestingly, it has also been shown that calcium signaling affects the activation of AKT, mTOR [Vaeth et al., 2017], and

AMPK [Tamas et al., 2006], three of the pivotal proteins in the regulation of cellular energetic homeostasis.

IL-1 elicits calcium signaling from internal stores and also from the extracellular space. This signaling is dependent on PLC and regulates ERK activation [Wang et al., 2003, Pritchard and Guilak, 2006]. Furthermore, calcium activates the three crucial Krebs cycle enzymes, pyruvate dehydrogenase, isocitrate dehydrogenase, and α-ketoglutarate dehydrogenase, in the mitochondrial matrix [Denton, 2009]. In the context of glucose uptake regulation, IL-1-induced calcium signaling is also important because calcium-dependent small GTPases, such as Rab11 are involved in the trafficking of GLUT vesicles [Savina et al., 2005, Wieman et al., 2007].

Mitochondria take up calcium via voltage-dependent anion-selective channels and mitochondrial Ca^{2+} uniporter complexes, following the electrochemical gradient generated by the respiratory chain. Simultaneously, calcium is externalized by the mitochondrial Na^+/Ca^{2+} exchanger and the mitochondrial H^+/Ca^{2+} exchanger, which reverse the activation and avoid calcium accumulation in the mitochondria (reviewed in [Giorgi et al., 2018]). Excess cytosolic Ca^{2+} in turn is externalized by plasma membrane Ca^{2+}-ATPases and Na^+/Ca^{2+} exchangers [Brini and Carafoli, 2011].

It is possible that the activation-dependent calcium influx that enhances metabolic activity has to be counteracted at some point by upregulating the machinery to externalize calcium in order to keep a steady state in the cell and in the mitochondria. If the calcium equilibrium is suddenly disturbed by a drastically reduced calcium influx, which could be the result of IL-1 blockade, then the intracellular calcium concentration may decrease to a level that impairs the proper function of mitochondrial enzymes. As consequence, the activity of the Krebs cycle would be reduced and oxygen consumption in the respiratory chain eventually decreases, as observed in the metabolic experiments reported here.

Isolated B cells from BCAP KO mice exhibit decreased calcium mobilization, which is attributed to reduced PLCγ2 activity [Yamazaki et al., 2002]. Since a decrease in IL-1R1 activity by IL-1Ra also results in a reduced PLCγ2 activation via BCAP, it can be assumed that intracellular calcium levels were decreased by IL-1Ra in the experiments shown in this work.

In conclusion, inhibition of IL-1-elicited calcium signaling could contribute to downregulate metabolism and possibly also to reduced glucose uptake, as we observed after IL-1 blockade.

4.6.8 AMPK

It is possible that the full magnitude of IL-1-mediated glucose uptake cannot be detected in the experiments reported here because the reduction of glucose uptake might be counteracted by AMPK after IL-1 blockade. A loss of PI3K/AKT signaling and the subsequent reduction of glucose uptake could activate ERK and p38 via AMPK, and result in a compensatory GLUT surface localization [Kim et al., 2010, Xi et al., 2001, Fujii et al., 2006]. Additionally, as mentioned above, AMPK inhibits GLUT internalization in response to a shortage of energy, and thus prevents a decrease in glucose uptake beyond a certain threshold [Wu et al., 2013].

4.6.9 K$_{ir}$6.2

The ion channel K$_{ir}$6.2 senses ATP/ADP levels in the cytoplasm and initiates protective stabilization of the membrane potential when the availability of ATP decreases [Seino and Miki, 2003]. It has also been shown that K$_{ir}$6.2 is involved in insulin-stimulated glucose uptake by skeletal muscles [Miki and Seino, 2005]. We hypothesized that K$_{ir}$6.2 could be involved in IL-1-mediated glucose uptake because we have previously shown that the hypoglycemia induced by IL-1β *in vivo* is significantly more pronounced in K$_{ir}$6.2 KO mice than in the WT mice [del Rey et al., 2016]. However, no difference in 2-NBDG uptake between spleen cells obtained from K$_{ir}$6.2 KO mice and WT mice was observed after IL-1 blockade. Therefore, it can be concluded that K$_{ir}$6.2 does not significantly contribute to IL-1-induced glucose uptake by immune cells under the experimental conditions used here.

4.6.10 Summary of pathways potentially involved in IL-1 effects

The preceding discussion illustrates the complexity of the potential pathways that could be involved in mediating the effect of IL-1 on glucose uptake and energetic metabolism. The mediators known to be involved in the regulation of glucose transport and/or metabolism that are also involved in transducing an IL-1 signal are summarized in Table 7.

Because the effects of IL-1 blockade on glucose uptake and metabolism are rather quick, it is expected that the signaling is mediated by a fast-reacting pathway. The MyD88 pathway has been shown to be involved in the induction of IL-1-elicited hypoglycemia in mice [del Rey et al., 2016]. However, IL-1 effects on metabolism and glucose uptake by immune cells *in vitro* was comparable in spleen cells derived from MyD88 KO and WT mice. Thus, the results indicate that the regulation of glucose homeostasis *in vivo* and at cellular levels might be mediated by different mechanisms. This is not surprising, since many mechanisms that control glucose homeostasis, such as those mediated by hormones and neurotransmitters, are integrated at brain level and only operate in vivo.

Regarding the *in vitro* experiments reported in this work, it can be concluded that either IL-1 signaling via mTORC1 and GSK3, which control glucose uptake, occurs redundantly via both MyD88 and PI3K/AKT, so that the loss of one pathway can be compensated by the other, or the effects of IL-1 blockade are mediated by another signaling pathway. As discussed above, there are many ways to affect the capacity to uptake glucose, and there are also many intracellular signaling pathways involved. Thus, further experiments are necessary to elucidate the molecular mechanism by which IL-1 affects glucose uptake and metabolism in immune cells.

Table 7. Potential intracellular mediators of IL-1-induced glucose uptake and metabolism. The intracellular mediators[1] mentioned in the table are involved in signaling pathways that regulate glucose transport and/or metabolism[2] (selected references and the cell type or cell line (CL) from which the evidence derives are indicated in[3]). It has been reported that either this mediator is also involved in transducing an IL-1-mediated signal[4] or that a comparable effect can be exerted by IL-1[5] in a given cell type. Selected references illustrating these aspects are provided in the last two columns.

| Mediator[1]	Effect[2]	Reference (cell type)[3]	Mediator involved in IL-1 signaling (cell type)[4]	Comparable effect exerted by IL-1 (cell type)[5]
PI3K/AKT	GLUT1 internalization ↓	Wieman 2007 (lymphocytic CL)	Reddy 1997 (hepatoma CL), Sizemore 1999 (hepatoma CL)	-
	GLUT1 internalization ↓ (TXNIP ↓)	Waldhart 2017 (hepatoma CL)	Reddy 1997 (hepatoma CL), Sizemore 1999 (hepatoma CL)	-
	GLUT1 surface expression ↑	Yang 1996 (adipocyte CL), Frauwirth 2002 (T cells), Doughty 2006 (B cells), Wieman 2007 (lymphocytic CL), Dimitriadis 2005 (monocytes), Jayachandran 2018 (B cells)	Reddy 1997 (hepatoma CL), Sizemore 1999 (hepatoma CL)	Garcia-Welsh 1990 (adipocytes), Kol 1997 (ovarian cells), Shikman 2001 (chondrocytes), Jager 2007 (adipocyte CL)
	Metabolism ↑ (glycolysis ↑)	Frauwirth 2002 (T cells), Doughty 2006 (B cells)	Reddy 1997 (hepatoma CL), Sizemore 1999 (hepatoma CL)	Shikman 2004 (chondrocytes), Park 2015 (Th17)
	Metabolism ↑ (hexokinase II ↑)	Roberts 2013 (cardiomyocytes)	Reddy 1997 (hepatoma CL), Sizemore 1999 (hepatoma CL)	-
	Metabolism+OCR ↑ (phosphofructokinase ↑)	Lee 2017 (glioblastoma CL, epidermoid carcinoma CL, breast cancer CL), Cerniglia 2015 (head and neck cancer CL)	Reddy 1997 (hepatoma CL), Sizemore 1999 (hepatoma CL)	-
ERK	Glucose uptake ↑	Marko 2010 (T cells)	Geng 1996 (chondrocytes)	Garcia-Welsh 1990 (adipocytes), Kol 1997 (ovarian cells), Shikman 2001 (chondrocytes), Jager 2007 (adipocyte CL)
	Metabolism ↑ (glycolysis ↑)	Marko 2010 (T cells)	Geng 1996 (chondrocytes)	-
	Metabolism ↑ (hexokinase ↑)	Marko 2010 (T cells)	Geng 1996 (chondrocytes)	-
p38	Glucose uptake ↑	Marko 2010 (T cells)	Shikman 2001 (chondrocytes), Geng 1996 (chondrocytes)	Garcia-Welsh 1990 (adipocytes), Kol 1997 (ovarian cells), Shikman 2001 (chondrocytes), Jager 2007 (adipocyte CL)
	Metabolism ↑ (glycolysis↑)	Marko 2010 (T cells)	Shikman 2001 (chondrocytes), Geng 1996 (chondrocytes)	Shikman 2004 (chondrocytes), Fultang 2019 (neuroblastoma)
PKC	GLUT1 surface expression ↑	Lee 2015 (fibroblast CL)	Shikman 2001 (chondrocytes)	Garcia-Welsh 1990 (adipocytes), Kol 1997 (ovarian cells), Shikman 2001 (chondrocytes), Jager 2007 (adipocyte CL)
PKCβ	Metabolism ↑ (glycolysis ↑)	Blair 2012 (B cells)	Halabi2017 (human embryonic kidney CL)	Park 2015 (Th17)
Calcium	Metabolism ↑ (mitochondrial dehydrogenases ↑)	Denton 2009 [review](various primary tissues)	Holliday 1993 (astrocytes), Luo 1997 (chondrocytes), Wang 2003 (fibroblasts), Pritchard 2006 (chondrocytes)	-
mTOR	Glucose uptake ↑	Wieman 2007 (lymphocytic CL)	Deason 2018 (Th17)	Garcia-Welsh 1990 (adipocytes), Kol 1997 (ovarian cells), Shikman 2001 (chondrocytes), Jager 2007 (adipocyte CL)
	GLUT1 surface expression ↑	Buller 2008 (embryonic fibroblast CL, renal tumor CL)	Deason 2018 (Th17)	Garcia-Welsh 1990 (adipocytes), Kol 1997 (ovarian cells), Shikman 2001 (chondrocytes), Jager 2007 (adipocyte CL)
GSK3β	Metabolism ↓ (pyruvate dehydrogenase ↓)	Hoshi 1996 (cell free assay)	Hermida 2017 [review]	-
	Metabolism ↓ (respiratory chain ↓)	King 2008 (isolated mitochondria)	Hermida 2017 [review]	-
	Metabolism ↓ (OCR ↓)	Martin 2018 (neuroglioma CL)	Hermida 2017 [review]	-
AMPK	GLUT1 internalization ↓ (TXNIP ↓)	Wu 13 (hepatoma CL, mouse embryonic fibroblast)	-	-
	GLUT1 surface expression ↑	Abbud 2000 (rat liver CL, preadipocyte CL, myoblast CL)	-	Garcia-Welsh 1990 (adipocytes), Kol 1997 (ovarian cells), Shikman 2001 (chondrocytes), Jager 2007 (adipocyte CL)

↑: increase; ↓: decrease/inhibition
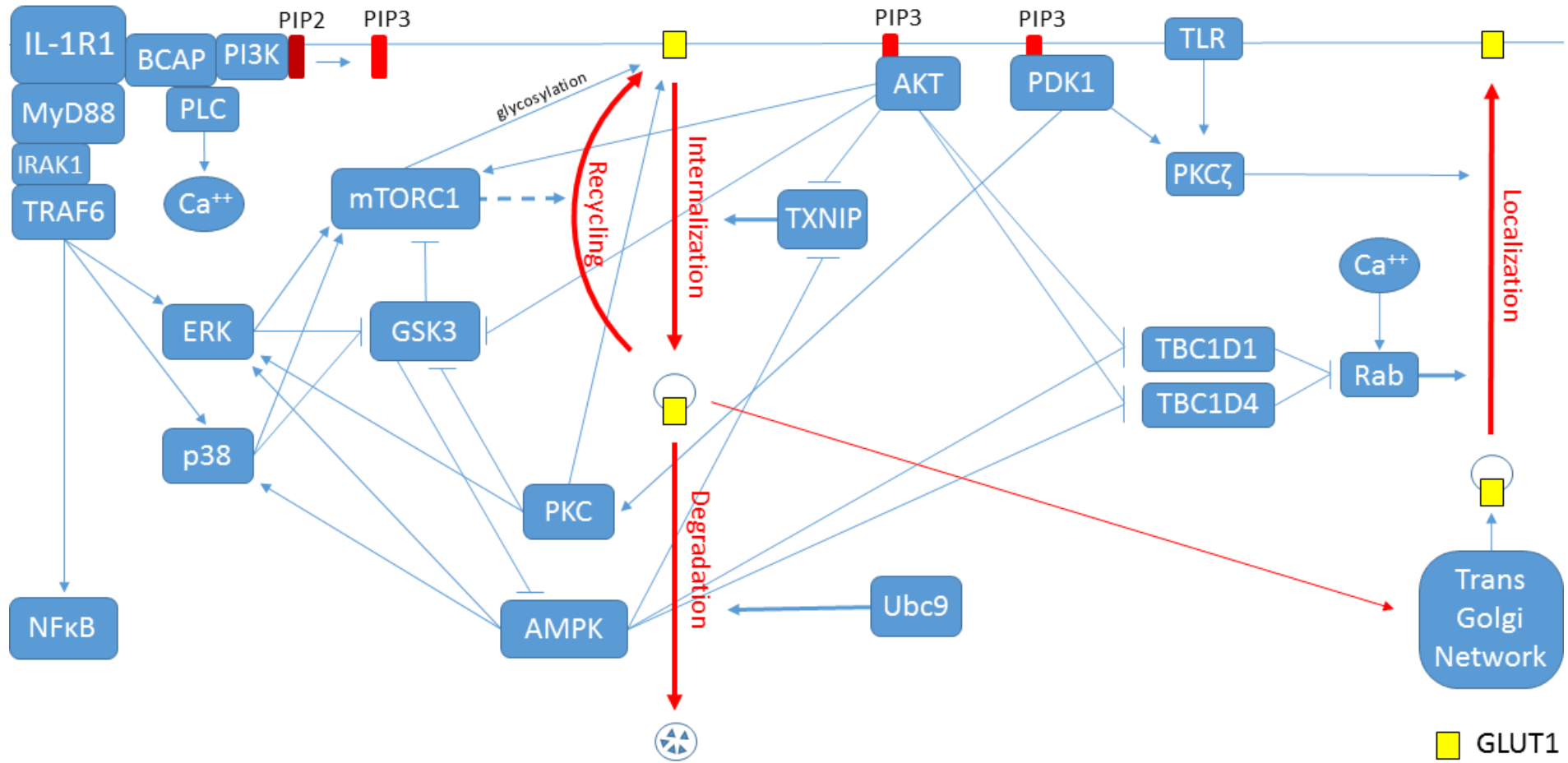
Figure 39. Connections of IL-1 signaling to pathways associated with glucose uptake

4.7 Conclusions

The relatively modest IL-1-dependent glucose uptake observed at short (4 h) incubation periods in B cells significantly increased when cells were stimulated for 24 h with LPS *in vitro*. This demonstrates that IL-1 signaling contributes to sustain the elevated energetic demand of activated B cells. A reduction of glucose uptake was also observed in T cells following IL-1Ra addition, but neither glucose uptake was increased after stimulation nor the proportion of IL-1-mediated glucose uptake changed in the observed timeframe. The magnitude by which IL-1Ra inhibits glucose uptake by T cells and LPS-stimulated B cells is comparable to the reduction caused by the GLUT blocker phloretin, indicating that the effect of endogenously produced IL-1 represents a substantial part of the overall glucose incorporation in immune cells.

It is also shown in this work that endogenous IL-1 profoundly supports lymphocyte energetic metabolism *in vitro*. Mitochondrial oxygen consumption was substantially reduced after blockade of IL-1 signaling and comparable to the effect caused by inhibition of ATP synthase with oligomycin. In LPS-stimulated cells, ECAR, which mainly reflects the rate of glycolysis, declined almost immediately after IL-1 blockade. It has been reported that IL-1 increases the expression of genes that are relevant for glycolysis via HIF-1α and c-Myc (reviewed in [Tan et al., 2018]). The fast decline of ECAR after IL-1Ra addition in LPS-stimulated cells makes it likely that IL-1 signaling also supports glycolysis by mechanisms other than transcription. The marked increase in ECAR after IL-1 blockade in non-LPS-stimulated cells suggests that the reduced mitochondrial OCR is not caused by a lack of fuel.

Some possible intracellular IL-1 signaling pathways that could be involved in the observed effects were examined. Neither the absence of MyD88 nor the inhibition of AKT prevented IL-1Ra effects on glucose uptake. These results indicate that the effects of IL-1 on glucose uptake are either downstream of both MyD88 and PI3K, and they can compensate each other, or that they are mediated by a different signaling pathway. Other possible mechanisms would include PLC pathways, which are activated by IL-1R1 via

BCAP [Yamazaki et al., 2002, Deason et al., 2018], IL-1R1-activated PKCζ [Yang et al., 2011], or a still unknown mechanism.

As already mentioned above, IL-1 signaling activates PLC [Halabi et al., 2017, Deason et al., 2018], which results in the elevation of intracellular calcium concentrations [Wang et al., 2003, Pritchard and Guilak, 2006]. Because calcium is a prominent regulator of mitochondrial activity, the mitochondria might be stimulated by the activation of enzymes involved in the Krebs cycle via an IL-1-induced elevation of calcium concentration.

Exogenous IL-1β was able to slightly elevate glucose uptake, but it did not enhance metabolism under the conditions tested in this work. It is possible that endogenous IL-1 production in the spleen cell suspension is able to maintain IL-1 signaling in an autocrine/paracrine manner *in vitro* and that it is sufficient to saturate the receptors depending on the incubation conditions.

In conclusion, this work demonstrates that IL-1 signaling promotes glucose uptake and energetic metabolism in lymphocytes, and contributes to the understanding of the physiology of glucose distribution to specific cells within the body. It has been reported that IL-1 (as well as TNFα) can induce insulin resistance in insulin-sensitive cells [Jager et al., 2007, Wellen and Hotamisligil, 2005]. On the other hand, we have already shown that neurons and astrocytes are among the different types of cells in which IL-1 can stimulate glucose uptake and that, *in vivo*, it can increase the energetic metabolism of the brain [del Rey et al., 2016]. Under certain pathological situations, the stimulation of glucose uptake by some types of cells and the induction of insulin-resistance in others may serve to deviate glucose to the activated immune system, which needs large amounts of energy to proliferate and to support humoral and cellular immune responses, but without markedly affecting brain functions. As a whole, these findings support previous work of our group showing the important role of IL-1 in the regulation of glucose homeostasis and energy relocation.

It is clear that the results reported in this work open many questions, and that further research is needed particularly to ascertain the physiological relevance of the effects of

IL-1 reported here. As an immediate continuation, it would be desirable to validate the effects of IL-1 on lymphocyte glucose uptake *in vivo*. In expansion of the *in vitro* results, cells from IL-1α/IL-1β double knockout mice could offer a valuable model to directly investigate IL-1β actions on lymphocyte glucose uptake without the interfering effects of endogenously produced IL-1. Regarding the signal transduction pathways that result in IL-1-induced metabolic effects and glucose uptake, PI3K and AKT inhibition in MyD88 KO mice and the comparison to the WT could elucidate the pathways involved. Further, the role of PLC, intracellular Ca^{2+}, MAPK, mTOR and PKCs remain to be clarified.

5 References

[Agilent Technologies, 2014] Agilent Technologies (2014). Cutaway graphic of a single probe and well. XF24 Training Manual.

[Agilent Technologies, 2017] Agilent Technologies (2017). Seahorse xf cell mito stress test profile. Agilent Seahorse XF Cell Mito Stress Test Kit User Guide.

[Ahmed and Berridge, 1999] Ahmed, N. and Berridge, M. V. (1999). N-glycosylation of glucose transporter-1 (glut-1) is associated with increased transporter affinity for glucose in human leukemic cells. Leukemia research, 23:395–401.

[Arencibia et al., 2013] Arencibia, J. M., Pastor-Flores, D., Bauer, A. F., Schulze, J. O., and Biondi, R. M. (2013). Agc protein kinases: from structural mechanism of regulation to allosteric drug development for the treatment of human diseases. Biochimica et biophysica acta, 1834:1302–1321.

[Arend, 2002] Arend, W. P. (2002). The balance between il-1 and il-1ra in disease. Cytokine & growth factor reviews, 13:323–340.

[Asano et al., 1991] Asano, T., Katagiri, H., Takata, K., Lin, J. L., Ishihara, H., Inukai, K., Tsukuda, K., Kikuchi, M., Hirano, H., and Yazaki, Y. (1991). The role of n-glycosylation of glut1 for glucose transport activity. The Journal of biological chemistry, 266:24632–24636.

[Avital et al., 2003] Avital, A., Goshen, I., Kamsler, A., Segal, M., Iverfeldt, K., Richter-Levin, G., and Yirmiya, R. (2003). Impaired interleukin-1 signaling is associated with deficits in hippocampal memory processes and neural plasticity. Hippocampus, 13:826–834.

[Bagchi et al., 2007] Bagchi, A., Herrup, E. A., Warren, H. S., Trigilio, J., Shin, H.-S., Valentine, C., and Hellman, J. (2007). Myd88-dependent and myd88-independent pathways in synergy, priming, and tolerance between tlr agonists. Journal of immunology (Baltimore, Md. : 1950), 178:1164–1171.

[Bandman et al., 2002] Bandman, O., Coleman, R. T., Loring, J. F., Seilhamer, J. J., and Cocks, B. G. (2002). Complexity of inflammatory responses in endothelial cells and vascular smooth muscle cells determined by microarray analysis. Annals of the New York Academy of Sciences, 975:77–90.

[Barros et al., 2001] Barros, L. F., Barnes, K., Ingram, J. C., Castro, J., Porras, O. H., and Baldwin, S. A. (2001). Hyperosmotic shock induces both activation and translocation

of glucose transporters in mammalian cells. Pflugers Archiv : European journal of physiology, 442:614–621.

[Barros et al., 2009] Barros, L. F., Bittner, C. X., Loaiza, A., Ruminot, I., Larenas, V., Moldenhauer, H., Oyarzun, C., and Alvarez, M. (2009). Kinetic validation of 6-nbdg as a probe for the glucose transporter glut1 in astrocytes. Journal of neurochemistry, 109 Suppl 1:94–100.

[Barros et al., 2005] Barros, L. F., Porras, O. H., and Bittner, C. X. (2005). Why glucose transport in the brain matters for pet. Trends in neurosciences, 28:117–119.

[Beeson, 1948] Beeson, P. B. (1948). Temperature-elevating effect of a substance obtained from polymorphonuclear leucocytes. The Journal of clinical investigation, 27:524.

[Ben Menachem-Zidon et al., 2011] Ben Menachem-Zidon, O., Avital, A., Ben-Menahem, Y., Goshen, I., Kreisel, T., Shmueli, E. M., Segal, M., Ben Hur, T., and Yirmiya, R. (2011). Astrocytes support hippocampal-dependent memory and long-term potentiation via interleukin-1 signaling. Brain, behavior, and immunity, 25:1008–1016.

[Ben-Sasson et al., 2013] Ben-Sasson, S. Z., Hogg, A., Hu-Li, J., Wingfield, P., Chen, X., Crank, M., Caucheteux, S., Ratner-Hurevich, M., Berzofsky, J. A., Nir-Paz, R., and Paul, W. E. (2013). Il-1 enhances expansion, effector function, tissue localization, and memory response of antigen-specific cd8 t cells. The Journal of experimental medicine, 210:491–502.

[Ben-Sasson et al., 2009] Ben-Sasson, S. Z., Hu-Li, J., Quiel, J., Cauchetaux, S., Ratner, M., Shapira, I., Dinarello, C. A., and Paul, W. E. (2009). Il-1 acts directly on cd4 t cells to enhance their antigen-driven expansion and differentiation. Proceedings of the National Academy of Sciences of the United States of America, 106:7119–7124.

[Besedovsky et al., 1986] Besedovsky, H., del Rey, A., Sorkin, E., and Dinarello, C. A. (1986). Immunoregulatory feedback between interleukin-1 and glucocorticoid hormones. Science, 233(4764):652–654.

[Besedovsky and del Rey, 2010] Besedovsky, H. O. and del Rey, A. (2010). Interleukin-1 resets glucose homeostasis at central and peripheral levels: relevance for immunoregulation. Neuroimmunomodulation, 17(3):139–141.

[Besedovsky and del Rey, 2011] Besedovsky, H. O. and del Rey, A. (2011). Central and peripheral cytokines mediate immune-brain connectivity. Neurochem Res, 36(1):1–6.

[Besedovsky and del Rey, 2014] Besedovsky, H. O. and del Rey, A. (2014). Physiologic versus diabetogenic effects of interleukin-1: a question of weight. Current pharmaceutical design, 20:4733–4740.

[Bhavsar et al., 2016] Bhavsar, S. K., Singh, Y., Sharma, P., Khairnar, V., Hosseinzadeh, Z., Zhang, S., Palmada, M., Sabolic, I., Koepsell, H., Lang, K. S., Lang, P. A., and Lang, F. (2016). Expression of jak3 sensitive na+ coupled glucose carrier sglt1 in activated cytotoxic t lymphocytes. Cellular physiology and biochemistry : international journal of experimental cellular physiology, biochemistry, and pharmacology, 39:1209–1228.

[Bird et al., 1990] Bird, T. A., Davies, A., Baldwin, S. A., and Saklatvala, J. (1990). Interleukin 1 stimulates hexose transport in fibroblasts by increasing the expression of glucose transporters. J Biol Chem, 265(23):13578–13583.

[Blair et al., 2012] Blair, D., Dufort, F. J., and Chiles, T. C. (2012). Protein kinase cβ is critical for the metabolic switch to glycolysis following b-cell antigen receptor engagement. The Biochemical journal, 448:165–169.

[Boonen et al., 2018] Boonen, B., Alpizar, Y. A., Meseguer, V. M., and Talavera, K. (2018). Trp channels as sensors of bacterial endotoxins. Toxins, 10.

[Boothby and Rickert, 2017] Boothby, M. and Rickert, R. C. (2017). Metabolic regulation of the immune humoral response. Immunity, 46:743–755.

[Braschi et al., 2018] Braschi, B., Denny, P., Gray, K., Jones, T., Seal, R., Tweedie, S., Yates, B., and Bruford, E. (2018). Genenames.org: the hgnc and vgnc resources in 2019. Nucleic acids research.

[Brini and Carafoli, 2011] Brini, M. and Carafoli, E. (2011). The plasma membrane ca^2+ atpase and the plasma membrane sodium calcium exchanger cooperate in the regulation of cell calcium. Cold Spring Harbor perspectives in biology, 3.

[Brinster and Shevach, 2008] Brinster, C. and Shevach, E. M. (2008). Costimulatory effects of il-1 on the expansion/differentiation of cd4+cd25+foxp3+ and cd4+cd25+foxp3- t cells. Journal of leukocyte biology, 84:480–487.

[Brissoni et al., 2006] Brissoni, B., Agostini, L., Kropf, M., Martinon, F., Swoboda, V., Lippens, S., Everett, H., Aebi, N., Janssens, S., Meylan, E., Felberbaum-Corti, M., Hirling, H., Gruenberg, J., Tschopp, J., and Burns, K. (2006). Intracellular trafficking of interleukin-1 receptor i requires tollip. Current biology : CB, 16:2265–2270.

[Broz and Dixit, 2016] Broz, P. and Dixit, V. M. (2016). Inflammasomes: mechanism of assembly, regulation and signalling. Nature reviews. Immunology, 16:407–420.

[Brunet et al., 1999] Brunet, A., Bonni, A., Zigmond, M. J., Lin, M. Z., Juo, P., Hu, L. S., Anderson, M. J., Arden, K. C., Blenis, J., and Greenberg, M. E. (1999). Akt promotes cell survival by phosphorylating and inhibiting a forkhead transcription factor. Cell, 96:857–868.

[Buller et al., 2008] Buller, C. L., Loberg, R. D., Fan, M.-H., Zhu, Q., Park, J. L., Vesely, E., Inoki, K., Guan, K.-L., and Brosius, F. C. (2008). A gsk-3/tsc2/mtor pathway regulates glucose uptake and glut1 glucose transporter expression. American journal of physiology. Cell physiology, 295:C836–C843.

[Calleja et al., 2007] Calleja, V., Alcor, D., Laguerre, M., Park, J., Vojnovic, B., Hemmings, B. A., Downward, J., Parker, P. J., and Larijani, B. (2007). Intramolecular and intermolecular interactions of protein kinase b define its activation in vivo. PLoS biology, 5:e95.

[Caro-Maldonado et al., 2014] Caro-Maldonado, A., Wang, R., Nichols, A. G., Kuraoka, M., Milasta, S., Sun, L. D., Gavin, A. L., Abel, E. D., Kelsoe, G., Green, D. R., and Rathmell, J. C. (2014). Metabolic reprogramming is required for antibody production that is suppressed in anergic but exaggerated in chronically baff-exposed b cells. Journal of immunology (Baltimore, Md. : 1950), 192:3626–3636.

[Cerniglia et al., 2015] Cerniglia, G. J., Dey, S., Gallagher-Colombo, S. M., Daurio, N. A., Tuttle, S., Busch, T. M., Lin, A., Sun, R., Esipova, T. V., Vinogradov, S. A., Denko, N., Koumenis, C., and Maity, A. (2015). The pi3k/akt pathway regulates oxygen metabolism via pyruvate dehydrogenase (pdh)-e1α phosphorylation. Molecular cancer therapeutics, 14:1928–1938.

[Chen et al., 2008] Chen, S., Murphy, J., Toth, R., Campbell, D. G., Morrice, N. A., and Mackintosh, C. (2008). Complementary regulation of tbc1d1 and as160 by growth factors, insulin and ampk activators. The Biochemical journal, 409:449–459.

[Coogan et al., 1999] Coogan, A. N., O'Neill, L. A., and O'Connor, J. J. (1999). The p38 mitogen-activated protein kinase inhibitor sb203580 antagonizes the inhibitory effects of interleukin-1beta on long-term potentiation in the rat dentate gyrus in vitro. Neuroscience, 93:57–69.

[Deason et al., 2018] Deason, K., Troutman, T. D., Jain, A., Challa, D. K., Mandraju, R., Brewer, T., Ward, E. S., and Pasare, C. (2018). Bcap links il-1r to the pi3k-mtor pathway and regulates pathogenic th17 cell differentiation. The Journal of experimental medicine, 215:2413–2428.

[del Rey and Besedovsky, 1987] del Rey, A. and Besedovsky, H. (1987). Interleukin 1 affects glucose homeostasis. Am J Physiol, 253(5 Pt 2):R794–R798.

[del Rey and Besedovsky, 1989] del Rey, A. and Besedovsky, H. (1989). Antidiabetic effects of interleukin 1. Proc Natl Acad Sci U S A, 86(15):5943–5947.

[del Rey et al., 1998] del Rey, A., Monge-Arditi, G., and Besedovsky, H. O. (1998). Central and peripheral mechanisms contribute to the hypoglycemia induced by interleukin-1. Ann N Y Acad Sci, 840:153–161.

[del Rey et al., 2006] del Rey, A., Roggero, E., Randolf, A., Mahuad, C., McCann, S., Rettori, V., and Besedovsky, H. O. (2006). Il-1 resets glucose homeostasis at central levels. Proc Natl Acad Sci U S A, 103(43):16039–16044.

[del Rey et al., 2016] del Rey, A., Verdenhalven, M., Lörwald, A. C., Meyer, C., Hernan-gomez, M., Randolf, A., Roggero, E., König, A. M., Heverhagen, J. T., Guaza, C., and Besedovsky, H. O. (2016). Brain-borne il-1 adjusts glucoregulation and provides fuel support to astrocytes and neurons in an autocrine/paracrine manner. Molecular psychiatry, 21:1309–1320.

[Denton, 2009] Denton, R. M. (2009). Regulation of mitochondrial dehydrogenases by calcium ions. Biochimica et biophysica acta, 1787:1309–1316.

[Dimitriadis et al., 2005] Dimitriadis, G., Maratou, E., Boutati, E., Psarra, K., Papasteriades, C., and Raptis, S. A. (2005). Evaluation of glucose transport and its regulation by insulin in human monocytes using flow cytometry. Cytometry. Part A : the journal of the International Society for Analytical Cytology, 64:27–33.

[Dinarello, 1991] Dinarello, C. A. (1991). Interleukin-1 and interleukin-1 antagonism. Blood, 77:1627–1652.

[Dinarello, 1996] Dinarello, C. A. (1996). Biologic basis for interleukin-1 in disease. Blood, 87:2095–2147.

[Dinarello, 2005] Dinarello, C. A. (2005). Blocking il-1 in systemic inflammation. The Journal of experimental medicine, 201:1355–1359.

[Dinarello, 2011] Dinarello, C. A. (2011). Interleukin-1 in the pathogenesis and treatment of inflammatory diseases. Blood, 117:3720–3732.

[Dinarello, 2015] Dinarello, C. A. (2015). The history of fever, leukocytic pyrogen and interleukin-1. Temperature (Austin, Tex.), 2:8–16.

[Dinarello, 2018] Dinarello, C. A. (2018). Overview of the il-1 family in innate inflammation and acquired immunity. Immunological reviews, 281:8–27.

[Dinarello et al., 1986] Dinarello, C. A., Cannon, J. G., Wolff, S. M., Bernheim, H. A., Beutler, B., Cerami, A., Figari, I. S., Palladino, M. A., and O'Connor, J. V. (1986). Tumor necrosis factor (cachectin) is an endogenous pyrogen and induces production of interleukin 1. The Journal of experimental medicine, 163:1433–1450.

[Dinarello et al., 1987] Dinarello, C. A., Ikejima, T., Warner, S. J., Orencole, S. F., Lonnemann, G., Cannon, J. G., and Libby, P. (1987). Interleukin 1 induces interleukin 1. i. induction of circulating interleukin 1 in rabbits in vivo and in human mononuclear cells in vitro. Journal of immunology (Baltimore, Md. : 1950), 139:1902–1910.

[Divakaruni et al., 2014] Divakaruni, A. S., Paradyse, A., Ferrick, D. A., Murphy, A. N., and Jastroch, M. (2014). Analysis and interpretation of microplate-based oxygen consumption and ph data. Methods in enzymology, 547:309–354.

[Donnelly and Finlay, 2015] Donnelly, R. P. and Finlay, D. K. (2015). Glucose, glycolysis and lymphocyte responses. Molecular immunology, 68:513–519.

[Doughty et al., 2006] Doughty, C. A., Bleiman, B. F., Wagner, D. J., Dufort, F. J., Mataraza, J. M., Roberts, M. F., and Chiles, T. C. (2006). Antigen receptor-mediated changes in glucose metabolism in b lymphocytes: role of phosphatidylinositol 3-kinase signaling in the glycolytic control of growth. Blood, 107:4458–4465.

[Dripps et al., 1991] Dripps, D. J., Verderber, E., Ng, R. K., Thompson, R. C., and Eisenberg, S. P. (1991). Interleukin-1 receptor antagonist binds to the type ii interleukin-1 receptor on b cells and neutrophils. The Journal of biological chemistry, 266:20311–20315.

[Ebner et al., 2017] Ebner, M., Lučić, I., Leonard, T. A., and Yudushkin, I. (2017). Pi(3,4,5)p$_3$ engagement restricts akt activity to cellular membranes. Molecular cell, 65:416–431.e6.

[Elgueta et al., 2009] Elgueta, R., Benson, M. J., de Vries, V. C., Wasiuk, A., Guo, Y., and Noelle, R. J. (2009). Molecular mechanism and function of cd40/cd40l engagement in the immune system. Immunological reviews, 229:152–172.

[Falkoff et al., 1983] Falkoff, R. J., Muraguchi, A., Hong, J. X., Butler, J. L., Dinarello, C. A., and Fauci, A. S. (1983). The effects of interleukin 1 on human b cell activation and proliferation. Journal of immunology (Baltimore, Md. : 1950), 131:801–805.

[Ferrer et al., 2014] Ferrer, C. M., Lynch, T. P., Sodi, V. L., Falcone, J. N., Schwab, L. P., Peacock, D. L., Vocadlo, D. J., Seagroves, T. N., and Reginato, M. J. (2014). O-glcnacylation regulates cancer metabolism and survival stress signaling via regulation of the hif-1 pathway. Molecular cell, 54:820–831.

[Fitzgerald et al., 2003] Fitzgerald, K. A., Rowe, D. C., Barnes, B. J., Caffrey, D. R., Visintin, A., Latz, E., Monks, B., Pitha, P. M., and Golenbock, D. T. (2003). Lps-tlr4 signaling to irf-3/7 and nf-kappab involves the toll adapters tram and trif. The Journal of experimental medicine, 198:1043–1055.

[Fowler et al., 2015] Fowler, T., Garruss, A. S., Ghosh, A., De, S., Becker, K. G., Wood, W. H., Weirauch, M. T., Smale, S. T., Aronow, B., Sen, R., and Roy, A. L. (2015). Divergence of transcriptional landscape occurs early in b cell activation. Epigenetics & chromatin, 8:20.

[Fox et al., 2005] Fox, C. J., Hammerman, P. S., and Thompson, C. B. (2005). Fuel feeds function: energy metabolism and the t-cell response. Nature reviews. Immunology, 5:844–852.

[Frauwirth et al., 2002] Frauwirth, K. A., Riley, J. L., Harris, M. H., Parry, R. V., Rathmell, J. C., Plas, D. R., Elstrom, R. L., June, C. H., and Thompson, C. B. (2002). The cd28 signaling pathway regulates glucose metabolism. Immunity, 16:769–777.

[Friedlander et al., 1996] Friedlander, R. M., Gagliardini, V., Rotello, R. J., and Yuan, J. (1996). Functional role of interleukin 1 beta (il-1 beta) in il-1 beta-converting enzyme-mediated apoptosis. The Journal of experimental medicine, 184:717–724.

[Fujii et al., 2006] Fujii, N., Jessen, N., and Goodyear, L. J. (2006). Amp-activated protein kinase and the regulation of glucose transport. American journal of physiology. Endocrinology and metabolism, 291:E867–E877.

[Fukuzumi et al., 1996] Fukuzumi, M., Shinomiya, H., Shimizu, Y., Ohishi, K., and Utsumi, S. (1996). Endotoxin-induced enhancement of glucose influx into murine peritoneal macrophages via glut1. Infection and immunity, 64:108–112.

[Garcia-Welsh et al., 1990] Garcia-Welsh, A., Schneiderman, J. S., and Baly, D. L. (1990). Interleukin-1 stimulates glucose transport in rat adipose cells. evidence for receptor discrimination between il-1 beta and il-1 alpha. FEBS Lett, 269(2):421–424.

[Geng et al., 1996] Geng, Y., Valbracht, J., and Lotz, M. (1996). Selective activation of the mitogen-activated protein kinase subgroups c-jun nh2 terminal kinase and p38 by il-1 and tnf in human articular chondrocytes. The Journal of clinical investigation, 98:2425–2430.

[Gharbi et al., 2007] Gharbi, S. I., Zvelebil, M. J., Shuttleworth, S. J., Hancox, T., Saghir, N., Timms, J. F., and Waterfield, M. D. (2007). Exploring the specificity of the pi3k family inhibitor ly294002. The Biochemical journal, 404:15–21.

[Giorgi et al., 2018] Giorgi, C., Marchi, S., and Pinton, P. (2018). The machineries, regulation and cellular functions of mitochondrial calcium. Nature reviews. Molecular cell biology, 19:713–730.

[Giorgino et al., 2000] Giorgino, F., de Robertis, O., Laviola, L., Montrone, C., Perrini, S., McCowen, K. C., and Smith, R. J. (2000). The sentrin-conjugating enzyme mubc9 interacts with glut4 and glut1 glucose transporters and regulates transporter levels in skeletal muscle cells. Proceedings of the National Academy of Sciences of the United States of America, 97:1125–1130.

[Gregory et al., 2003] Gregory, M. A., Qi, Y., and Hann, S. R. (2003). Phosphorylation by glycogen synthase kinase-3 controls c-myc proteolysis and subnuclear localization. The Journal of biological chemistry, 278:51606–51612.

[Halabi et al., 2017] Halabi, S., Sekine, E., Verstak, B., Gay, N. J., and Moncrieffe, M. C. (2017). Structure of the toll/interleukin-1 receptor (tir) domain of the b-cell adaptor that links phosphoinositide metabolism with the negative regulation of the toll-like receptor (tlr) signalosome. The Journal of biological chemistry, 292:652–660.

[Hambleton et al., 1996] Hambleton, J., Weinstein, S. L., Lem, L., and DeFranco, A. L. (1996). Activation of c-jun n-terminal kinase in bacterial lipopolysaccharide-stimulated macrophages. Proceedings of the National Academy of Sciences of the United States of America, 93:2774–2778.

[Herst and Berridge, 2007] Herst, P. M. and Berridge, M. V. (2007). Cell surface oxygen consumption: a major contributor to cellular oxygen consumption in glycolytic cancer cell lines. Biochimica et biophysica acta, 1767:170–177.

[Herst et al., 2004] Herst, P. M., Tan, A. S., Scarlett, D.-J. G., and Berridge, M. V. (2004). Cell surface oxygen consumption by mitochondrial gene knockout cells. Biochimica et biophysica acta, 1656:79–87.

[Holliday and Gruol, 1993] Holliday, J. and Gruol, D. L. (1993). Cytokine stimulation increases intracellular calcium and alters the response to quisqualate in cultured cortical astrocytes. Brain research, 621:233–241.

[Holzberg et al., 2003] Holzberg, D., Knight, C. G., Dittrich-Breiholz, O., Schneider, H., Dörrie, A., Hoffmann, E., Resch, K., and Kracht, M. (2003). Disruption of the c-jun-jnk complex by a cell-permeable peptide containing the c-jun delta domain induces apoptosis and affects a distinct set of interleukin-1-induced inflammatory genes. The Journal of biological chemistry, 278:40213–40223.

[Huber et al., 1998] Huber, M., Beuscher, H. U., Rohwer, P., Kurrle, R., Röllinghoff, M., and Lohoff, M. (1998). Costimulation via tcr and il-1 receptor reveals a novel il-1alpha-mediated autocrine pathway of th2 cell proliferation. Journal of immunology (Baltimore, Md. : 1950), 160:4242–4247.

[Huber et al., 1996] Huber, M., Rutherford, A., Meister, W., Weiss, A., Röllinghoff, M., and Lohoff, M. (1996). Tcr- and il-1-mediated co-stimulation reveals an il-4-independent way of th2 cell proliferation. International immunology, 8:1257–1263.

[Jacobs et al., 2008] Jacobs, S. R., Herman, C. E., Maciver, N. J., Wofford, J. A., Wieman, H. L., Hammen, J. J., and Rathmell, J. C. (2008). Glucose uptake is limiting in t cell activation and requires cd28-mediated akt-dependent and independent pathways. Journal of immunology (Baltimore, Md. : 1950), 180:4476–4486.

[Jager et al., 2007] Jager, J., Grémeaux, T., Cormont, M., Le Marchand-Brustel, Y., and Tanti, J.-F. (2007). Interleukin-1beta-induced insulin resistance in adipocytes through down-regulation of insulin receptor substrate-1 expression. Endocrinology, 148:241–251.

[Jayachandran et al., 2018] Jayachandran, N., Mejia, E. M., Sheikholeslami, K., Sher, A. A., Hou, S., Hatch, G. M., and Marshall, A. J. (2018). Tapp adaptors control b cell metabolism by modulating the phosphatidylinositol 3-kinase signaling pathway: A novel regulatory circuit preventing autoimmunity. Journal of immunology (Baltimore, Md. : 1950), 201:406–416.

[Johnson et al., 2018] Johnson, M. O., Wolf, M. M., Madden, M. Z., Andrejeva, G., Sugiura, A., Contreras, D. C., Maseda, D., Liberti, M. V., Paz, K., Kishton, R. J., Johnson, M. E., de Cubas, A. A., Wu, P., Li, G., Zhang, Y., Newcomb, D. C., Wells, A. D., Restifo, N. P., Rathmell, W. K., Locasale, J. W., Davila, M. L., Blazar, B. R., and Rathmell, J. C. (2018). Distinct regulation of th17 and th1 cell differentiation by glutaminase-dependent metabolism. Cell, 175:1780–1795.e19.

[Jope and Johnson, 2004] Jope, R. S. and Johnson, G. V. W. (2004). The glamour and gloom of glycogen synthase kinase-3. Trends in biochemical sciences, 29:95–102.

[Kawai et al., 1999] Kawai, T., Adachi, O., Ogawa, T., Takeda, K., and Akira, S. (1999). Unresponsiveness of myd88-deficient mice to endotoxin. Immunity, 11:115–122.

[Kaye et al., 1984] Kaye, J., Gillis, S., Mizel, S. B., Shevach, E. M., Malek, T. R., Dinarello, C. A., Lachman, L. B., and Janeway, C. A. (1984). Growth of a cloned helper t cell line induced by a monoclonal antibody specific for the antigen receptor: interleukin 1 is required for the expression of receptors for interleukin 2. Journal of immunology (Baltimore, Md. : 1950), 133:1339–1345.

[Khoruts et al., 2004] Khoruts, A., Osness, R. E., and Jenkins, M. K. (2004). Il-1 acts on antigen-presenting cells to enhance the in vivo proliferation of antigen-stimulated naive cd4 t cells via a cd28-dependent mechanism that does not involve increased expression of cd28 ligands. European journal of immunology, 34:1085–1090.

[Kim et al., 2010] Kim, J. H., Park, J.-M., Yea, K., Kim, H. W., Suh, P.-G., and Ryu, S. H. (2010). Phospholipase d1 mediates amp-activated protein kinase signaling for glucose uptake. PloS one, 5:e9600.

[Kobayashi et al., 2002] Kobayashi, K., Hernandez, L. D., Galàn, J. E., Janeway, C. A., Medzhitov, R., and Flavell, R. A. (2002). Irak-m is a negative regulator of toll-like receptor signaling. Cell, 110:191–202.

[Koopman et al., 1994] Koopman, G., Reutelingsperger, C. P., Kuijten, G. A., Keehnen, R. M., Pals, S. T., and van Oers, M. H. (1994). Annexin v for flow cytometric detection of phosphatidylserine expression on b cells undergoing apoptosis. Blood, 84:1415–1420.

[Land and Tee, 2007] Land, S. C. and Tee, A. R. (2007). Hypoxia-inducible factor 1alpha is regulated by the mammalian target of rapamycin (mtor) via an mtor signaling motif. The Journal of biological chemistry, 282:20534–20543.

[Laplante and Sabatini, 2012] Laplante, M. and Sabatini, D. M. (2012). mtor signaling in growth control and disease. Cell, 149:274–293.

[Lee et al., 2015] Lee, E. E., Ma, J., Sacharidou, A., Mi, W., Salato, V. K., Nguyen, N., Jiang, Y., Pascual, J. M., North, P. E., Shaul, P. W., Mettlen, M., and Wang, R. C. (2015). A protein kinase c phosphorylation motif in glut1 affects glucose transport and is mutated in glut1 deficiency syndrome. Molecular cell, 58:845–853.

[Lee et al., 2017] Lee, J.-H., Liu, R., Li, J., Zhang, C., Wang, Y., Cai, Q., Qian, X., Xia, Y., Zheng, Y., Piao, Y., Chen, Q., de Groot, J. F., Jiang, T., and Lu, Z. (2017). Stabilization of phosphofructokinase 1 platelet isoform by akt promotes tumorigenesis. Nature communications, 8:949.

[Li et al., 2010] Li, Q., Zhang, H., Chen, Q., and Quan, N. (2010). Existence of seven human il-1r1 promoters. Journal of inflammation research, 2010:17–24.

[Lichtman et al., 1988] Lichtman, A. H., Chin, J., Schmidt, J. A., and Abbas, A. K. (1988). Role of interleukin 1 in the activation of t lymphocytes. Proceedings of the National Academy of Sciences of the United States of America, 85:9699–9703.

[Liu et al., 2014] Liu, T., Kishton, R. J., Macintyre, A. N., Gerriets, V. A., Xiang, H., Liu, X., Abel, E. D., Rizzieri, D., Locasale, J. W., and Rathmell, J. C. (2014). Glucose transporter 1-mediated glucose uptake is limiting for b-cell acute lymphoblastic leukemia anabolic metabolism and resistance to apoptosis. Cell death & disease, 5:e1470.

[Lukens et al., 2012] Lukens, J. R., Gross, J. M., and Kanneganti, T.-D. (2012). Il-1 family cytokines trigger sterile inflammatory disease. Frontiers in immunology, 3:315.

[Lučić et al., 2018] Lučić, I., Rathinaswamy, M. K., Truebestein, L., Hamelin, D. J., Burke, J. E., and Leonard, T. A. (2018). Conformational sampling of membranes by akt controls its activation and inactivation. Proceedings of the National Academy of Sciences of the United States of America, 115:E3940–E3949.

[MacIver et al., 2013] MacIver, N. J., Michalek, R. D., and Rathmell, J. C. (2013). Metabolic regulation of t lymphocytes. Annual review of immunology, 31:259–283.

[Macintyre et al., 2014] Macintyre, A. N., Gerriets, V. A., Nichols, A. G., Michalek, R. D., Rudolph, M. C., Deoliveira, D., Anderson, S. M., Abel, E. D., Chen, B. J., Hale, L. P., and Rathmell, J. C. (2014). The glucose transporter glut1 is selectively essential for cd4 t cell activation and effector function. Cell metabolism, 20:61–72.

[Maciver et al., 2008] Maciver, N. J., Jacobs, S. R., Wieman, H. L., Wofford, J. A., Coloff, J. L., and Rathmell, J. C. (2008). Glucose metabolism in lymphocytes is a regulated process with significant effects on immune cell function and survival. Journal of leukocyte biology, 84:949–957.

[Manning and Toker, 2017] Manning, B. D. and Toker, A. (2017). Akt/pkb signaling: Navigating the network. Cell, 169:381–405.

[Mantovani et al., 2001] Mantovani, A., Locati, M., Vecchi, A., Sozzani, S., and Allavena, P. (2001). Decoy receptors: a strategy to regulate inflammatory cytokines and chemokines. Trends in immunology, 22:328–336.

[Maratou et al., 2007] Maratou, E., Dimitriadis, G., Kollias, A., Boutati, E., Lambadiari, V., Mitrou, P., and Raptis, S. A. (2007). Glucose transporter expression on the plasma membrane of resting and activated white blood cells. European journal of clinical investigation, 37:282–290.

[Mariathasan et al., 2004] Mariathasan, S., Newton, K., Monack, D. M., Vucic, D., French, D. M., Lee, W. P., Roose-Girma, M., Erickson, S., and Dixit, V. M. (2004). Differential activation of the inflammasome by caspase-1 adaptors asc and ipaf. Nature, 430:213–218.

[Marko et al., 2010] Marko, A. J., Miller, R. A., Kelman, A., and Frauwirth, K. A. (2010). Induction of glucose metabolism in stimulated t lymphocytes is regulated by mitogen-activated protein kinase signaling. PloS one, 5:e15425.

[Marshall et al., 2000] Marshall, A. J., Niiro, H., Lerner, C. G., Yun, T. J., Thomas, S., Disteche, C. M., and Clark, E. A. (2000). A novel b lymphocyte-associated adaptor protein, bam32, regulates antigen receptor signaling downstream of phosphatidylinositol 3-kinase. The Journal of experimental medicine, 191:1319–1332.

[Martinon et al., 2004] Martinon, F., Agostini, L., Meylan, E., and Tschopp, J. (2004). Identification of bacterial muramyl dipeptide as activator of the nalp3/cryopyrin inflammasome. Current biology : CB, 14:1929–1934.

[Matsushima et al., 1986] Matsushima, K., Yodoi, J., Tagaya, Y., and Oppenheim, J. J. (1986). Down-regulation of interleukin 1 (il 1) receptor expression by il 1 and fate of internalized 125i-labeled il 1 beta in a human large granular lymphocyte cell line. Journal of immunology (Baltimore, Md. : 1950), 137:3183–3188.

[McBrayer et al., 2012] McBrayer, S. K., Cheng, J. C., Singhal, S., Krett, N. L., Rosen, S. T., and Shanmugam, M. (2012). Multiple myeloma exhibits novel dependence on glut4, glut8, and glut11: implications for glucose transporter-directed therapy. Blood, 119:4686–4697.

[McIntyre et al., 1991] McIntyre, K. W., Stepan, G. J., Kolinsky, K. D., Benjamin, W. R., Plocinski, J. M., Kaffka, K. L., Campen, C. A., Chizzonite, R. A., and Kilian, P. L. (1991). Inhibition of interleukin 1 (il-1) binding and bioactivity in vitro and modulation of acute inflammation in vivo by il-1 receptor antagonist and anti-il-1 receptor monoclonal antibody. The Journal of experimental medicine, 173:931–939.

[Melchers et al., 1975] Melchers, F., Von Boehmer, H., and Phillips, R. A. (1975). B-lymphocyte subpopulations in the mouse. organ distribution and ontogeny of immunoglobulin-synthesizing and of mitogen-sensitive cells. Transplantation reviews, 25:26–58.

[Mendoza et al., 2011] Mendoza, M. C., Er, E. E., and Blenis, J. (2011). The ras-erk and pi3k-mtor pathways: cross-talk and compensation. Trends in biochemical sciences, 36:320–328.

[Michalek et al., 2011] Michalek, R. D., Gerriets, V. A., Jacobs, S. R., Macintyre, A. N., MacIver, N. J., Mason, E. F., Sullivan, S. A., Nichols, A. G., and Rathmell, J. C. (2011). Cutting edge: distinct glycolytic and lipid oxidative metabolic programs are essential for effector and regulatory cd4+ t cell subsets. Journal of immunology (Baltimore, Md. : 1950), 186:3299–3303.

[Mier and Gallo, 1980] Mier, J. W. and Gallo, R. C. (1980). Purification and some characteristics of human t-cell growth factor from phytohemagglutinin-stimulated lymphocyte-conditioned media. Proceedings of the National Academy of Sciences of the United States of America, 77:6134–6138.

[Miki et al., 2001] Miki, T., Liss, B., Minami, K., Shiuchi, T., Saraya, A., Kashima, Y., Horiuchi, M., Ashcroft, F., Minokoshi, Y., Roeper, J., and Seino, S. (2001). Atp-sensitive k+ channels in the hypothalamus are essential for the maintenance of glucose homeostasis. Nat Neurosci, 4(5):507–512.

[Miki and Seino, 2005] Miki, T. and Seino, S. (2005). Roles of katp channels as metabolic sensors in acute metabolic changes. J Mol Cell Cardiol, 38(6):917–925.

[Monos et al., 1984] Monos, D., Gray, I., and Cooper, H. L. (1984). Glycogen regulation in lps-stimulated murine splenocytes. Experimental cell research, 151:306–313.

[Mora et al., 2004] Mora, A., Komander, D., van Aalten, D. M. F., and Alessi, D. R. (2004). Pdk1, the master regulator of agc kinase signal transduction. Seminars in cell & developmental biology, 15:161–170.

[Mueckler and Thorens, 2013] Mueckler, M. and Thorens, B. (2013). The slc2 (glut) family of membrane transporters. Molecular aspects of medicine, 34:121–138.

[Neary and Pastorino, 2013] Neary, C. L. and Pastorino, J. G. (2013). Akt inhibition promotes hexokinase 2 redistribution and glucose uptake in cancer cells. Journal of cellular physiology, 228:1943–1948.

[Netea et al., 2015] Netea, M. G., van de Veerdonk, F. L., van der Meer, J. W. M., Dinarello, C. A., and Joosten, L. A. B. (2015). Inflammasome-independent regulation of il-1-family cytokines. Annual review of immunology, 33:49–77.

[O'Neill et al., 2013] O'Neill, L. A. J., Golenbock, D., and Bowie, A. G. (2013). The history of toll-like receptors - redefining innate immunity. Nature reviews. Immunology, 13:453–460.

[Orlinska and Newton, 1993] Orlinska, U. and Newton, R. C. (1993). Role of glucose in interleukin-1 beta production by lipopolysaccharide-activated human monocytes. Journal of cellular physiology, 157:201–208.

[Osthus et al., 2000] Osthus, R. C., Shim, H., Kim, S., Li, Q., Reddy, R., Mukherjee, M., Xu, Y., Wonsey, D., Lee, L. A., and Dang, C. V. (2000). Deregulation of glucose transporter 1 and glycolytic gene expression by c-myc. The Journal of biological chemistry, 275:21797–21800.

[Papatheodorou et al., 2018] Papatheodorou, I., Fonseca, N. A., Keays, M., Tang, Y. A., Barrera, E., Bazant, W., Burke, M., Füllgrabe, A., Fuentes, A. M.-P., George, N., Huerta, L., Koskinen, S., Mohammed, S., Geniza, M., Preece, J., Jaiswal, P., Jarnuczak, A. F., Huber, W., Stegle, O., Vizcaino, J. A., Brazma, A., and Petryszak, R. (2018). Expression atlas: gene and protein expression across multiple studies and organisms. Nucleic acids research, 46:D246–D251.

[Park et al., 2015] Park, M.-J., Lee, S. H., Lee, S.-H., Lee, E.-J., Kim, E.-K., Choi, J. Y., and Cho, M.-L. (2015). Il-1 receptor blockade alleviates graft-versus-host disease through downregulation of an interleukin-1β-dependent glycolytic pathway in th17 cells. Mediators of inflammation, 2015:631384.

[Pearce et al., 2009] Pearce, E. L., Walsh, M. C., Cejas, P. J., Harms, G. M., Shen, H., Wang, L.-S., Jones, R. G., and Choi, Y. (2009). Enhancing cd8 t-cell memory by modulating fatty acid metabolism. Nature, 460:103–107.

[Pei et al., 2018] Pei, H., He, L., Shao, M., Yang, Z., Ran, Y., Li, D., Zhou, Y., Tang, M., Wang, T., Gong, Y., Chen, X., Yang, S., Xiang, M., and Chen, L. (2018). Discovery of a highly selective jak3 inhibitor for the treatment of rheumatoid arthritis. Scientific reports, 8:5273.

[Penton-Rol et al., 1999] Penton-Rol, G., Orlando, S., Polentarutti, N., Bernasconi, S., Muzio, M., Introna, M., and Mantovani, A. (1999). Bacterial lipopolysaccharide causes rapid shedding, followed by inhibition of mrna expression, of the il-1 type ii receptor, with concomitant up-regulation of the type i receptor and induction of incompletely spliced transcripts. Journal of immunology (Baltimore, Md. : 1950), 162:2931–2938.

[Pétrilli et al., 2007] Pétrilli, V., Papin, S., Dostert, C., Mayor, A., Martinon, F., and Tschopp, J. (2007). Activation of the nalp3 inflammasome is triggered by low intracellular potassium concentration. Cell death and differentiation, 14:1583–1589.

[Pfleger et al., 2015] Pfleger, J., He, M., and Abdellatif, M. (2015). Mitochondrial complex ii is a source of the reserve respiratory capacity that is regulated by metabolic sensors and promotes cell survival. Cell death & disease, 6:e1835.

[Pizarro and Cominelli, 2007] Pizarro, T. T. and Cominelli, F. (2007). Cloning il-1 and the birth of a new era in cytokine biology. Journal of immunology (Baltimore, Md. : 1950), 178:5411–5412.

[Pritchard and Guilak, 2006] Pritchard, S. and Guilak, F. (2006). Effects of interleukin-1 on calcium signaling and the increase of filamentous actin in isolated and in situ articular chondrocytes. Arthritis and rheumatism, 54:2164–2174.

[Puente et al., 2006] Puente, L. G., He, J.-S., and Ostergaard, H. L. (2006). A novel pkc regulates erk activation and degranulation of cytotoxic t lymphocytes: Plasticity in pkc regulation of erk. European journal of immunology, 36:1009–1018.

[Qian et al., 2012] Qian, J., Zhu, L., Li, Q., Belevych, N., Chen, Q., Zhao, F., Herness, S., and Quan, N. (2012). Interleukin-1r3 mediates interleukin-1-induced potassium current increase through fast activation of akt kinase. Proceedings of the National Academy of Sciences of the United States of America, 109:12189–12194.

[Rathmell and Thompson, 2002] Rathmell, J. C. and Thompson, C. B. (2002). Pathways of apoptosis in lymphocyte development, homeostasis, and disease. Cell, 109 Suppl:S97–107.

[Roberts et al., 2013] Roberts, D. J., Tan-Sah, V. P., Smith, J. M., and Miyamoto, S. (2013). Akt phosphorylates hk-ii at thr-473 and increases mitochondrial hk-ii association to protect cardiomyocytes. The Journal of biological chemistry, 288:23798–23806.

[Rosenwasser, 1998] Rosenwasser, L. J. (1998). Biologic activities of il-1 and its role in human disease. The Journal of allergy and clinical immunology, 102:344–350.

[Sarbassov et al., 2005] Sarbassov, D. D., Guertin, D. A., Ali, S. M., and Sabatini, D. M. (2005). Phosphorylation and regulation of akt/pkb by the rictor-mtor complex. Science (New York, N.Y.), 307:1098–1101.

[Sasaki et al., 2016] Sasaki, A., Nagatomo, K., Ono, K., Yamamoto, T., Otsuka, Y., Teshima, T., and Yamada, K. (2016). Uptake of a fluorescent l-glucose derivative 2-nbdlg into three-dimensionally accumulating insulinoma cells in a phloretin-sensitive manner. Human cell, 29:37–45.

[Savina et al., 2005] Savina, A., Fader, C. M., Damiani, M. T., and Colombo, M. I. (2005). Rab11 promotes docking and fusion of multivesicular bodies in a calcium-dependent manner. Traffic (Copenhagen, Denmark), 6:131–143.

[Saxton and Sabatini, 2017] Saxton, R. A. and Sabatini, D. M. (2017). mtor signaling in growth, metabolism, and disease. Cell, 168:960–976.

[Schieke et al., 2006] Schieke, S. M., Phillips, D., McCoy, J. P., Aponte, A. M., Shen, R.-F., Balaban, R. S., and Finkel, T. (2006). The mammalian target of rapamycin (mtor) pathway regulates mitochondrial oxygen consumption and oxidative capacity. The Journal of biological chemistry, 281:27643–27652.

[Schindelin et al., 2012] Schindelin, J., Arganda-Carreras, I., Frise, E., Kaynig, V., Longair, M., Pietzsch, T., Preibisch, S., Rueden, C., Saalfeld, S., Schmid, B., Tinevez, J.-Y., White, D. J., Hartenstein, V., Eliceiri, K., Tomancak, P., and Cardona, A. (2012). Fiji: an open-source platform for biological-image analysis. Nature methods, 9:676–682.

[Schneider et al., 1998] Schneider, H., Pitossi, F., Balschun, D., Wagner, A., del Rey, A., and Besedovsky, H. O. (1998). A neuromodulatory role of interleukin-1beta in the hippocampus. Proceedings of the National Academy of Sciences of the United States of America, 95:7778–7783.

[Seino and Miki, 2003] Seino, S. and Miki, T. (2003). Physiological and pathophysiological roles of atp-sensitive k+ channels. Progress in biophysics and molecular biology, 81:133–176.

[Sena et al., 2013] Sena, L. A., Li, S., Jairaman, A., Prakriya, M., Ezponda, T., Hildeman, D. A., Wang, C.-R., Schumacker, P. T., Licht, J. D., Perlman, H., Bryce, P. J., and Chandel, N. S. (2013). Mitochondria are required for antigen-specific t cell activation through reactive oxygen species signaling. Immunity, 38:225–236.

[Sherwin, 2008] Sherwin, R. S. (2008). Bringing light to the dark side of insulin: a journey across the blood-brain barrier. Diabetes, 57(9):2259–2268.

[Shikhman et al., 2004] Shikhman, A. R., Brinson, D. C., and Lotz, M. K. (2004). Distinct pathways regulate facilitated glucose transport in human articular chondrocytes during anabolic and catabolic responses. American journal of physiology. Endocrinology and metabolism, 286:E980–E985.

[Shikhman et al., 2001] Shikhman, A. R., Brinson, D. C., Valbracht, J., and Lotz, M. K. (2001). Cytokine regulation of facilitated glucose transport in human articular chondrocytes. Journal of immunology (Baltimore, Md. : 1950), 167:7001–7008.

[Simpson et al., 2008] Simpson, I. A., Dwyer, D., Malide, D., Moley, K. H., Travis, A., and Vannucci, S. J. (2008). The facilitative glucose transporter glut3: 20 years of distinction. American journal of physiology. Endocrinology and metabolism, 295:E242–E253.

[Sims and Smith, 2010] Sims, J. E. and Smith, D. E. (2010). The il-1 family: regulators of immunity. Nature reviews. Immunology, 10:89–102.

[Slack et al., 2015] Slack, M., Wang, T., and Wang, R. (2015). T cell metabolic reprogramming and plasticity. Molecular immunology, 68:507–512.

[Smith et al., 2009] Smith, D. E., Lipsky, B. P., Russell, C., Ketchem, R. R., Kirchner, J., Hensley, K., Huang, Y., Friedman, W. J., Boissonneault, V., Plante, M.-M., Rivest, S., and Sims, J. E. (2009). A central nervous system-restricted isoform of the interleukin-1 receptor accessory protein modulates neuronal responses to interleukin-1. Immunity, 30:817–831.

[Smith et al., 1980] Smith, K. A., Lachman, L. B., Oppenheim, J. J., and Favata, M. F. (1980). The functional relationship of the interleukins. The Journal of experimental medicine, 151:1551–1556.

[So and Fruman, 2012] So, L. and Fruman, D. A. (2012). Pi3k signalling in b- and t-lymphocytes: new developments and therapeutic advances. The Biochemical journal, 442:465–481.

[Speizer et al., 1985] Speizer, L., Haugland, R., and Kutchai, H. (1985). Asymmetric transport of a fluorescent glucose analogue by human erythrocytes. Biochim Biophys Acta, 815(1):75–84.

[Spulber et al., 2009] Spulber, S., Mateos, L., Oprica, M., Cedazo-Minguez, A., Bartfai, T., Winblad, B., and Schultzberg, M. (2009). Impaired long term memory consolidation in transgenic mice overexpressing the human soluble form of il-1ra in the brain. Journal of neuroimmunology, 208:46–53.

[Sun et al., 2006] Sun, C.-C., Su Pang, J.-H., Cheng, C.-Y., Cheng, H.-F., Lee, Y.-S., Ku, W.-C., Hsiao, C.-H., Chen, J.-K., and Yang, C.-M. (2006). Interleukin-1 receptor antagonist (il-1ra) prevents apoptosis in ex vivo expansion of human limbal epithelial cells cultivated on human amniotic membrane. Stem cells (Dayton, Ohio), 24:2130–2139.

[Sutton et al., 2006] Sutton, C., Brereton, C., Keogh, B., Mills, K. H. G., and Lavelle, E. C. (2006). A crucial role for interleukin (il)-1 in the induction of il-17-producing t cells that mediate autoimmune encephalomyelitis. The Journal of experimental medicine, 203:1685–1691.

[Tamas et al., 2006] Tamas, P., Hawley, S. A., Clarke, R. G., Mustard, K. J., Green, K., Hardie, D. G., and Cantrell, D. A. (2006). Regulation of the energy sensor amp-activated protein kinase by antigen receptor and ca2+ in t lymphocytes. The Journal of experimental medicine, 203:1665–1670.

[Tan et al., 2018] Tan, Q., Huang, Q., Ma, Y. L., Mao, K., Yang, G., Luo, P., Ma, G., Mei, P., and Jin, Y. (2018). Potential roles of il-1 subfamily members in glycolysis in disease. Cytokine & growth factor reviews, 44:18–27.

[Teshima et al., 2004] Teshima, S., Nakanishi, H., Nishizawa, M., Kitagawa, K., Kaibori, M., Yamada, M., Habara, K., Kwon, A.-H., Kamiyama, Y., Ito, S., and Okumura, T. (2004). Up-regulation of il-1 receptor through pi3k/akt is essential for the induction of inos gene expression in hepatocytes. Journal of hepatology, 40:616–623.

[Thorens and Mueckler, 2010] Thorens, B. and Mueckler, M. (2010). Glucose transporters in the 21st century. American journal of physiology. Endocrinology and metabolism, 298:E141–E145.

[Trebak and Kinet, 2019] Trebak, M. and Kinet, J.-P. (2019). Calcium signalling in t cells. Nature reviews. Immunology, 19:154–169.

[Treebak et al., 2010] Treebak, J. T., Taylor, E. B., Witczak, C. A., An, D., Toyoda, T., Koh, H.-J., Xie, J., Feener, E. P., Wojtaszewski, J. F. P., Hirshman, M. F., and Goodyear, L. J. (2010). Identification of a novel phosphorylation site on tbc1d4 regulated by amp-activated protein kinase in skeletal muscle. American journal of physiology. Cell physiology, 298:C377–C385.

[Troutman et al., 2012] Troutman, T. D., Bazan, J. F., and Pasare, C. (2012). Toll-like receptors, signaling adapters and regulation of the pro-inflammatory response by pi3k. Cell cycle (Georgetown, Tex.), 11:3559–3567.

[Tsuchiya et al., 2018] Tsuchiya, M., Sekiai, S., Hatakeyama, H., Koide, M., Chaweewannakorn, C., Yaoita, F., Tan-No, K., Sasaki, K., Watanabe, M., Sugawara, S., Endo, Y., Itoi, E., Hagiwara, Y., and Kanzaki, M. (2018). Neutrophils provide a favorable il-1-mediated immunometabolic niche that primes glut4 translocation and performance in skeletal muscles. Cell reports, 23:2354–2364.

[Ueda et al., 1996] Ueda, Y., Hirai, S. i., Osada, S. i., Suzuki, A., Mizuno, K., and Ohno, S. (1996). Protein kinase c activates the mek-erk pathway in a manner independent of ras and dependent on raf. The Journal of biological chemistry, 271:23512–23519.

[Vaeth et al., 2017] Vaeth, M., Maus, M., Klein-Hessling, S., Freinkman, E., Yang, J., Eckstein, M., Cameron, S., Turvey, S. E., Serfling, E., Berberich-Siebelt, F., Possemato, R., and Feske, S. (2017). Store-operated ca, javax.xml.bind.jaxbelement@123a8b, entry controls clonal expansion of t cells through metabolic reprogramming. Immunity, 47:664–679.e6.

[van der Windt et al., 2012] van der Windt, G. J. W., Everts, B., Chang, C.-H., Curtis, J. D., Freitas, T. C., Amiel, E., Pearce, E. J., and Pearce, E. L. (2012). Mitochondrial respiratory capacity is a critical regulator of cd8+ t cell memory development. Immunity, 36:68–78.

[van Engeland et al., 1998] van Engeland, M., Nieland, L. J., Ramaekers, F. C., Schutte, B., and Reutelingsperger, C. P. (1998). Annexin v-affinity assay: a review on an apoptosis detection system based on phosphatidylserine exposure. Cytometry, 31:1–9.

[Vander Heiden et al., 2009] Vander Heiden, M. G., Cantley, L. C., and Thompson, C. B. (2009). Understanding the warburg effect: the metabolic requirements of cell proliferation. Science (New York, N.Y.), 324:1029–1033.

[Vogel et al., 1983] Vogel, S. N., Hilfiker, M. L., and Caulfield, M. J. (1983). Endotoxin-induced t lymphocyte proliferation. Journal of immunology (Baltimore, Md. : 1950), 130:1774–1779.

[von Bernuth et al., 2008] von Bernuth, H., Picard, C., Jin, Z., Pankla, R., Xiao, H., Ku, C.-L., Chrabieh, M., Mustapha, I. B., Ghandil, P., Camcioglu, Y., Vasconcelos, J., Sirvent, N., Guedes, M., Vitor, A. B., Herrero-Mata, M. J., Arostegui, J. I., Rodrigo, C., Alsina, L., Ruiz-Ortiz, E., Juan, M., Fortuny, C., Yague, J., Anton, J., Pascal, M., Chang, H.-H., Janniere, L., Rose, Y., Garty, B.-Z., Chapel, H., Issekutz, A., Marodi, L., Rodriguez-Gallego, C., Banchereau, J., Abel, L., Li, X., Chaussabel, D., Puel, A., and Casanova, J.-L. (2008). Pyogenic bacterial infections in humans with myd88 deficiency. Science (New York, N.Y.), 321:691–696.

[Wald et al., 2003] Wald, D., Qin, J., Zhao, Z., Qian, Y., Naramura, M., Tian, L., Towne, J., Sims, J. E., Stark, G. R., and Li, X. (2003). Sigirr, a negative regulator of toll-like receptor-interleukin 1 receptor signaling. Nature immunology, 4:920–927.

[Waldhart et al., 2017] Waldhart, A. N., Dykstra, H., Peck, A. S., Boguslawski, E. A., Madaj, Z. B., Wen, J., Veldkamp, K., Hollowell, M., Zheng, B., Cantley, L. C., McGraw, T. E., and Wu, N. (2017). Phosphorylation of txnip by akt mediates acute influx of glucose in response to insulin. Cell reports, 19:2005–2013.

[Wang et al., 2003] Wang, Q., Downey, G. P., Choi, C., Kapus, A., and McCulloch, C. A. (2003). Il-1 induced release of ca2+ from internal stores is dependent on cell-matrix interactions and regulates erk activation. FASEB journal : official publication of the Federation of American Societies for Experimental Biology, 17:1898–1900.

[Wang et al., 2011] Wang, R., Dillon, C. P., Shi, L. Z., Milasta, S., Carter, R., Finkelstein, D., McCormick, L. L., Fitzgerald, P., Chi, H., Munger, J., and Green, D. R. (2011). The transcription factor myc controls metabolic reprogramming upon t lymphocyte activation. Immunity, 35:871–882.

[Wang and Green, 2012] Wang, R. and Green, D. R. (2012). Metabolic reprogramming and metabolic dependency in t cells. Immunological reviews, 249:14–26.

[Watanabe et al., 2012] Watanabe, M., Abe, N., Oshikiri, Y., Stanbridge, E. J., and Kitagawa, T. (2012). Selective growth inhibition by glycogen synthase kinase-3 inhibitors in tumorigenic hela hybrid cells is mediated through nf-κb-dependent glut3 expression. Oncogenesis, 1:e21.

[Watanabe and Kobayashi, 1994] Watanabe, N. and Kobayashi, Y. (1994). Selective release of a processed form of interleukin 1 alpha. Cytokine, 6:597–601.

[Waters et al., 2018] Waters, L. R., Ahsan, F. M., Wolf, D. M., Shirihai, O., and Teitell, M. A. (2018). Initial b cell activation induces metabolic reprogramming and mitochondrial remodeling. iScience, 5:99–109.

[Weaver et al., 1988] Weaver, C. T., Hawrylowicz, C. M., and Unanue, E. R. (1988). T helper cell subsets require the expression of distinct costimulatory signals by antigen-presenting cells. Proceedings of the National Academy of Sciences of the United States of America, 85:8181–8185.

[Weber et al., 2010] Weber, A., Wasiliew, P., and Kracht, M. (2010). Interleukin-1 (il-1) pathway. Science signaling, 3:cm1.

[Wellen and Hotamisligil, 2005] Wellen, K. E. and Hotamisligil, G. S. (2005). Inflammation, stress, and diabetes. The Journal of clinical investigation, 115:1111–1119.

[Werman et al., 2004] Werman, A., Werman-Venkert, R., White, R., Lee, J.-K., Werman, B., Krelin, Y., Voronov, E., Dinarello, C. A., and Apte, R. N. (2004). The precursor form of il-1alpha is an intracrine proinflammatory activator of transcription. Proceedings of the National Academy of Sciences of the United States of America, 101:2434–2439.

[Wheeler and Defranco, 2012] Wheeler, M. L. and Defranco, A. L. (2012). Prolonged production of reactive oxygen species in response to b cell receptor stimulation promotes b cell activation and proliferation. Journal of immunology (Baltimore, Md. : 1950), 189:4405–4416.

[Wieman et al., 2009] Wieman, H. L., Horn, S. R., Jacobs, S. R., Altman, B. J., Kornbluth, S., and Rathmell, J. C. (2009). An essential role for the glut1 pdz-binding motif in growth factor regulation of glut1 degradation and trafficking. The Biochemical journal, 418:345–367.

[Wieman et al., 2007] Wieman, H. L., Wofford, J. A., and Rathmell, J. C. (2007). Cytokine stimulation promotes glucose uptake via phosphatidylinositol-3 kinase/akt regulation of glut1 activity and trafficking. Molecular biology of the cell, 18:1437–1446.

[Wofford et al., 2008] Wofford, J. A., Wieman, H. L., Jacobs, S. R., Zhao, Y., and Rathmell, J. C. (2008). Il-7 promotes glut1 trafficking and glucose uptake via stat5-mediated activation of akt to support t-cell survival. Blood, 111:2101–2111.

[Wu et al., 2013] Wu, N., Zheng, B., Shaywitz, A., Dagon, Y., Tower, C., Bellinger, G., Shen, C.-H., Wen, J., Asara, J., McGraw, T. E., Kahn, B. B., and Cantley, L. C. (2013). Ampk-dependent degradation of txnip upon energy stress leads to enhanced glucose uptake via glut1. Molecular cell, 49:1167–1175.

[Xi et al., 2001] Xi, X., Han, J., and Zhang, J. Z. (2001). Stimulation of glucose transport by amp-activated protein kinase via activation of p38 mitogen-activated protein kinase. The Journal of biological chemistry, 276:41029–41034.

[Xu et al., 2008] Xu, H., Liew, L. N., Kuo, I. C., Huang, C. H., Goh, D. L.-M., and Chua, K. Y. (2008). The modulatory effects of lipopolysaccharide-stimulated b cells on differential t-cell polarization. Immunology, 125:218–228.

[Yamada, 2018] Yamada, K. (2018). Aberrant uptake of a fluorescent l-glucose analogue (flg) into tumor cells expressing malignant phenotypes. Biological & pharmaceutical bulletin, 41:1508–1516.

[Yamada et al., 2007] Yamada, K., Saito, M., Matsuoka, H., and Inagaki, N. (2007). A real-time method of imaging glucose uptake in single, living mammalian cells. Nature protocols, 2:753–762.

[Yamazaki et al., 2002] Yamazaki, T., Takeda, K., Gotoh, K., Takeshima, H., Akira, S., and Kurosaki, T. (2002). Essential immunoregulatory role for bcap in b cell development and function. The Journal of experimental medicine, 195:535–545.

[Yang et al., 1996] Yang, J., Clarke, J. F., Ester, C. J., Young, P. W., Kasuga, M., and Holman, G. D. (1996). Phosphatidylinositol 3-kinase acts at an intracellular membrane site to enhance glut4 exocytosis in 3t3-l1 cells. The Biochemical journal, 313 (Pt 1):125–131.

[Yang et al., 2011] Yang, M., Wang, C., Zhu, X., Tang, S., Shi, L., Cao, X., and Chen, T. (2011). E3 ubiquitin ligase chip facilitates toll-like receptor signaling by recruiting and polyubiquitinating src and atypical pkczeta. The Journal of experimental medicine, 208:2099–2112.

[Ye et al., 1992] Ye, K., Koch, K. C., Clark, B. D., and Dinarello, C. A. (1992). Interleukin-1 down-regulates gene and surface expression of interleukin-1 receptor type i by destabilizing its mrna whereas interleukin-2 increases its expression. Immunology, 75:427–434.

[Yoshida et al., 2008] Yoshida, H., Kwon, A.-H., Kaibori, M., Tsuji, K., Habara, K., Yamada, M., Kamiyama, Y., Nishizawa, M., Ito, S., and Okumura, T. (2008). Edaravone prevents inos expression by inhibiting its promoter transactivation and mrna stability in cytokine-stimulated hepatocytes. Nitric oxide : biology and chemistry, 18:105–112.

[Zanin-Zhorov et al., 2007] Zanin-Zhorov, A., Tal-Lapidot, G., Cahalon, L., Cohen-Sfady, M., Pevsner-Fischer, M., Lider, O., and Cohen, I. R. (2007). Cutting edge: T cells respond to lipopolysaccharide innately via tlr4 signaling. Journal of immunology (Baltimore, Md. : 1950), 179:41–44.

[Zhao et al., 2007] Zhao, Y., Altman, B. J., Coloff, J. L., Herman, C. E., Jacobs, S. R., Wieman, H. L., Wofford, J. A., Dimascio, L. N., Ilkayeva, O., Kelekar, A., Reya, T., and Rathmell, J. C. (2007). Glycogen synthase kinase 3alpha and 3beta mediate a glucose-sensitive antiapoptotic signaling pathway to stabilize mcl-1. Molecular and cellular biology, 27:4328–4339.

[Zhou et al., 2010] Zhou, R., Tardivel, A., Thorens, B., Choi, I., and Tschopp, J. (2010). Thioredoxin-interacting protein links oxidative stress to inflammasome activation. Nature immunology, 11:136–140.

6 Appendix

6.1 List of Abbreviations

2-DG	2-deoxy-D-glucose
2-NBDG	2-deoxy-2-[(7-nitro-2,1,3-benzoxadiazol-4-yl)amino]-D-glucose
6-NBDG	6-deoxy-6-[(7-nitro-2,1,3-benzoxadiazol-4-yl)amino]-D-glucose
7-AAD	7-aminoactinomycin D
Acetyl-CoA	Acetyl coenzyme A
ACK	Ammonium-chloride-potassium
ADP	Adenosine diphosphate
AKTi8	AKT inhibitor VIII
AMPK	AMP-activated protein kinase
ANOVA	Analysis of variance
AP1	Activator protein 1
AS160	AKT substrate of 160 kDa
ATP	Adenosine triphosphate
AU	Arbitrary unit
Bam32	32 kDa B cell adapter molecule
BCAP	B cell adapter for phosphoinositide 3-kinase
cJNK	c-Jun N-terminal kinases
DAG	Diacyl glycerol
ECAR	Extracellular acidification rate
ERK	extracellular-signal regulated kinase
FACS	Fluorescence activated cell sorting
FCCP	Carbonyl cyanide-4-(trifluoromethoxy)phenylhydrazone
FCS	Fetal calf serum
FITC	Fluorescein isothiocyanate
FLGA	Fluorescence-labeled glucose analogues
FOX	Forkhead box
FSC	Forward scatter
GAP	GTPase-activating proteins
GLUT	Glucose transporter
GSK3β	Glycogen synthase kinase 3β
HIF-1α	Hypoxia-inducible factor 1α

H$^+$leak	Proton leak
HSA	Human serum albumin
ICE	IL-1β converting enzyme
IKK	IκB kinase
IL-1	Interleukin-1
IL-1α	Interleukin-1α
IL-1β	Interleukin-1β
IL-1R1	IL-1 receptor 1
IL-1R2	IL-1 receptor 2
IL-1Ra	Interleukin-1 receptor antagonist
IL-1RAcP	IL-1 receptor accessory protein
IL-1RAcPb	IL-1 receptor accessory protein b
i.p.	Intraperitoneal
IP$_3$	Inositol 1,4,5-trisphosphate
IRAK	IL-1 receptor-associated kinase
K$_{ir}$6.2	Inward-rectifier potassium channel 6.2
KO	Knockout
LPS	Lipopolysaccharide
LSM	Laser scanning microscope
MAPK	Mitogen-activated protein kinase
MFI	Mean fluorescence intensity
mTOR	Mechanistic target of rapamycin
MyD88	Myeloid differentiation primary response 88
NBD	7-nitrobenzo-2-oxa-1,3-diazol
NFκB	Nuclear factor kappa-light-chain-enhancer of activated B cells
NMOC	Non-mitochondrial oxygen consumption
OCR	Oxygen consumption rate
PBS	Phosphate buffered saline
PDH	Pyruvate dehydrogenase
PDK	Pyruvate dehydrogenase kinase
PDK1	Phosphoinoisitide dependent kinase 1
PE	Phycoerythrin
PH	Pleckstrin homology
pH	Potential of hydrogen
PI3K	Phosphoinositide 3-kinase

PIP$_2$	Phosphatidylinositol 4,5-biphosphate
PIP$_3$	Phosphatidylinositol (3,4,5)-triphosphate
PKB	Protein kinase B
PKC	Protein kinase C
PLCγ2	Phospholipase Cγ2
PTEN	Phosphatase and tensin homolog
Rab	Ras-associated binding
Ras	Rat sarcoma
RM-ANOVA	Repeated measure analysis of variance
R$_{max}$	Maximal respiratory capacity
ROS	Reactive oxygen species
S6K	p70 ribosomal S6 kinase
SGK	Serum- and glucocorticoid-induced protein kinase
SGLT	Sodium-glucose-linked transporter
SIGIRR	Single Ig IL-1-related receptor
SOCE	Store-operated calcium entry
SPF	Specific pathogen free
SSC	Side scatter
SSC-H	SSC pulse height
SSC-W	SSC pulse width
TAPP	Tandem PH-domain containing protein
TBC1D1	TBC1 domain family member 1
TBC1D4	TBC1 domain family member 4
TIR	Toll-IL-1 receptor
TLR	Toll-like receptor
TNFα	Tumor necrosis factor α
TOLLIP	Toll interacting protein
TRP	Transient receptor potential
TXNIP	Thioredoxin-interacting protein
Ubc9	Ubiquitin conjugating enzyme 9
WT	Wildtype

6.2 List of Figures

6.3 List of Tables

6.4 Academic Teachers

My academic teachers in Marburg were:

Prof. Dr. Bauer, S.
Prof. Dr. Bauer, U.
Dr. Bertoune
Prof. Dr. Besedovski
Dr. Bette
Dr. Braun
Prof. Dr. Brehm
Prof. Dr. Bremmer
Prof. Dr. Daut
Prof. Dr. Decher
Prof. Dr. Dehnen
Prof. Dr. del Rey
Prof. Dr. Dodel
Prof. Dr. Elsässer
Dr. Feuser
Prof. Dr. Garten
Prof. Dr. Jacob
Dr. Käuser
Prof. Dr. Koolman
Dr. Leitner
Prof. Dr. Lill
Prof. Dr. Maisner
Dr. Milani
Prof. Dr. Müller
Prof. Dr. Oliver
Prof. Dr. Pagenstecher
Prof. Dr. Plant
Dr. Preisig-Müller
Prof. Dr. Röhm
Dr. Schäfer
Prof. Dr. Schütz
Prof. Dr. Suske
Prof. Dr. Weihe
Dr. Westermann
Dr. Wildmann
Dr. Wrocklage

6.5 Acknowledgements